ENDF-334

ORNL/TM-8880

ornl

OAK RIDGE NATIONAL LABORATORY

MARTIN MARIETTA

ORELA Flight Path 1: Determinations of Its Effective Length vs Energy, Experimental Energies, and Energy Resolution Function and Their Uncertainties

D. C. Larson
N. M. Larson
J. A. Harvey

OPERATED BY
MARTIN MARIETTA ENERGY SYSTEMS, INC.
FOR THE UNITED STATES
DEPARTMENT OF ENERGY

Printed in the United States of America. Available from
National Technical Information Service
U.S. Department of Commerce
5285 Port Royal Road, Springfield, Virginia 22161
NTIS price codes—Printed Copy: A06; Microfiche A01

ORNL/TM-8880

Engineering Physics and Mathematics Division

ORELA FLIGHT PATH 1: DETERMINATIONS OF ITS EFFECTIVE LENGTH vs ENERGY, EXPERIMENTAL ENERGIES, AND ENERGY RESOLUTION FUNCTION AND THEIR UNCERTAINTIES

D. C. Larson, N. M. Larson,* and J. A. Harvey

Manuscript Completed: April 15, 1984
Date Published - June 1984

*Computer Sciences

NOTICE This document contains information of a preliminary nature. It is subject to revision or correction and therefore does not represent a final report.

Prepared by the
OAK RIDGE NATIONAL LABORATORY
Oak Ridge, Tennessee 37831
operated by
Martin Marietta Energy Systems, Inc.
Under Contract No. DE-AC05-840R21400
for the
Division of Basic Energy Sciences
U.S. DEPARTMENT OF ENERGY

CONTENTS

ORELA FLIGHT PATH 1: DETERMINATIONS OF ITS EFFECTIVE LENGTH vs ENERGY, EXPERIMENTAL ENERGIES, AND ENERGY RESOLUTION FUNCTION AND THEIR UNCERTAINTIES

D. C. Larson, N. M. Larson, and J. A. Harvey

ABSTRACT

Flight path 1 at ORELA is nominally 200 m in length and has been extensively used for neutron transmission and scattering measurements. Due to moderation effects in the neutron-producing target and to the finite thickness of the neutron detector, the effective flight-path length is a function of neutron energy. In this report, we determine the effective length as a function of energy, its uncertainty, and time-of-flight energies and their uncertainties. Finally, we determine the resolution function and its uncertainty and compare the width of this resolution function with an experimental determination of this quantity.

1. INTRODUCTION AND DEFINITIONS

Flight path 1 at ORELA has been used for neutron transmission and scattering measurements on many materials and isotopes. It has a nominal length of 200 m, with intermediate flight-path stations at 80 and 18 m. With the recent development of an R-matrix code, SAMMY (LA80), based on Bayes' equations, more in-house data analyses are being performed. Such analyses demand precise information for the flight-path length, timing parameters, and the resolution function, and their uncertainties, in order to obtain reliable resonance parameters and realistic uncertainties. This report is a scoping study to develop this information using approximate analytic models for the neutron-producing target, the NE110 proton recoil detector, the neutron burst shape, and the timing channels. We evaluate energy dependent effects which contribute to the effective flight-path length and resolution function and give a first-order treatment of those which appear to be important. Finally, we note those areas which should be treated in more depth. This report is a companion to our report on the measurement of the total cross section of natural nickel (LA83), and the experimental parameters used in this report are consistent with the experimental configuration used for the nickel measurement.

In Sect. 2 we describe the general properties of flight path 1, including a description of a recent laser measurement of the drift tube length.

In Sect. 3 we develop distribution functions for components of the flight-path length from the target and the detector, and we use these to evaluate the first moment (mean value of the length) and second moment or width (variance) of the distributions. Uncertainties of the moments are also evaluated.

In Sect. 4 we concern ourselves with properties associated with the flight time. We develop distribution functions for the ORELA pulse width and the channel width of the data-acquisition program. Means and variances of these distributions are computed, along with their uncertainties.

In Sect. 5 the results from Sects. 3 and 4 are combined to develop a distribution function for the time-of-flight (t-o-f) energy. The first moment of this energy distribution function gives the mean t-o-f energy, and we identify the second moment with the width of the energy resolution function. Uncertainties of the mean energy and the resolution function parameters are also derived. Finally, in this section we compare parameters of our resolution function with those extracted from a recent analysis of experimental data.

Section 6 is a summary of what we have learned in this scoping study. Also noted are areas where more thorough treatments are called for.

1.1 METHOD AND DEFINITIONS

We approach this problem by developing analytic models for the distribution functions of the flight-path length and flight time. From these distribution functions we obtain the desired results for the energy scale and energy-resolution function and their associated uncertainties. Considering as an example the flight-path length, we identify the length with the *mean value* of the convolution of the various distribution functions associated with the effective flight-path length. The *uncertainty* in the length is identified as the uncertainty in the mean value. The contribution to the energy resolution function from the flight path is identified with the *widths* of the above distributions, and the *uncertainties* in the resolution functions result from the uncertainties associated with the distribution widths. Quantities associated with the flight time are similarly obtained from the distribution functions for the components of the flight time. Figures 1 and 2 are graphic representations of the various distributions, means and uncertainties.

In this work we will be dealing with distributions which describe physical properties of the target, detector, and beam from the accelerator. We now explicitly state our definitions and rules for calculating mean values and variances associated with these distributions and *uncertainties* on the means and variances. We feel that it is important to be very clear on this point. For example, looking ahead we will find that to first order, the expressions for the energy uncertainty ΔE and the resolution function width ω_E are identical in form; however, corresponding parameters in the two expressions have very different meanings. For this reason, we consistently apply the following definitions and methods of calculating the various means, variances, and uncertainties.

Each distribution, $\rho(y)$, where y is an arbitrary parameter or set of parameters, will be expressed in an appropriate analytic form utilizing parameters which can be either calculated or estimated. We define the mean value of a quantity (assumed to be the experimentally observed value) as

$$<y> = \int y\rho(y)dy \quad , \tag{1.1.1}$$

and the variance of y (which is a measure of the width of the distribution) as

$$\omega_y^2 = <(y - <y>)^2> \quad , \tag{1.1.2}$$

or equivalently

$$\omega_y^2 = <y^2> - <y>^2 \quad , \tag{1.1.3}$$

where

$$<y^2> = \int y^2\rho(y)dy \quad , \tag{1.1.4}$$

and $<y>^2$ is obtained from Eq. (1.1.1).

ORNL-DWG 83-19667

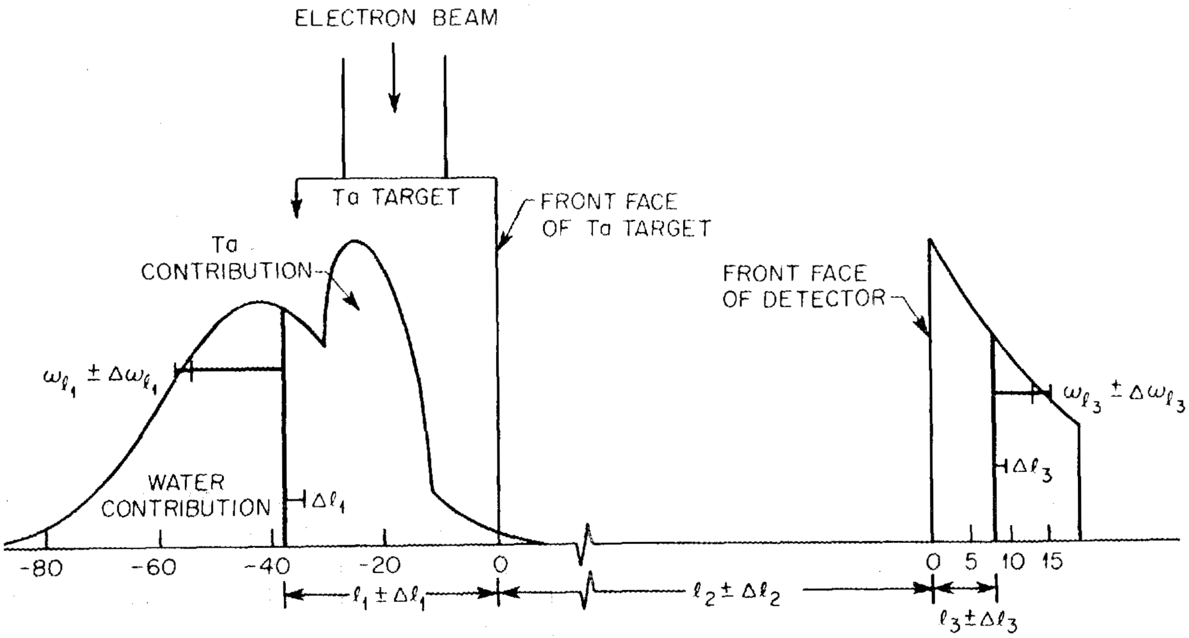

Fig. 1. This figure schematically illustrates the various quantities and their uncertainties associated with the target and detector. l_1 is the mean distance from the effective point of neutron production to the front face of the Ta target. The distribution is a superposition of a Gaussian for the water and a parabola for the Ta for a neutron energy of 100 keV (see text). l_2 is the mean distance from the front face of the target to the front face of the detector, and l_3 is the mean distance from the front face of the detector to the first collision. Widths of the target and detector distributions are also shown. ω_{l_1} is the width of the neutron distribution associated with the target, and ω_{l_3} is the width of the distribution associated with the detector. Uncertainties (standard deviations) for the mean lengths Δl_1, Δl_2, and Δl_3, as well as for the widths $\Delta\omega_{l_1}$ and $\Delta\omega_{l_3}$, are also illustrated. The Ta contribution to the neutron production is offset from the center of the incident electron beam by s (6 mm for 1-MeV neutrons), the correction for multiple scattering in the Ta (see text).

ORNL-DWG 83-19666

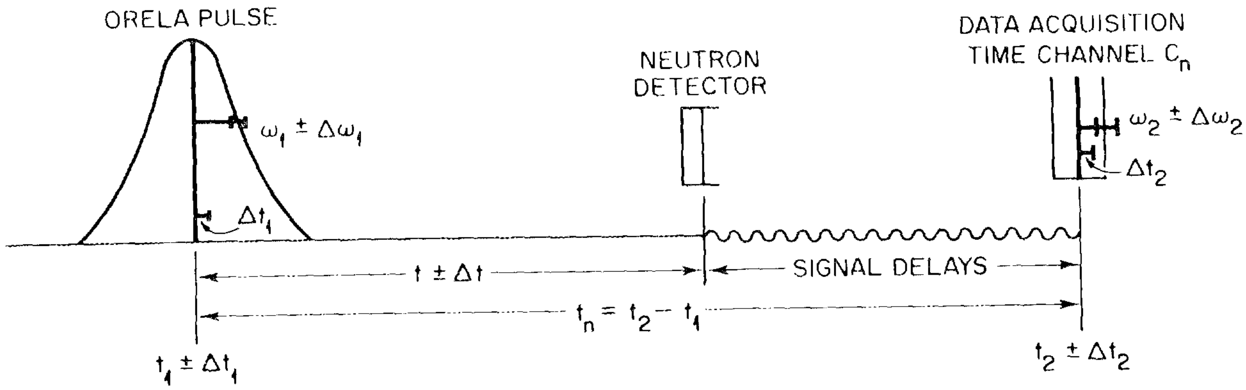

Fig. 2. This figure schematically serves to define the various times used in this report as well as the time distributions. The ORELA pulse is represented by a Gaussian of width $\omega_1 \pm \Delta\omega_1$ and mean value $t_1 \pm \Delta t_1$ (t_1 is taken as zero in the text). The flight time t is the flight time of the neutron from the target to the detector. t_2 is the center of a time channel defined by the data-acquisition program, and ω_2 is the width (standard deviation) of this channel. t_n is the "observed flight time" of a neutron event in the data-acquisition system. Uncertainties in the various times and widths are also illustrated.

As noted earlier, in this work we will develop distribution functions for each component of the flight-path length and flight times. From the mean values of the flight-path length and flight-time distributions, we can calculate the observed mean energy E, and from the widths (and higher moments) of the distributions associated with the flight-path length and flight times we can calculate the width (square root of variance) ω_E of the energy resolution function. We can also calculate the uncertainties associated with the energy scale and resolution function, as well as the correlations among the parameters of the distributions, by calculating small increments of E and ω_E. In particular, for the energy uncertainty we will generate a small increment δE via the chain rule

$$\delta E = \sum_i \frac{\partial E}{\partial p_i} \delta p_i \quad , \tag{1.1.5}$$

where the p_i are the values of the parameters in the expression for E, and δp_i are small increments of those parameters. The variance ΔE^2 (squared uncertainty) on E is then given by forming the product

$$<\delta E \delta E> \equiv \Delta E^2 \quad . \tag{1.1.6}$$

The energy and its uncertainty is then given by $E \pm \Delta E$. Similarly, the uncertainty associated with the width of the resolution function is obtained from

$$\delta(\omega_E) = \sum_i \frac{\partial \omega_E}{\partial p_i} \delta p_i \quad , \tag{1.1.7}$$

and the standard deviation $\Delta\omega_E$ is obtained from

$$\Delta\omega_E = \sqrt{<\delta\omega_E \delta\omega_E>} \quad . \tag{1.1.8}$$

Our evaluation of the quantities ΔE, ω_E, and $\Delta\omega_E$ (Sect. 5) involves second, third, and fourth moments of the length- and time-distribution functions as well as the uncertainties of those moments. The rest of this report is concerned with developing approximations for the various distribution functions $\rho(y)$ and evaluating the means, widths, uncertainties, and higher moments.

Before proceeding to the task of developing the distribution functions, we digress to point out that the term "distribution function" often has another meaning when used in an uncertainty analysis context. We are using the term to refer to a physical property of the experimental system. However, the parameters p_i which occur in the analytic expressions for these distributions are also characterized by a mean value and an uncertainty. The parameters p_i are distributed according to some probability density function *(pdf)*. Nevertheless, when evaluating the parameters p_i and their uncertainties Δp_i, we need only give the mean values and standard deviations and do not require knowledge of the explicit form of the *pdf*.

2. GENERAL PROPERTIES OF FLIGHT PATH 1

Flight path 1 is positioned at 90° with respect to the incident electron beam and is perpendicular to the face of the neutron-producing target (see Fig. 3). Three computer-controlled sample changers are available, located at 5 m, 9 m, and 10 m from the target. Two changers have five paddles and one has four positions available for filters or samples. Various collimators are inserted at ~8 m from the target to view neutrons from only the tantalum target, only the water moderator (above the tantalum), or a combination of the two sources. We treat the latter case in this report. The neutron spectrum from the tantalum has a higher average energy than that from the water moderator. A rectangular (5.4 by 4.8 cm) shadow bar which consists of 2.9 cm uranium, 2.5 cm thorium, and 2.5 cm tantalum is normally located at ~4 m from the source. The thickness and composition of the shadow bar have been chosen to reduce the gamma flash from the tantalum to an acceptable intensity, while still allowing neutrons from the tantalum to reach the detector.

The neutron time-of-flight spectrum from the bare tantalum target has been compared to that from the surrounding water moderator (HA75). The spectral comparisons are shown in Fig. 4. After renormalizing those results to collimator sizes, filters, shadow bars, and neutron production as a function of distance from the target center for the nickel measurement (LA83), we find that the neutron intensities from the water moderator and from the tantalum metal are equal at about 300 keV, with the tantalum target producing more neutrons at 1 MeV by a factor of about 10. The water-moderated neutrons have significantly greater intensity below ~100 keV, since the production cross section for neutrons in the tantalum is decreasing with decreasing energy, and multiple scattering is increasing since the tantalum target is >1 mean-free-path thick for neutrons less than ~100 keV.

For this report we need an accurate measurement of the length of the 200-m flight path. In March 1983 a Hewlett-Packard electronic distance meter (laser) was used to measure distances along the 200-m flight path. This measurement and analysis is detailed in (LA84). At that time we were not able to measure directly to the target center and had to satisfy ourselves with measurements to various benchmarks along the 200-m flight path and to the 20-m station, which is on line with, but on the other side of, the target from the 200-m flight path. Sufficient measurements were taken to determine the offset of the measuring device, and the statistical uncertainty associated with the measurements. Combining the laser results with results from engineering drawings (HA 69) which give distances from the center of the target room to existing benchmarks allowed us to determine a mean flight-path length from the center of the target room to the east benchmark at the 200-m station. In this analysis, provision was made for the possibility that the target is not located perfectly at the center of the target room. The mean value of this displacement parameter was taken as zero, with an uncertainty of ±2 mm. An uncertainty analysis using Bayes' equations and including correlations introduced by the measurement process provided the uncertainty. The preliminary result is 201858.6 ± 4.0 mm.

3. PROPERTIES ASSOCIATED WITH THE FLIGHT-PATH LENGTH

The total flight-path length l can be separated into three components (see Fig. 1): (1) l_1, the mean distance from the point where the neutron is "produced" to the front face of the neutron-producing target; (2) l_2, the distance from the face of the target to the face of the detector; and (3) l_3, the distance from the face of the detector to the point of the first collision. Each component will be discussed separately in Sects. 3.1, 3.2, and 3.3, and the combined flight-path length is discussed in Sect. 3.4.

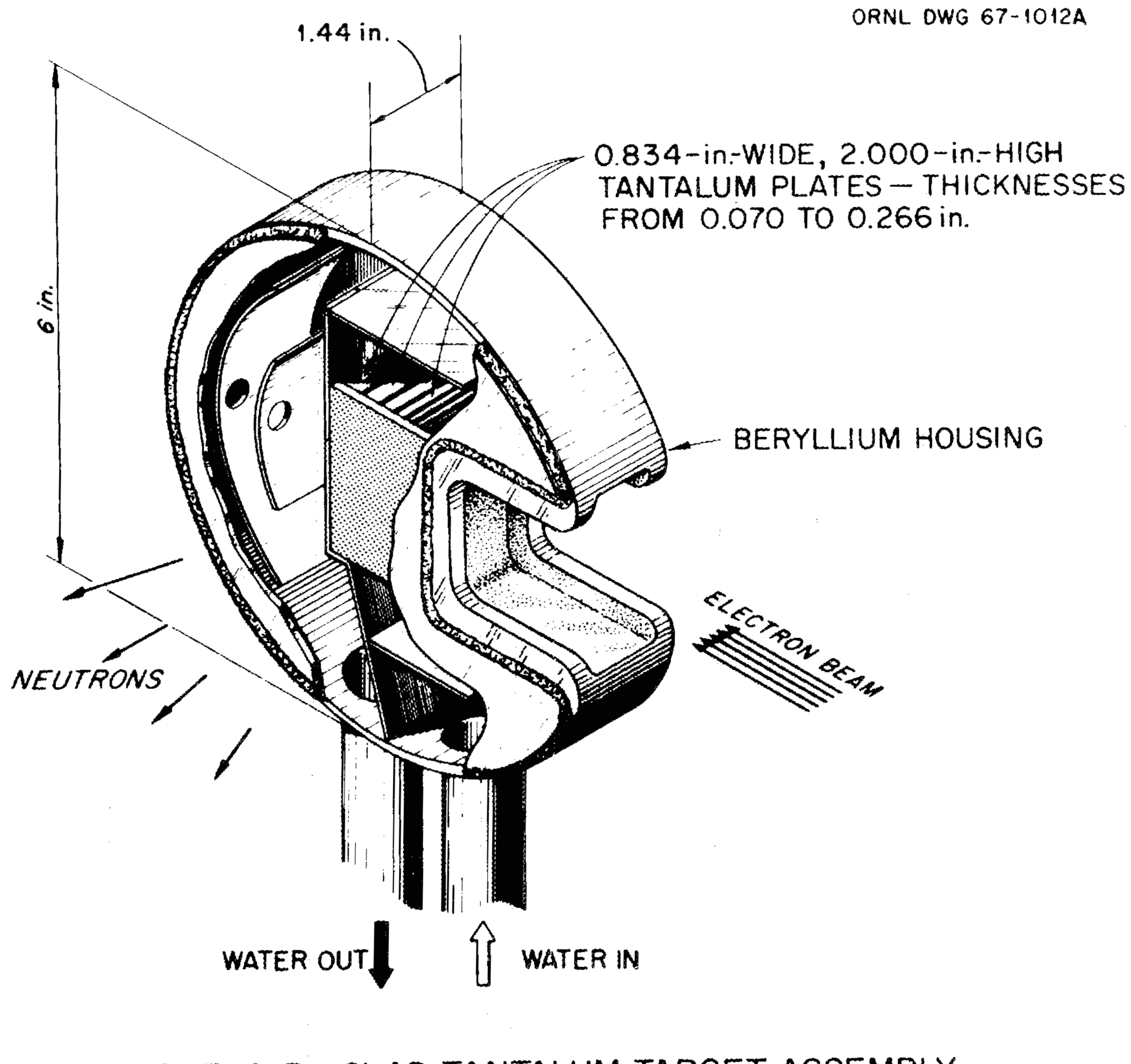

Fig. 3. This figure is an illustration of the ORELA Ta target. The 200-m flight path is in the direction of the neutron arrows, perpendicular to the face of the target.

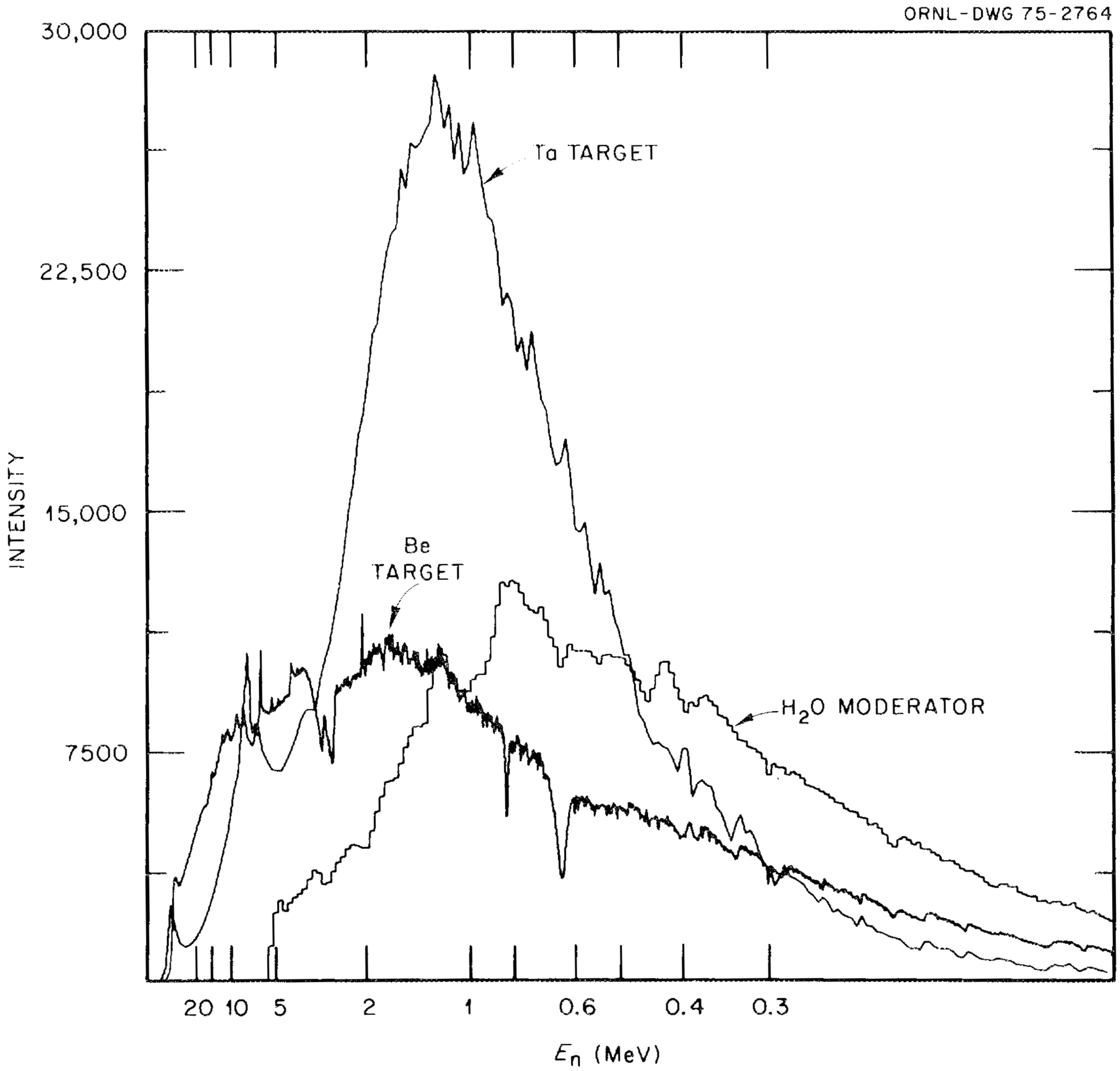

Fig. 4. This figure is an illustration of the measured flux as a function of neutron energy at 200 m from two different areas of the target (Fig. 3) and from a separate Be block target which is not treated in this report. The "Ta target" spectrum results from using a collimator which views only the Ta plates of the target, while the "H_2O moderator" spectrum results from using a collimator which views only neutrons emanating from the water moderator above the Ta plates. These spectral measurements were done with a different experimental configuration than that treated in the present work; however, the present analysis has been normalized for the different filters, collimator sizes, etc., used for the present work (see text). In particular, for the present analysis we have a larger collimator which views both the Ta and the water moderator, and we used a "thin" shadow bar to reduce the intensity of the gamma flash and neutrons emanating from electrons striking the Ta plates. This figure and analysis served to provide the "crossover energy" E_m, where the spectra from the Ta and H_2O have approximately equal intensity. For the present experimental configuration, this was found to be $\sim$300 $\pm$ 90 keV.

3.1 DISTRIBUTION FUNCTION FOR x_1: THE CONTRIBUTION TO THE FLIGHT-PATH LENGTH FROM THE TARGET

The first component l_1 of the total flight-path length l is the most difficult to assess since in the experiments of immediate concern we view neutrons both from the tantalum metal target and from the cooling-water moderator surrounding the target. For the nickel measurement, the 7.6-cm-diam collimator at 8 m views 45.4 cm^2 of the target, of which 20.8 cm^2 is the tantalum and the remaining 24.6 cm^2 is water moderator. The cross-sectional area of the shadow bar is 25.9 cm^2 and thus shadows the tantalum target plus some of the water moderator. Neutrons which emanate from the tantalum target are assumed to be born near the centerline of the target (along the direction of the incident electron beam, see Figs. 1 and 3). For these neutrons, the length $W/2$ from the center of the tantalum target to the target face (from where l_1 is measured) is 18.3 mm and is assumed to be energy independent. However, scattering of the primary neutrons in the Ta target changes the distribution of neutrons leaving the exit surface of the Ta target. To estimate these effects, we consider what happens to 1-MeV neutrons produced in the Ta by the electron beam. We assume a value of $\sigma_{Ta} = 7.56$ b for the following approximate calculation. The unscattered neutrons produced at the center of the Ta target moving in the direction of the detector at 200 m escape with a 47% probability. These primary neutrons have a mean value length of $W/2 = 18.3$ mm. Numerical analytic calculations have been made to estimate the contributions to the effective flight-path length $q = W/2 + s$ of the *scattered* neutrons in the Ta target. The intensity of singly scattered neutrons in the direction of the detector is ~60% of the unscattered neutron intensity. Combining the unscattered and first scattered neutrons gives a value of $s = 3.3$ mm. Estimating the contribution of higher order scattering (to eighth order) approximately doubles this correction to 6 mm. In this work we use a value of $s = 6$ mm with $\Delta s = 30\%$, giving $q = W/2 + s = 24.3$ mm. We also note that the correction factor s is expected to be energy dependent; however, that complication is not treated in this work. In addition, the possibility that the electron beam is not centered about $W/2$ must be considered. For instance, if the electron beam strikes the target between $W/2$ and the front face, the correction s due to multiple scattering in the Ta may be reduced. To account for this possibility, we add another parameter Z, which we assume has a mean value $Z = 0$, but with the uncertainty $\Delta Z = \pm 2$ mm. Thus, finally $q = W/2 + s + Z$.

The neutrons which come from the water moderator are also difficult to characterize since the moderation process produces a distribution of neutron delay times. These delay time distributions are conventionally converted to distributions of equivalent moderation distances d, which are the product of delay times and escape velocities. The mean equivalent moderation distance d for the ORELA target is described in (CO83). The quantity d is energy-dependent and increases with energy according to

$$d(E) = 22.8 - 1.60\times\ln E + 0.283\times(\ln E)^2 \quad , \tag{3.1.1}$$

where d is in mm and E in eV. This equation is quoted to be valid for 10-ev to 1-MeV neutrons which come from the water moderator (CO83). A calculation similar to this should be done for the Ta.

We now see that for the energy region from ~1 keV to 1 MeV (a region of interest for resonance parameter analysis) we have an energy-dependent flight-path length, since useful neutrons come from both the tantalum and the water sources. For the case of 300-keV neutrons emerging from the face of the target (recall that both sources contribute about equally at 300 keV), those neutrons coming from the tantalum target have a mean effective flight-path length of 24.3 mm, while those coming from the water moderator have a mean effective flight-path length of 47.6 mm. Thus, for the water-moderated neutrons, the effective flight path is ~23 mm longer than for the neutrons which come directly from the tantalum.

We now derive a distribution function for the production of neutrons from the target. If we let $\rho_{l_1}(x_1)$ describe the distribution of neutrons as a function of x_1, the distance from the front face of the target measured in the direction away from the detector, we can write

$$\rho_{l_1}(E,x_1) = f_W(E)\rho_W(E,x_1) + f_T(E)\rho_T(x_1) \quad , \tag{3.1.2}$$

where $f_W(E)$ and $f_T(E)$ represent the fraction of neutrons originating in the water moderator and in the tantalum target respectively for energy E. $\rho_W(E,x_1)$ and $\rho_T(x_1)$ represent the effective spatial distributions of neutrons originating in the water and tantalum, respectively. Note that for water the distribution is a function of energy and position, while the distribution from the tantalum is assumed to be independent of energy.

We somewhat arbitrarily specify the energy dependence of the fractions $f_W(E)$ and $f_T(E)$ as

$$f_W(E) = \frac{2}{1 + e^{\frac{E\ln 3}{E_m}}} \quad , \tag{3.1.3}$$

with $E_m = 300$ keV and

$$f_T(E) = 1 - f_W(E) \quad . \tag{3.1.4}$$

Note that this choice gives

$$f_W(E=0) = 1 \quad , \quad f_T(E=0) = 0 \quad ,$$

$$f_W(E=E_m) = 0.5 \quad , \quad f_T(E=E_m) = 0.5 \quad ,$$

$$f_W(E=1 \text{ MeV}) \simeq 0.05 \quad , \quad f_T(E=1 \text{ MeV}) \simeq 0.95;$$

i.e., this choice for the two fractions is consistent with the energy dependence of the observed spectra from the tantalum and water (Fig. 4).

For $\rho_W(E,x_1)$, we choose a Gaussian distribution centered at $d(E)$, with a standard deviation width $\omega_W(E)$. The distributions actually given in (CO83) are slightly asymmetric, and are described by the functional form x^2e^{-x}, but we ignore that complication in this work. Thus

$$\rho_W(E,x_1) = \frac{1}{\omega_W\sqrt{2\pi}} e^{-\frac{(x_1-d)^2}{2\omega_W^2}} , \tag{3.1.5}$$

where the mean value is calculated from Eq. (1.1.1).

$$<x_1>_W = d(E) , \tag{3.1.6}$$

with *d(E)* given in Eq. (3.1.1). The variance of the distribution is calculated from Eq. (1.1.2):

$$<(x_1 - <x_1>)^2>_W = \omega_W^2(E) . \tag{3.1.7}$$

An expression for $\omega_W(E)$ was obtained by fitting a curve to the square root of values given in the "Var d" column of Table 1 of (CO83):

$$\omega_W(E) = 10.0 - 0.63\times\ln E + 0.112\times(\ln E)^2 , \quad E \text{ in eV} . \tag{3.1.8}$$

We now develop an expression for $\rho_T(x_1)$, the distribution function for neutrons from the tantalum. The electron beam strikes the tantalum target directly. Thus for $\rho_T(x_1)$ we assume that a uniform electron beam of radius r (= 9.2 mm) (LE70) is incident on the tantalum plates of the target, and we find

$$\rho_T(x_1) = \begin{cases} \frac{2}{\pi r^2}\left[r^2 - (q - x_1)^2\right]^{1/2} & \text{for } |x_1 - q| \leqslant r \\ 0 \text{ otherwise} & \end{cases} \tag{3.1.9}$$

where $q = W/2 + s + Z$, W is the width of the tantalum target (= 36.6 mm), s (6 mm) is the correction for multiple scattering and attenuation in the tantalum, and Z is the possible offset of the electron beam from the center of the target ($Z = 0$). From this distribution and Eq. (1.1.1) we find the mean value

$$<x_1>_T = q , \tag{3.1.10}$$

and from Eq. (1.1.2) the variance

$$<x_1^2>_T \; - \; <x_1>_T^2 \; = \; \frac{r^2}{4} \; = \; \omega_T^2 \quad . \tag{3.1.11}$$

The distribution function $\rho_{l_1}(E,x_1)$ is then given by the weighted sum of the water plus tantalum distributions, as stated in Eq. (3.1.2), with Eqs. (3.1.5) and (3.1.9) for the individual distributions.

3.1.1 *Mean Value l_1 for Distribution of x_1*

From Eq. (1.1.1) we can write the expression for the mean value of the contribution to the flight path length from the neutron target:

$$l_1 \; = \; <x_1>_{l_1} \; = \; \int x_1 \rho_{l_1}(x_1) dx_1 \; = \; f_W <x_1>_W \; + \; f_T <x_1>_T \; = \; f_W d \; + \; f_T q \quad . \tag{3.1.12}$$

Replacing q by $W/2 + s + Z$ and f_T by $1 - f_W$, this equation becomes

$$l_1 \; = \; (d \; - \; W/2 \; - \; s \; - \; Z) f_W \; + \; W/2 \; + \; s \; + \; Z \quad . \tag{3.1.13}$$

This contribution to the flight-path length is given as a function of energy in Table 1.

3.1.2 *Uncertainty in l_1*

We now evaluate the uncertainty associated with l_1. Taking small increments and using the chain rule for partial derivatives give

$$\delta l_1 \; = \; \frac{\partial l_1}{\partial d} \, \delta d \; + \; \frac{\partial l_1}{\partial W} \, \delta W \; + \; \frac{\partial l_1}{\partial s} \, \delta s \; + \; \frac{\partial l_1}{\partial Z} \, \delta Z \; + \; \frac{\partial l_1}{\partial f_W} \, \delta f_W \quad . \tag{3.1.14}$$

Using Eq. (3.1.3) for f_W gives δf_W in terms of δE_m, which is a parameter of interest,

$$\delta f_W \; = \; \frac{\partial f_W}{\partial E_m} \, \delta E_m \; = \; f_W^2 \, \frac{E \ln 3}{2 E_m^2} \, e^{\frac{E \ln 3}{E_m}} \, \delta E_m \quad . \tag{3.1.15}$$

Table 1. The energy uncertainty ΔE and the total flight-path length l and its uncertainty Δl are given as a function of energy. Also given are the contributions from the target (l_1) and the detector (l_3) to l and their uncertainties. All energies are in eV, lengths are in mm, and uncertainties are one standard deviation.

E	ΔE	$\Delta E/E$	l	Δl	l_1	Δl_1	l_3	Δl_3	l_1+l_3	$\Delta(l_1+l_3)$
10.000	0.001	6.699E−05	201466.604	5.413	20.616	2.062	5.986	0.220	26.602	2.073
1000.000	0.069	6.853E−05	201471.238	5.604	25.250	2.521	5.989	0.220	31.239	2.530
2000.000	0.138	6.917E−05	201472.984	5.681	26.979	2.689	6.005	0.220	32.984	2.698
5000.000	0.351	7.021E−05	201475.703	5.806	29.653	2.943	6.051	0.222	35.704	2.952
10000.000	0.711	7.114E−05	201478.055	5.913	31.928	3.149	6.127	0.224	38.055	3.157
20000.000	1.443	7.215E−05	201480.592	6.022	34.330	3.349	6.263	0.230	40.592	3.357
50000.000	3.670	7.341E−05	201483.910	6.136	37.311	3.548	6.600	0.244	43.911	3.557
100000.000	7.430	7.430E−05	201485.699	6.180	38.705	3.623	6.995	0.266	45.700	3.633
200000.000	15.273	7.636E−05	201485.490	6.305	38.023	3.830	7.466	0.296	45.489	3.841
300000.000	23.788	7.929E−05	201483.803	6.541	35.966	4.205	7.835	0.323	43.802	4.218
400000.000	32.764	8.191E−05	201481.605	6.744	33.668	4.513	7.937	0.331	41.604	4.525
700000.000	59.068	8.438E−05	201476.617	6.698	28.338	4.442	8.279	0.360	36.618	4.457
1000000.000	85.044	8.504E−05	201474.301	6.420	25.823	4.009	8.478	0.377	34.301	4.027
2000000.000	186.289	9.314E−05	201473.156	6.318	24.346	3.841	8.811	0.408	33.157	3.862
5000000.000	578.663	1.157E−04	201473.375	6.322	24.300	3.845	9.074	0.433	33.374	3.869
10000000.000	1457.753	1.458E−04	201473.486	6.323	24.300	3.845	9.186	0.444	33.486	3.870
20000000.000	3845.079	1.923E−04	201473.514	6.323	24.300	3.845	9.213	0.447	33.513	3.870

Note: Insignificant digits have been retained in all tables to facilitate comparisons with future calculations.

Evaluating the partial derivations in Eq. (3.1.14) explicitly from Eq. (3.1.13) gives

$$\delta l_1 = f_W \delta d + \left(\frac{1 - f_W}{2}\right)\delta W + (1 - f_W)(\delta s + \delta Z) + \left(d - \frac{W}{2} - s - Z\right)\left(f_W^2 \frac{E\ln 3}{2E_m^2} e^{\frac{E\ln 3}{E_m}}\right)\delta E_m \quad . \tag{3.1.16}$$

Forming the product $<\delta l_1 \delta l_1> \equiv \Delta l_1^2$, and assuming all variables are uncorrelated, we find

$$\Delta l_1 = \left\{ f_W^2 \Delta d^2 + \left(\frac{1 - f_W}{2}\right)^2 \Delta W^2 + (1 - f_W)^2(\Delta s^2 + \Delta Z^2) + \left(d - \frac{W}{2} - s - Z\right)^2 \left(f_W^2 \frac{E\ln 3}{2E_m^2} e^{\frac{E\ln 3}{E_m}}\right)^2 \Delta E_m^2 \right\}^{1/2} \tag{3.1.17}$$

for the uncertainty on l_1.

We assume values of $\Delta d/d = 10\%$, $\Delta W/W = 2\%$, $\Delta s/s = 30\%$, $\Delta Z = 2$ mm, $\Delta r/r = 20\%$, and $\Delta E_m/E_m = 30\%$. Using these values, we obtain results for Δl_1 as in Table 1.

This completes our evaluation of the contribution to the flight-path length from the target end and its uncertainty ($l_1 \pm \Delta l_1$) as a function of neutron energy.

3.1.3 *Higher Moments of the Target Distribution Function*

Later on this report when we derive expressions for the mean energy and the energy resolution function, we will need higher moments of x_1; in particular, the second, third, and fourth moments. We shall evaluate these moments "about the mean" and define $\omega_{l_1}^2$ as the second moment about the mean (i.e., the variance),

$$\omega_{l_1}^2 = \langle (x_1 - \langle x_1 \rangle_{l_1})^2 \rangle_{l_1} \quad , \tag{3.1.18}$$

$\nu_{l_1}^3$ as the third moment,

$$\nu_{l_1}^3 = \langle (x_1 - \langle x_1 \rangle_{l_1})^3 \rangle_{l_1} \quad , \tag{3.1.19}$$

and $\mu_{l_1}^4$ as the fourth moment,

$$\mu_{l_1}^4 = \langle (x_1 - \langle x_1 \rangle_{l_1})^4 \rangle_{l_1} \quad . \tag{3.1.20}$$

We now evaluate these moments for future reference. The n^{th} moment about the mean is given by

$$\langle x_1^n \rangle_{l_1} = \int (x_1 - \langle x_1 \rangle_{l_1})^n \rho_{l_1}(x_1) dx_1 \quad , \tag{3.1.21}$$

where $\rho_{l_1}(x_1)$ is given by Eq. (3.1.2) in terms of the water and tantalum distributions. For the water contribution, $\rho_W(x_1)$ is a Gaussian with moments given by

$$\langle x_1 \rangle_W = d \quad , \tag{3.1.22}$$

$$<(x_1 - d)^2>_W = \omega_W^2 \quad , \tag{3.1.23}$$

$$\nu_W^3 = <(x_1 - d)^3>_W = 0 \quad , \tag{3.1.24}$$

and

$$\mu_W^4 = <(x_1 - d)^4>_W = 3\omega_W^4 \quad . \tag{3.1.25}$$

For the tantalum, $\rho_T(x_1)$ is given by Eq. (3.1.9). The moments of this distribution are

$$<x_1>_T = q \quad , \tag{3.1.26}$$

$$\omega_T^2 = <(x_1 - q)^2>_T = \frac{r^2}{4} \quad , \tag{3.1.27}$$

$$\nu_T^3 = <(x_1 - q)^3>_T = 0 \quad , \tag{3.1.28}$$

and

$$\mu_T^4 = <(x_1 - q)^4>_T = \frac{r^4}{8} \quad . \tag{3.1.29}$$

Combining these results, we obtain

$$l_1 = <x_1>_{l_1} = f_W d + (1 - f_W)q \quad , \tag{3.1.30}$$

$$\omega_{l_1}^2 = <(x_1 - l_1)^2>_{l_1} = f_W\omega_W^2 + (1 - f_W)r^2/4 + f_W(1 - f_W)(d - q)^2 \quad , \tag{3.1.31}$$

$$\begin{aligned} \nu_{l_1}^3 &= <(x_1 - l_1)^3>_{l_1} \\ &= f_W(1 - f_W)(d - q)[3(\omega_W^2 - r^2/4) + (1 - 2f_W)(d - q)^2] \quad . \end{aligned} \tag{3.1.32}$$

(Note that even though the third-order moments about their means are zero, the combined distribution is asymmetric about its mean, and hence the third-order moment is non-zero.)

$$\mu_{l_1}^4 = \langle (x_1 - l_1)^4 \rangle_{l_1}$$

$$= f_W \mu_W^4 + (1 - f_W)\mu_T^4 + 6 f_W (1 - f_W)(d-q)^2 \, [(1 - f_W)^2 \omega_W^2 + f_W^2 r^2/4]$$

$$+ f_W (1 - f_W)[(1 - f_W)^3 + f_W^3](d - q)^4 \quad . \tag{3.1.33}$$

3.1.4 *Width* ω_{l_1} *of Target Distribution Function*

The distribution function $\rho_{l_1}(x_1)$ is the contribution of the target end of the flight path to the energy resolution function. The width of this distribution function is given by the square root of Eq. (3.1.31). Tabulated values of $\omega_{l_1} = \sqrt{\omega_{l_1}^2}$ are given as a function of energy in Table 2.

Table 2. The width of the energy resolution function ω_E and its uncertainty $\Delta\omega_E$ are given as a function of energy. In addition, the contribution of ω_l to ω_E is given, as well as the components ω_{l_1} and ω_{l_3} of ω_l. All energy widths and uncertainties are in eV, and length widths and uncertainties are in mm. All uncertainties are one standard deviation. The contribution of ω_t to ω_E is energy independent and not given in the table. ($\omega_t \pm \Delta\omega_t = 3.21 \pm 0.21$ ns.) See Sect. 3.4.5 for a discussion of why $\Delta\omega_l < \Delta\omega_{l_1}$.

E	ω_E	ω_E/E	$\Delta\omega_E$	ω_l	$\Delta\omega_l$	ω_{l_1}	$\Delta\omega_{l_1}$	ω_{l_3}	$\Delta\omega_{l_3}$
10.000	0.001	1.025E−04	0.000	10.321	0.815	9.143	0.914	4.788	0.191
1000.000	0.120	1.198E−04	0.010	11.983	1.009	10.984	1.098	4.790	0.191
2000.000	0.253	1.267E−04	0.021	12.613	1.081	11.665	1.166	4.796	0.191
5000.000	0.693	1.385E−04	0.058	13.599	1.188	12.718	1.268	4.815	0.193
10000.000	1.501	1.501E−04	0.121	14.462	1.277	13.627	1.353	4.844	0.196
20000.000	3.305	1.653E−04	0.253	15.429	1.365	14.631	1.438	4.896	0.201
50000.000	9.716	1.943E−04	0.655	16.893	1.482	16.132	1.550	5.015	0.213
100000.000	22.749	2.275E−04	1.395	18.153	1.625	17.411	1.693	5.136	0.227
200000.000	54.817	2.741E−04	3.328	19.263	1.992	18.532	2.069	5.256	0.242
300000.000	92.245	3.075E−04	5.857	19.300	2.432	18.549	2.530	5.332	0.252
400000.000	133.381	3.335E−04	8.889	18.594	2.933	17.808	3.062	5.350	0.255
700000.000	276.447	3.949E−04	18.736	14.596	3.936	13.560	4.236	5.403	0.262
1000000.000	452.296	4.523E−04	29.330	10.922	3.403	9.478	3.918	5.428	0.266
2000000.000	1250.421	6.252E−04	81.587	7.302	0.710	4.850	1.024	5.459	0.270
5000000.000	4922.198	9.844E−04	323.789	7.151	0.628	4.600	0.920	5.475	0.273
10000000.000	13903.978	1.390E−03	916.989	7.154	0.628	4.600	0.920	5.479	0.273
20000000.000	39300.716	1.965E−03	2595.324	7.155	0.628	4.600	0.920	5.480	0.274

3.1.5 *Uncertainty on* ω_{l_1}

Eventually we wish to determine the uncertainty associated with the energy resolution function. For this it is necessary to determine the uncertainty on ω_{l_1}, which is found by first evaluating the square of the uncertainty on $\omega_{l_1}^2$, or $(\Delta\omega_{l_1}^2)^2$. The uncertainty $\Delta\omega_{l_1}$ will then be expressed in terms of $(\Delta\omega_{l_1}^2)^2$.

Our procedure is the same as that used to evaluate $(\Delta I_1)^2$ in Sect. 3.1.2. A small increment on $\omega_{l_1}^2$ can be written as

$$\delta\omega_{l_1}^2 = \frac{\partial\omega_{l_1}^2}{\partial f_W}\,\delta f_W + \frac{\partial\omega_{l_1}^2}{\partial\omega_W}\,\delta\omega_W + \frac{\partial\omega_{l_1}^2}{\partial d}\,\delta d + \frac{\partial\omega_{l_1}^2}{\partial r}\,\delta r + \frac{\partial\omega_{l_1}^2}{\partial W}\,\delta W + \frac{\partial\omega_{l_1}^2}{\partial s}\,\delta s + \frac{\partial\omega_{l_1}^2}{\partial Z}\,\delta Z \quad . \tag{3.1.34}$$

If the partial derivatives in Eq. (3.1.34) are evaluated directly from Eq. (3.1.31) (remembering that $q = W/2 + s + Z$) and Eq. (3.1.15) is used for δf_W, then $\delta\omega_{l_1}^2$ becomes

$$\delta\omega_{l_1}^2 = [\omega_W^2 + (1 - 2f_W)(d - q)^2 - r^2/4]\left[f_W^2\,\frac{E\,\ln 3}{2E_m^2}\,e^{\frac{E\,\ln 3}{E_m}}\right]\delta E_m + 2f_W\omega_W\delta\omega_W + 2f_W(1 - f_W)(d - q)[\delta d - \delta s - \delta Z - \delta W/2] + (1 - f_W)r\delta r/2 \quad . \tag{3.1.35}$$

Forming the product $<\delta\omega_{l_1}^2\delta\omega_{l_1}^2> = (\Delta\omega_{l_1}^2)^2$ and assuming all parameters are uncorrelated give

$$(\Delta\omega_{l_1}^2)^2 = [\omega_W^2 + (1 - 2f_W)(d - q)^2 - r^2/4]^2\left[f_W^2\,\frac{E\,\ln 3}{2E_m}\,e^{\frac{E\,\ln 3}{E_m}}\right]^2\Delta E_m^2 + (2f_W\omega_W\Delta\omega_W)^2 + ((1 - f_W)r\frac{\Delta r}{2})^2 + [2f_W(1 - f_W)(d - q)]^2\,[\Delta d^2 + \Delta s^2 + \Delta Z^2 + \Delta W^2/4] \quad . \tag{3.1.36}$$

To convert from this expression to an uncertainty on ω_{l_1}, we note that

$$\delta\omega_{l_1}^2 = 2\omega_{l_1}\delta\omega_{l_1} \tag{3.1.37}$$

which gives $(\Delta\omega_{l_1})^2$ as

$$(\Delta\omega_{l_1})^2 = <\delta\omega_{l_1}\delta\omega_{l_1}> = \frac{1}{4\omega_{l_1}^2}<\delta\omega_{l_1}^2\delta\omega_{l_1}^2> \tag{3.1.38}$$

or

$$\Delta\omega_{l_1} = \frac{1}{2\omega_{l_1}}\Delta\omega_{l_1}^2 \quad . \tag{3.1.39}$$

Thus, the uncertainty on ω_{l_1} is evaluated using Eq. (3.1.39) with the square root of Eq. (3.1.36) for $\Delta\omega_{l_1}^2$ and the square root of Eq. (3.1.31) for ω_{l_1}. We assume $(\Delta\omega_W)/(\omega_W) = 10\%$. Values of ω_{l_1} and $\Delta\omega_{l_1}$ are tabulated in Table 2.

This completes derivation of the mean flight-path length from the target end [Eq. (3.1.13)], its uncertainty [Eq. (3.1.17)], the width of the distribution [Eq. (3.1.31)], and the uncertainty on the width [Eq. (3.1.39)]. We note that these quantities are all functions of neutron energy.

3.2 DISTRIBUTION FUNCTION FOR x_2: THE CONTRIBUTION TO THE FLIGHT-PATH LENGTH FROM THE FLIGHT TUBE

We now evaluate the second component of the flight-path length, l_2, measured from the face of the target to the face of the detector. The distance from the center of the neutron-producing target to the east benchmark in the 200-m station was measured to be (preliminary value) 201858.6 ± 4.0 mm (LA84). However, since the target flight-path length l_1 is measured from the front face of the target, we subtract one-half of the tantalum target thickness W, 18.3 mm, which gives 201840.3 ± 4.0 mm. The distance from the benchmark to the front face of the NE110 detector was measured to be 400 ± 3 mm, giving a mean value of the flight-path length from the front face of the target to the face of the detector $l_2 \pm \Delta l_2 = 201440 \pm 5$ mm.

No distribution is associated with this component of the flight-path length; i.e., $\omega_{l_2}^2 = 0$. Equivalently, we may say that the distribution function is a δ-function:

$$\rho_{l_2}(x_2) = \delta(x_2 - l_2) \quad . \tag{3.2.1}$$

(We note, however, that if the target vibrates back and forth, and we developed a physical model for this phenomenon described by a distribution function $\rho_{l_2}(x_2)$, $\omega_{l_2}^2$ would not be zero. However, we neglect such phenomena in this study.) The mean of this distribution is

$$<x_2>_{l_2} = l_2 \quad , \tag{3.2.2}$$

which has uncertainty Δl_2. Higher moments about the mean vanish, since

$$<(x_2 - l_2)^m>_{l_2} = \int \delta(x_2 - l_2)(x_2 - l_2)^m \, dx_2 = 0 \quad . \tag{3.2.3}$$

Explicitly, the second, third, and fourth moments are

$$\omega_{l_2}^2 = 0 \quad , \tag{3.2.4}$$

$$\nu_{l_2}^3 = 0 \quad , \tag{3.2.5}$$

and

$$\mu_{l_2}^4 = 0 \quad . \tag{3.2.6}$$

3.3 DISTRIBUTION FUNCTION FOR x_3: THE CONTRIBUTION TO THE FLIGHT-PATH LENGTH FROM THE DETECTOR

The final contribution to the flight-path length is from the 19-mm-thick NE110 detector. Since the transmission of neutrons through the detector ranges from 9% at 10 keV (2.4 mfp thick) to 82% at 10 MeV (0.2 mfp thick), the effective flight-path length of the neutrons in the detector is a function of energy. The low-energy neutrons will interact in the first few millimeters of the detector, while the high-energy neutrons will interact, on the average, near the center. To estimate the flight-path length in the detector as a function of neutron energy, we calculate the mean-path length l_3 before the first scattering. This assumes that we detect light from both hydrogen and carbon first-collision recoils in the NE110. The neutron distribution in the detector should be calculated using Monte Carlo techniques to account for multiple scattering effects, but for this work we choose the simpler "distance to first collision" approximation.

We represent the neutron distribution in the detector by

$$\rho_{l_3}(x_3) = \begin{cases} Ae^{-\lambda\sigma x_3} & \text{for } 0 \leqslant x_3 \leqslant L \\ 0 & \text{otherwise} \end{cases} \tag{3.3.1}$$

where $\lambda = 0.0047$, the number of molecules per mm·b of NE110 ($CH_{1.104}$), $\sigma(E)$ is the total cross section of $CH_{1.104}$, with numerical values calculated from ENDF/B-V (EN79), and L is the average thickness of the NE110 scintillator, taken as 19 mm. The normalization A is found by setting

$$\int_0^L \rho_{l_3}(x_3)dx_3 = 1 \quad , \tag{3.3.2}$$

giving

$$A = \frac{\lambda\sigma}{1 - e^{-\lambda\sigma L}} \quad . \tag{3.3.3}$$

3.3.1 *Mean Value l_3 for Distribution of x_3*

We can write the mean distance to the first collision as

$$\langle x_3 \rangle_{l_3} = A\int_0^L x_3 e^{-\lambda\sigma x_3} dx_3 \quad , \tag{3.3.4}$$

which gives

$$l_3 = \langle x_3 \rangle_{l_3} = \frac{1}{\lambda\sigma} + \frac{L}{1 - e^{\lambda\sigma L}} \quad . \tag{3.3.5}$$

This contribution to the flight-path length is given in Table 1.

3.3.2 *Uncertainty in l_3*

We now calculate the uncertainty on l_3. Taking small increments gives

$$\delta l_3 = \frac{\partial l_3}{\partial \lambda}\,\delta\lambda + \frac{\partial l_3}{\partial \sigma}\,\delta\sigma + \frac{\partial l_3}{\partial L}\,\delta L \quad , \tag{3.3.6}$$

which, after evaluating derivatives, becomes

$$\delta l_3 = \left[-\frac{1}{\lambda^2\sigma} + \frac{\sigma L^2 e^{\lambda\sigma L}}{(1 - e^{\lambda\sigma L})^2} \right] \delta\lambda + \left[-\frac{1}{\lambda\sigma^2} + \frac{\lambda L^2 e^{\lambda\sigma L}}{(1 - e^{\lambda\sigma L})^2} \right] \delta\sigma$$
$$+ \left[\frac{1}{1 - e^{\lambda\sigma L}} + \frac{\lambda\sigma L e^{\lambda\sigma L}}{(1 - e^{\lambda\sigma L})^2} \right] \delta L \quad . \tag{3.3.7}$$

Forming the product $<\delta l_3 \delta l_3> \equiv \Delta l_3^2$ and assuming $<\delta\lambda\delta\sigma> = <\delta\sigma\delta L> = <\delta\lambda\delta L> = 0$, we obtain

$$\Delta l_3 = \left\{ \left[-\frac{1}{\lambda^2\sigma^2 L^2} + \frac{e^{\lambda\sigma L}}{(1 - e^{\lambda\sigma L})^2} \right]^2 \left[\left(\frac{\Delta\lambda}{\lambda} \right)^2 + \left(\frac{\Delta\sigma}{\sigma} \right)^2 \right] \right.$$
$$\left. + \left[\frac{1}{\lambda\sigma L(1 - e^{\lambda\sigma L})} + \frac{e^{\lambda\sigma L}}{(1 - e^{\lambda\sigma L})^2} \right]^2 \left(\frac{\Delta L}{L} \right)^2 \right\}^{1/2} \lambda\sigma L^2 \tag{3.3.8}$$

for the uncertainty on l_3.

We assume uncertainties of $\Delta\lambda/\lambda = 2\%$, $\Delta\sigma/\sigma = 5\%$, and $\Delta L/L = 5\%$. Results for Δl_3 are given in Table 1.

3.3.3 *Higher Moments of the Detector Distribution Function*

We will also need the higher moments of x_3, and we present those results here for future convenience. In general,

$$<(x_3 - l_3)^m>_{l_3} = \frac{\int_0^L (x_3 - l_3)^m \, e^{-\lambda\sigma x_3} dx_3}{\int_0^L e^{-\lambda\sigma x_3} dx_3} \quad , \tag{3.3.9}$$

so that after considerable algebra we find

$$\omega_{l_3}^2 = <(x_3 - l_3)^2>_{l_3} = \frac{1}{(\lambda\sigma)^2} - \frac{L^2 e^{\lambda\sigma L}}{(1 - e^{\lambda\sigma L})^2} \quad , \tag{3.3.10}$$

$$\nu_{l_3}^3 = <(x_3 - l_3)^3>_{l_3} = \frac{2}{(\lambda\sigma)^3} + \frac{L^3 e^{\lambda\sigma L}(1 - e^{\lambda\sigma L})}{(1 - e^{\lambda\sigma L})^3} \quad , \tag{3.3.11}$$

and

$$\mu_{l_3}^4 = \frac{9}{(\lambda\sigma)^4} - \frac{6L^2 e^{\lambda\sigma L}}{(\lambda\sigma)^2(1 - e^{\lambda\sigma L})^2} - \frac{L^4 e^{\lambda\sigma L}\,(1 + e^{\lambda\sigma L} + e^{2\lambda\sigma L})}{(1 - e^{\lambda\sigma L})^4} \quad . \tag{3.3.12}$$

3.3.4 *Width ω_{l_3} of Detector Distribution Function*

The variance of the distribution function for x_3 is given by Eq. (3.3.10) and is identified with the contribution to the energy resolution function from the detector. Values of the width of the distribution $\omega_{l_3} = \sqrt{\omega_{l_3}^2}$ are given in Table 2 as a function of neutron energy.

3.3.5 *Uncertainty on ω_{l_3}*

The uncertainty on $\omega_{l_3}^2$ is found from

$$\delta\omega_{l_3}^2 = \frac{\partial\omega_{l_3}^2}{\partial\lambda}\,\delta\lambda + \frac{\partial\omega_{l_3}^2}{\partial\sigma}\,\delta\sigma + \frac{\partial\omega_{l_3}^2}{\partial L}\,\delta L \quad , \tag{3.3.13}$$

where the partial derivatives may be evaluated from Eq. (3.3.10),

$$\begin{aligned} \delta\omega_{l_3}^2 = {} & L\left\{ - \frac{2}{\lambda\sigma L} + \frac{1 + e^{\lambda\sigma L}}{1 - e^{\lambda\sigma L}} \right\} \omega_{l_3}^2 \left[\sigma\delta\lambda + \lambda\delta\sigma \right] \\ & + \lambda\sigma\left\{ \frac{2}{\lambda\sigma L} + \frac{1 + e^{\lambda\sigma L}}{1 - e^{\lambda\sigma L}} \right\} \omega_{l_3}^2 \delta L \quad . \end{aligned} \tag{3.3.14}$$

Thus the squared uncertainty on $\omega_{l_3}^2$ is

$$\begin{aligned} (\Delta\omega_{l_3}^2)^2 & = \langle \delta\omega_{l_3}^2 \; \delta\omega_{l_3}^2 \rangle \\ & = (\omega_{l_3}^2)^2 \left[\left\{ - \frac{2}{\lambda\sigma L} + \frac{1 + e^{\lambda\sigma L}}{1 - e^{\lambda\sigma L}} \right\}^2 \left[L^2\sigma^2(\Delta\lambda)^2 + L^2\lambda^2(\Delta\sigma)^2 \right] \right. \\ & \left. + \left\{ \frac{2}{\lambda\sigma L} + \frac{1 + e^{\lambda\sigma L}}{1 - e^{\lambda\sigma L}} \right\}^2 \lambda^2\sigma^2(\Delta L)^2 \right] \quad . \end{aligned} \tag{3.3.15}$$

To convert to the uncertainty on ω_{l_3}, recall that

$$\Delta\omega_{l_3} = \frac{1}{2\omega_{l_3}} \Delta\omega_{l_3}^2 \quad , \tag{3.3.16}$$

in analogy with Eq. (3.1.39). Thus, the uncertainty on the width ω_{l_3} is given by

$$\begin{aligned}\Delta\omega_{l_3} = \frac{\lambda\sigma L}{2} \Bigg[\left\{ -\frac{2}{\lambda\sigma L} + \frac{1 + e^{\lambda\sigma L}}{1 - e^{\lambda\sigma L}} \right\} \left\{ \left(\frac{\Delta\lambda}{\lambda} \right)^2 + \left(\frac{\Delta\sigma}{\sigma} \right)^2 \right\} \\ + \left\{ \frac{2}{\lambda\sigma L} + \frac{1 + e^{\lambda\sigma L}}{1 - e^{\lambda\sigma L}} \right\} \left\{ \left(\frac{\Delta L}{L} \right)^2 \right\} \Bigg]^{1/2} \quad .\end{aligned} \tag{3.3.17}$$

Values for $\Delta\omega_{l_3}$ are given in Table 2 as a function of neutron energy. This completes the derivation of the mean flight path length in the detector [Eq. (3.3.5)] and its uncertainty [Eq. (3.3.8)], and the width of the distribution [Eq. (3.3.10)] and its uncertainty [Eq. (3.3.17)]. We note that these quantities are all energy dependent.

3.4 DISTRIBUTION FUNCTION FOR x: THE TOTAL FLIGHT-PATH LENGTH

We now have the necessary results which allow us to calculate the distribution function for the total flight-path length x. Since x is the sum of x_1, x_2, and x_3, the distribution function for x is

$$\rho_l(x) = \int \rho_{l_1}(x_1)dx_1 \int \rho_{l_2}(x_2)dx_2 \int \rho_{l_3}(x_3)dx_3 \; \delta((x_1 + x_2 + x_3) - x) \quad , \tag{3.4.1}$$

where $\delta(\cdot)$ is the Dirac delta function. By using Eqs. (3.1.2), (3.2.1), and (3.3.1), this expression could be explicitly evaluated to give $\rho_l(x)$ in terms of the parameters of the target (d, W, s, Z, and f_W), the flight tube (l_2), and the detector (λ, σ, and L). However, for this study we will not determine the combined distribution function directly, but will be satisfied with the moments of the distribution.

3.4.1 Mean Value l for Distribution of x

The mean value for the distribution function given in Eq. (3.4.1) is

$$
\begin{aligned}
l = \langle x\rangle_l = & \int \rho_l(x)xdx \\
= & \int \rho_{l_1}(x_1)dx_1 \int \rho_{l_2}(x_2)dx_2 \int \rho_{l_3}(x_3)dx_3 \int xdx\delta((x_1 + x_2 + x_3) - x) \\
= & \int \rho_{l_1}(x_1)dx_1 \int \rho_{l_2}(x_2)dx_2 \int \rho_{l_3}(x_3)dx_3(x_1 + x_2 + x_3) \\
= & \int \rho_{l_1}(x_1)x_1dx_1 \int \rho_{l_2}(x_2)dx_2 \int \rho_{l_3}(x_3)dx_3 \\
+ & \int \rho_{l_1}(x_1)dx_1 \int \rho_{l_2}(x_2)x_2dx_2 \int \rho_{l_3}(x_3)dx_3 \\
+ & \int \rho_{l_1}(x_1)dx_1 \int \rho_{l_1}(x_2)dx_2 \int \rho_{l_3}(x_3)x_3dx_3 \\
= & \langle x_1\rangle_{l_1} + \langle x_2\rangle_{l_2} + \langle x_3\rangle_{l_3} \\
= & l_1 + l_2 + l_3 \quad .
\end{aligned} \tag{3.4.2}
$$

The final step in Eq. (3.4.2) results from substituting Eq. (3.1.12), (3.2.2), and (3.3.5) for the three individual mean values. Note that the total flight-path length l is energy dependent; i.e.,

$$
l(E) = l_1(E) + l_2 + l_3(E) \quad , \tag{3.4.3}
$$

or, substituting explicit results from Eqs. (3.1.13) and (3.3.5),

$$
l = (d - \frac{W}{2} - s - Z)f_W + \frac{W}{2} + s + Z + l_2 + \frac{1}{\lambda\sigma} + \frac{L}{1 - e^{\lambda\sigma L}} \quad . \tag{3.4.4}
$$

3.4.2 *Uncertainty in l*

A small increment in l can be written in terms of small increments in l_1, l_2, and l_3 as

$$
\delta l = \delta l_1 + \delta l_2 + \delta l_3 \quad , \tag{3.4.5}
$$

so that

$$
(\Delta l)^2 = \langle\delta l\delta l\rangle = \langle(\delta l_1 + \delta l_2 + \delta l_3)^2\rangle \quad . \tag{3.4.6}
$$

Since l_1, l_2. and l_3 are independent, the cross terms (e.g.,$<\delta l_1 \delta l_2>$) in Eq. (3.4.6) vanish, yielding for the uncertainty in l:

$$\Delta l = [\Delta l_1^2 + \Delta l_2^2 + \Delta l_3^2]^{1/2} \quad . \tag{3.4.7}$$

where Δl_1 and Δl_3 are evaluated from Eqs. (3.1.17) and (3.3.8) respectively, and Δl_2 is taken from the measurement process for l_2. The total flight-path length and its uncertainty $l \pm \Delta l$ are given in Table 1. We see that there is about a 20-mm variation in the effective flight-path length as a function of energy, and this is larger than the uncertainty at any energy. Figure 5 shows a plot of $l_1 + l_3$ as a function of neutron energy.

3.4.3 *Higher Moments of the Flight-Path Length Distribution Function*

In evaluating $<x>_l$ in the previous subsection, we explicitly displayed each step of the process, for clarity's sake. In evaluating the higher moments, those steps shall be implicitly understood. Details are given in Appendix A.

The second moment about the mean is given by

$$\omega_l^2 = <(x - l)^2>_l = \omega_{l_1}^2 + \omega_{l_2}^2 + \omega_{l_3}^2 = \omega_{l_1}^2 + \omega_{l_3}^2 \quad \text{since} \quad \omega_{l_2}^2 = 0 \quad . \tag{3.4.8}$$

The third moment becomes

$$\nu_l^3 = \nu_{l_1}^3 + \nu_{l_2}^3 + \nu_{l_3}^3 = \nu_{l_1}^3 + \nu_{l_3}^3 \quad \text{since} \quad \nu_{l_2}^3 = 0 \quad . \tag{3.4.9}$$

Finally, the fourth moment is given by

$$\begin{aligned} \mu_{l_1}^4 &= \mu_{l_1}^4 + \mu_{l_2}^4 + \mu_{l_3}^4 + 6(\omega_{l_1}^2\omega_{l_2}^2 + \omega_{l_1}^2\omega_{l_3}^2 + \omega_{l_2}^2\omega_{l_3}^2) \\ &= \mu_{l_1}^4 + \mu_{l_3}^4 + 6(\omega_{l_1}^2\omega_{l_3}^2) \quad \text{since} \quad \mu_{l_2}^4 = \omega_{l_2}^2 = 0 \quad . \end{aligned} \tag{3.4.10}$$

3.4.4 *Width ω_l of Flight-Path Length Distribution Function*

The width ω_l of the distribution function for the total flight-path length is given in Eq. (3.4.8), with values for ω_{l_1} and ω_{l_3} taken from Sects. 3.1 and 3.3 respectively. Values of ω_l as a function of energy are shown in Table 2.

ORNL-DWG 84-8209

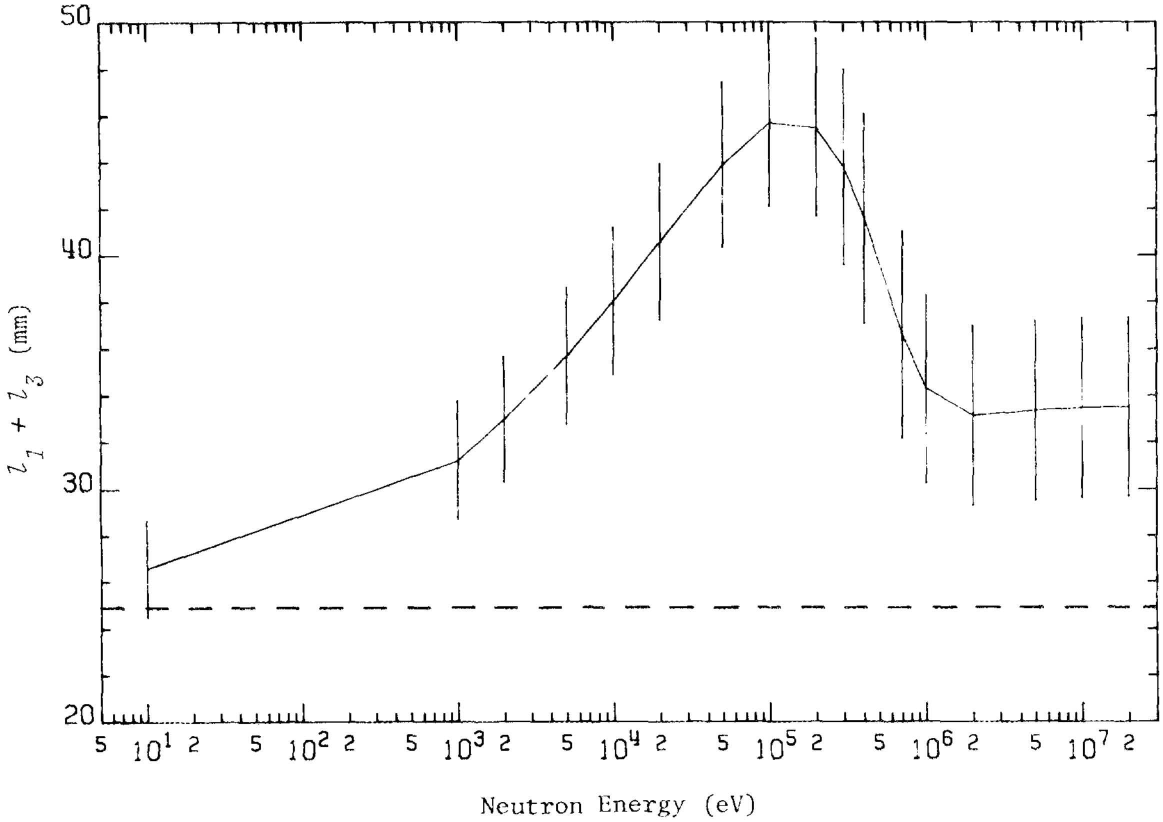

Fig. 5. This figure illustrates the energy dependence of the mean flight-path length as a function of neutron energy. The energy-independent length l_2 was not included; only the sum $l_1 + l_3$ (and its uncertainty) is shown. We note there is approximately a 20-mm difference in the mean effective flight-path length as a function of neutron energy. Simply adding the measured distance from the center of the Ta target to its face, 18.3 mm, and (arbitrarily) one-third of the detector thickness, 6.3 mm, would give a length of 24.6 mm (shown as dashed line), significantly different from the results found in this report.

3.4.5 *Uncertainty on* ω_l

The uncertainty on ω_l is found by using Eqs. (3.1.36) and (3.3.15) and Eq. (3.4.8), which gives

$$(\Delta\omega_l^2)^2 = (\Delta\omega_{l_1}^2)^2 + (\Delta\omega_{l_3}^2)^2 \quad . \tag{3.4.11}$$

The uncertainty $\Delta\omega_l$ is then given by

$$\Delta\omega_l = \frac{1}{2\omega_l} \Delta\omega_l^2 \quad . \tag{3.4.12}$$

Values for this uncertainty are shown in Table 2. We note that although the uncertainties on $\omega_{l_1}^2$ and $\omega_{l_3}^2$ combine quadratically to give $\Delta\omega_l^2$, this is *not* true for the uncertainties on ω_{l_1} and ω_{l_2}. $\Delta\omega_l$ must be obtained using results from Eq. (3.4.12). This is illustrated in Table 2, where $\Delta\omega_l$ is observed to be smaller than $\Delta\omega_{l_1}$, a somewhat surprising result.

4. PROPERTIES ASSOCIATED WITH THE FLIGHT TIME

In order to calculate the neutron energy, we must have information about the flight time as well as the flight-path length. In this section we describe how the neutron flight times are determined. Figure 2 illustrates the various times defined below. For each burst, the time digitizer (clock) is started with a signal from a bare phototube viewing the gamma flash produced when the electron beam strikes the target. t_0'' is the time for the signal to travel from the phototube to the clock. The gamma flash reaches the detector at time l/c, where l is the length of the flight path and c is the speed of light. The gamma-flash signal then leaves the detector and at time t_0' later is stored in channel C_γ (at time t_γ) in the data-acquisition computer. Thus

$$\frac{l}{c} + (t_0' - t_0'') = t_\gamma \quad . \tag{4.1}$$

Properties of t_0' and t_0'' need not be developed since we are only interested in the relative time $t_0' - t_0''$, so we define a time parameter t_0 as

$$t_0 \equiv t_0' - t_0'' \quad ,$$

or

$$t_0 = t_\gamma - \frac{l}{c} \quad . \tag{4.2}$$

Thus t_0 is related to the time to process a signal from the detector to the computer and is a constant for a given experiment. To get the flight time t associated with a neutron-induced event, we subtract t_0 from the time t_n the event is observed at the computer. That is,

$$t = t_n - t_0 \tag{4.3}$$

This time t_n can be identified with the difference in the means of two distributions: (1) t_1, the mean time at which the neutrons are born, and (2) t_2, the mean time at which the neutron is registered in the data-taking computer at channel c_n. That is,

$$t_n = t_2 - t_1 \tag{4.4}$$

The mean flight time is then given by

$$t = (t_2 - t_1) - t_0 \quad . \tag{4.5}$$

The first component, t_1, is associated with the pulse width of the ORELA beam and may be described approximately by a Gaussian distribution. The second component represents the finite channel width of the data-acquisition program and is approximated by a square distribution.

4.1 DISTRIBUTION FUNCTION FOR t_1: THE ORELA PULSE WIDTH

The ORELA pulse width may be approximated by a Gaussian shape (for pulse widths <10 ns) whose standard deviation is a. For the nickel measurement, the FWHM of the gamma flash pulse width was 7.5 ± 0.5 ns, corresponding to a = 3.2 ± 0.2 ns. The distribution may be written as

$$\rho_{t_1}(\tau_1) = \frac{1}{a\sqrt{2\pi}} e^{-\frac{\tau_1^2}{2a^2}} \quad . \tag{4.1.1}$$

4.1.1 *Mean Value t_1 for Distribution of τ_1*

The mean value for the distribution in Eq. (4.1.1) is

$$t_1 = \langle\tau_1\rangle_{t_1} = \int \tau_1 \rho_{t_1}(\tau_1) d\tau_1 = 0 \quad . \tag{4.1.2}$$

4.1.2 *Uncertainty in t_1*

The uncertainty in t_1 is simply the accuracy with which t_1 can be determined experimentally, which we will call Δt_1. A more complete description is given in Sect. 4.3.2.

4.1.3 *Higher Moments of the Pulse Width Distribution Function*

The variance and other moments of the Gaussian distribution about the mean (= 0 for this case) in Eq. (4.1.1) are given by

$$\omega_{t_1}^2 = a^2 \quad , \tag{4.1.3}$$

$$\nu_{t_1}^3 = 0 \quad , \tag{4.1.4}$$

$$\mu_{t_1}^4 = 3a^4 \quad . \tag{4.1.5}$$

4.1.4 *Width ω_{t_1} of Pulse Width Distribution Function*

The width, ω_{t_1}, of the pulse is given by the square root of the variance, or

$$\omega_{t_1} = a \quad . \tag{4.1.6}$$

This width is identified with the contribution to the energy resolution function from the neutron burst width.

4.1.5 *Uncertainty on ω_{t_1}*

The uncertainty on this width reflects the accuracy with which a can be determined experimentally; that is

$$\Delta\omega_{t_1} = \Delta a = 0.2 \text{ ns} \quad . \tag{4.1.7}$$

4.2 DISTRIBUTION FUNCTION FOR t_2: THE CHANNEL WIDTH

Neutrons are accumulated in the data acquisition computer in channels of width b (typically 1 ns). Since the time distributions which enter in this work (e.g., ω_{t_1}) are large compared with b, this section will be important only if wide channel widths (>10 ns) are used. It is included here for completeness. This square distribution may be written as

$$\rho_{t_2}(\tau_2) = \begin{cases} 1/b \text{ for } -b/2 \leqslant \tau_2 - t_2 \leqslant b/2 \\ 0 \text{ otherwise.} \end{cases} \tag{4.2.1}$$

4.2.1 *Mean Value t_2 for Distribution of τ_2*

The 1-ns-wide channels are probably not square distributions in fact, but trapezoidal or even triangular. However, for wide channels where this section is important, a square distribution is a good approximation. The mean of this distribution is

$$<\tau_2>_{t_2} = \frac{1}{b} \int_{t_2-b/2}^{t_2+b/2} \tau_2 d\tau_2 = t_2 \quad . \tag{4.2.2}$$

4.2.2 *Uncertainty in t_2*

The uncertainty Δt_2 reflects the accuracy with which the value t_2 can be determined experimentally. See Sect. 4.3.2 for a more complete description.

4.2.3 *Higher Moments of the Channel Width Distribution Function*

The second moment about the mean (i.e., the variance) for the channel width distribution is given by

$$\omega_{t_2}^2 = <(\tau_2 - t_2)^2> = \frac{1}{b} \int_{t_2-b/2}^{t_2+b/2} (\tau_2 - t_2)^2 d\tau_2 = \frac{b^2}{12} \quad . \tag{4.2.3}$$

Similarly the third moment is equal to

$$\nu_{t_2}^3 = 0 \quad , \tag{4.2.4}$$

and the fourth to

$$\mu_{t_2}^4 = b^4/80 \quad . \tag{4.2.5}$$

4.2.4 *Width ω_{t_2} of Channel Width Distribution Function*

The width (square root of variance) ω_{t_2} is given by the full width b of the square distribution divided by $\sqrt{12}$:

$$\omega_{t_2} = b/\sqrt{12} \quad . \tag{4.2.6}$$

This width is the contribution to the energy resolution function from the data-acquisition channel width.

4.2.5 *Uncertainty on ω_{t_2}*

The uncertainty on the width ω_{t_2} is simply

$$\Delta\omega_{t_2} = \Delta b/\sqrt{12} \quad , \tag{4.2.7}$$

where Δb was estimated by accumulating ~100,000 cts/channel from a random source and looking for deviations from the statistical uncertainty. From this we estimate $\Delta b/b = 0.3\%$.

4.3 DISTRIBUTION FUNCTION FOR τ: THE TOTAL FLIGHT TIME

The mean flight time $t = t_n - t_0$ (where $t_n = t_2 - t_1$) is given by the difference between the mean time t_2 at which the neutron is registered by the data-acquisition system and the mean time t_1 at which the neutron left the source, minus the time t_0 to transfer and process the signal. Thus, the t-o-f distribution is the convolution of the Gaussian and the square distributions. That is, the distribution function for τ is

$$\rho_t(\tau) = \int \rho_{t_1}(\tau_1)d\tau_1 \int \rho_{t_2}(\tau_2)d\tau_2 \; \delta((\tau_2 - \tau_1 - t_0) - \tau) \quad , \tag{4.3.1}$$

where ρ_{t_1} and ρ_{t_2} are given in Eqs. (4.1.1) and (4.2.1) respectively.

4.3.1 *Mean Value t for Distribution of τ*

The mean value t for the distribution given in Eq. (4.3.1) is

$$t = <\tau>_t = \int_{-\infty}^{\infty} d\tau_1 \rho_{t_1}(\tau_1) \int_{t_2-b/2}^{t_2+b/2} d\tau_2 \rho_{t_2}(\tau_2)(\tau_2 - \tau_1 - t_0) \tag{4.3.2}$$

$$= t_2 - t_1 - t_0 = t_n - t_0 \quad . \tag{4.3.3}$$

4.3.2 *Uncertainty in t*

The uncertainty in the flight time is given by

$$\delta t = \delta<\tau_2 - \tau_1 - t_0> = \delta t_n - \delta t_0 = \delta(t_n - t_0) \quad , \tag{4.3.4}$$

so that

$$(\Delta t)^2 = \Delta^2(\tau_2 - \tau_1 - t_0) = <\delta(t_n - t_0)^2> \quad . \tag{4.3.5}$$

To evaluate these terms, we consider the possibility of a scale error in both t_n and t_0 and an absolute error in t_0. Thus

$$t_n \rightarrow t_n g \quad \text{and} \quad t_0 \rightarrow t_0 g \quad , \tag{4.3.6}$$

with $<g> = 1$, so that

$$\delta t_n = t_n \delta g \quad \text{and} \quad \delta t_0 = t_0 \delta g + g \delta t_0 \quad , \tag{4.3.7}$$

or

$$\delta(t_n - t_0) = (t_n - t_0)\delta g - g\delta t_0 \quad . \tag{4.3.8}$$

Squaring and taking expectation values gives

$$(\Delta t)^2 = \Delta(t_n - t_0)^2 = (t_n - t_0)^2\Delta g^2 + \Delta t_0^2 = t^2\Delta g^2 + \Delta t_0^2 \quad . \tag{4.3.9}$$

The standard deviation of the uncertainty in t_0, Δt_0, is estimated to be 0.3 ns, based on comparison of the gamma flash centroids in the four bias spectra (LA83).

The scale uncertainty Δg may be identified with uncertainties in the timing clock oscillator. Such uncertainties have been measured for the ORELA clocks and are found to be less than 1 part in 50,000, i.e., $\Delta g = 2 \times 10^{-5}$.

4.3.3 *Higher Moments of the Total Flight-Time Distribution Function*

We shall define ω_t^2, ν_t^3, and μ_t^4 as the second, third, and fourth moments about the mean, respectively, of the flight-time distribution function. These moments are given by

$$\begin{aligned} <(\tau - t)^m>_t &= \int (\tau - t)^m \rho_t(\tau) d\tau \\ &= \int \rho_{t_1}(\tau_1)d\tau_1 \int \rho_{t_2}(\tau_2)d\tau_2 \, ((\tau_2 - \tau_1 - t_0) - t)^m \quad , \end{aligned} \tag{4.3.10}$$

in which we have used Eq. (4.3.1) to replace the integral over τ by the double integrals over τ_1 and τ_2 and to replace τ by $\tau_2 - \tau_1 - t_0$. Since t is equal to $t_2 - t_1 - t_0$ and t_1 is zero, Eq. (4.3.10) can be written in the form

$$<(\tau - t)^m>_t = \int \rho_{t_1}(\tau_1)d\tau_1 \int \rho_{t_2}(\tau_2)d\tau_2((\tau_2 - t_2) - \tau_1)^m \quad . \tag{4.3.11}$$

Thus the variance ω_t^2 becomes

$$\omega_t^2 = <(\tau - t)^2>_t = \omega_{t_2}^2 + \omega_{t_1}^2 = \frac{b^2}{12} + a^2 \quad , \tag{4.3.12}$$

where we have used results from Eqs. (4.1.3) and (4.2.3) for values of $\omega_{t_2}^2$ and $\omega_{t_1}^2$.

Similarly, the third moment is

$$\nu_t^3 = <(\tau - t)^3>_t = \nu_{t_2}^3 - 3\omega_{t_2}^2<\tau_2>_{t_1} + 3\omega_{t_1}^2<\tau_2 - t_2>_{t_2} - \nu_{t_1}^3 = \nu_{t_2}^3 - \nu_{t_1}^3 \quad . \tag{4.3.13}$$

Each of the two terms $\nu_{t_2}^3$ and $\nu_{t_1}^3$ are zero [see Eqs. (4.2.4) and (4.1.4)] by virtue of the symmetry of the square and Gaussian distributions. Thus, we have

$$\nu_t^3 = 0 \quad . \tag{4.3.14}$$

The fourth moment is

$$\mu_t^4 = \langle(\tau - t)^4\rangle_t = \mu_{t_2}^4 - 4\nu_{t_2}^3\langle\tau_1\rangle_{t_1} + 6\omega_t t_2{}^2\omega_{t_1}^2 - 4\nu_{t_1}^3\langle\tau_2 - t\rangle_{t_2} + \mu_{t_1}^4 \quad , \tag{4.3.15}$$

or, again using the value zero for $\nu_{t_2}^3$ and $\nu_{t_1}^3$,

$$\mu_t^4 = \mu_{t_2}^4 + 6\omega_{t_2}^2\omega_{t_1}^2 + \mu_{t_1}^4 \quad . \tag{4.3.16}$$

Substituting values found in Sect. 4.1 and 4.2, we find

$$\mu_t^4 = b^4/80 + 6(b^2/12)(a^2) + 3a^4 \quad . \tag{4.3.17}$$

In Sect. 5 we shall require expectation values of powers of $1/\tau$. These are evaluated in Appendix B in terms of the quantities ω_t^2, ν_t^3, and μ_t^4 whose values we have just derived.

4.3.4 *Width ω_t of Total Flight-Time Distribution Function*

The width ω_t of the *time*-resolution function is the square root of the variance ω_t^2 given in Eq. (4.3.12), or

$$\omega_t = \sqrt{b^2/12 + a^2} \quad . \tag{4.3.18}$$

4.3.5 *Uncertainty on ω_t*

The uncertainty $\Delta\omega_t$ may be found directly from Eq. (4.3.18)

$$\Delta\omega_t = (b\Delta b/12 + a\Delta a)\,\frac{1}{\omega_t} \quad . \tag{4.3.19}$$

5. PROPERTIES OF THE ENERGY SCALE AND THE RESOLUTION FUNCTION

We now focus our attention on two objects of ultimate interest - the energy scale and the associated energy resolution function. Work done in the preceding two sections can be viewed as prologue, laying the framework for this section.

5.1 DISTRIBUTION FUNCTION OF ϵ: THE ENERGY SCALE

The (non-relativistic) energy ϵ can be written in terms of the time-of-flight length x and travel time τ as

$$\epsilon = \frac{m}{2}\left(\frac{x}{\tau}\right)^2 \quad , \tag{5.1.1}$$

where m is the neutron mass. The distribution function for the energy can therefore be written

$$\rho(\epsilon) = \int \rho_t(\tau)d\tau \int \rho_l(x)dx \;\delta\left(\epsilon - \frac{m}{2}\left(\frac{x}{\tau}\right)^2\right) \quad , \tag{5.1.2}$$

where the time and length distribution functions are given in Eqs. (4.3.1) and (3.4.1) respectively. We do not explicitly evaluate this expression for $\rho(\epsilon)$, but calcuate the first and second moments of the distribution.

5.1.1 *Mean Value E for Distribution of ϵ*

The mean energy E is found from Eq. (5.1.2) as

$$E = \langle\epsilon\rangle = \int \epsilon\rho(\epsilon)d\epsilon = \int \rho_t(\tau)d\tau \int \rho_l(x)dx\frac{m}{2}\left(\frac{x}{\tau}\right)^2 \quad . \tag{5.1.3}$$

This expression can be divided naturally into the product form

$$E = \frac{m}{2}\langle\tau^{-2}\rangle_t\langle x^2\rangle_l \quad , \tag{5.1.4}$$

where

$$<\tau^{-2}>_t = \int \tau^{-2} \rho_t(\tau) d\tau \quad , \tag{5.1.5}$$

and

$$<x^2>_l = \int x^2 \rho_l(x) dx \quad . \tag{5.1.6}$$

In Appendix A we show that the second moment about the origin is equal to the variance plus the square of the mean; thus Eq. (5.1.6) becomes

$$<x^2>_l = \omega_l^2 + l^2 \quad , \tag{5.1.7}$$

where values of ω_l^2 and l^2 are given in Sect. 3.

In Appendix B we show that the expression in Eq. (5.1.5) may be expanded about t to give the approximate value

$$<\tau^{-2}>_t \simeq t^{-2} \left(1 + 3\omega_t^2 t^{-2} + 5\mu_t^4 t^{-4} \right) \quad , \tag{5.1.8}$$

where values for the second and fourth moments about the mean ω_t^2 and μ_t^4 are given in Sect. 4.

Substituting Eqs. (5.1.7) and (5.1.8) into (5.1.4) gives

$$E \simeq E_0(l + \omega_l^2/l^2)(1 + 3\omega_t^2 t^{-2} + 5\mu_t^4 t^{-4}) \quad , \tag{5.1.9}$$

where we have set

$$E_o = \frac{m}{2} \frac{l^2}{t^2} \quad . \tag{5.1.10}$$

Thus, in addition to the usual term E_0 for the mean energy, we have correction factors which depend on the variances (and higher moments) of the distributions in length and time. We can estimate the magnitude of these correction terms from results previously determined. Values for l and ω_l as a function of energy are given in Tables 1 and 2. At $E_0 = 300$ keV, we see that

$$\frac{\omega_l^2}{l^2} \simeq 1.0 \times 10^{-8} \quad . \tag{5.1.11}$$

Likewise, using $\omega_t^2 = a^2 + b^2/12$ gives

$$3\omega_t^2/t^2 \simeq 4.1 \times 10^{-8} \quad , \tag{5.1.12}$$

and a far smaller number for the μ_t^4 term. Therefore, these corrections can be neglected, and the mean energy is well approximated by

$$E \simeq E_0 = \frac{m}{2}\left(\frac{l}{t}\right)^2 \quad . \tag{5.1.13}$$

5.1.2 *Uncertainty in E*

We can now evaluate the uncertainty on the mean energy. Taking small increments gives

$$\delta E = \frac{\partial E}{\partial l}\,\delta l + \frac{\partial E}{\partial t}\,\delta t \quad . \tag{5.1.14}$$

Evaluation of the derivatives, using the approximation in Eq. (5.1.13), gives

$$\delta E = 2E_0\left(\frac{\delta l}{l} - \frac{\delta t}{t}\right) \quad . \tag{5.1.15}$$

Forming the product $<\delta E\,\delta E> \equiv \Delta E^2$, we find

$$\Delta E = 2E_0\left[\left(\frac{\Delta l}{l}\right)^2 + \left(\frac{\Delta t}{t}\right)^2\right]^{1/2} \quad , \tag{5.1.16}$$

where Δl^2 is obtained from Table 1 as a function of energy by squaring the standard deviation, and Δt^2 was evaluated in Sect. 4.3.2. Table 1 contains the energy uncertainty as a function of energy.

5.1.3 *Higher Moments of the Energy Distribution Function*

We shall evaluate only the second moment of the energy distribution function, since higher moments are not needed. The second moment (the variance) is given by

$$\omega_E^2 = <(\epsilon - E)^2> = <\epsilon^2> - E^2 \quad , \tag{5.1.17}$$

where $<\epsilon^2>$, the second moment about the origin, is given by

$$<\epsilon^2> = \int \epsilon^2 \rho(\epsilon) d\epsilon = (m/2)^2 <\tau^{-4}>_t <x^4>_l \quad . \tag{5.1.18}$$

In Appendix A (Eq. A.9), the fourth moment about the origin $<x^4>_l$ is shown to be given by

$$<x^4>_l = \mu_l^4 + 4\nu_l^3 l + 6\omega_l^2 l^2 + l^4 \quad . \tag{5.1.19}$$

Values for μ_l^4, ν_l^3, and ω_l^2 are given in Sect. 3.4 and in Table 3.

Table 3. The second, third, and fourth moments of the flight-path length distribution function.

E (eV)	ω_l^2 (mm^2)	ν_l^3 (mm^3)	μ_l^4 (mm^4)
10.	106.52	89.77	12944.99
1000.	143.59	90.29	18053.78
2000.	159.08	92.99	20232.67
5000.	184.94	108.80	23968.89
10000.	209.15	150.46	27696.27
20000.	238.05	266.91	32714.38
50000.	285.38	755.24	43905.53
100000.	329.54	1818.09	59994.09
200000.	371.08	4328.43	82187.19
300000.	372.50	6593.78	87614.68
400000.	345.74	7971.24	77657.39
700000.	213.06	6729.15	25648.56
1000000.	119.29	3378.89	4965.63
2000000.	53.32	159.46	5741.62
5000000.	51.13	15.25	6307.69
10000000.	51.18	10.81	6142.88
20000000.	51.19	9.97	6187.93

In Appendix B we show that the inverse fourth moment of the time distribution is approximately

$$<\tau^{-4}>_t \simeq t^{-4}\ (1 + 10\omega_t^2 t^{-2} + 35\mu_t^4 t^{-4}) \quad , \tag{5.1.20}$$

where the various moments are evaluated explicitly in Sect. 4, and where we have set $\nu_t^3 = 0$. Combining Eqs. (5.1.18) through (5.1.20) and keeping only terms of fourth order or less gives

$$\begin{aligned} <E^2> \simeq E_0^2\ (1 &+ 6\omega_l^2 l^{-2} + 4\nu_l^3 l^{-3} + \mu_l^4 l^{-4} \\ &+ 10\omega_t^2 t^{-2} + 35\mu_t^4 t^{-4} + 60\omega_l^2 l^{-2}\omega_t^2 t^{-2}) \quad . \end{aligned} \tag{5.1.21}$$

Similarly, squaring Eq. (5.1.9) and keeping only terms of fourth order or less gives

$$E^2 = <E>^2(1 + 2\omega_l^2 l^{-2} + \omega_l^4 l^{-4} + 6\omega_t^2 t^{-2} + 10\mu_t^4 t^{-4} + 9\omega_t^4 t^{-4} + 12\omega_l^2 l^{-2}\omega_t^2 t^{-2}). \tag{5.1.22}$$

Finally, substituting Eqs. (5.1.21) and (5.1.22) into (5.1.17) yields

$$\begin{aligned} \omega_E^2 \simeq E_0^2 \Big\{ & (2\omega_l l^{-1})^2 + (2\omega_t t^{-1})^2 + 3(2\omega_l l^{-1} 2\omega_t t^{-1})^2 \\ & + 4\nu_l^3 l^{-3} + (\mu_l^4 - \omega_l^4) l^{-4} + (25\mu_t^4 - 9\omega_t^4) t^{-4} \Big\} \end{aligned} \tag{5.1.23}$$

for the variance of our energy distribution function.

5.1.4 *Width ω_E of Energy Distribution Function: Identification with the Energy Resolution Function*

The energy distribution function given in Eq. (5.1.2) is precisely the energy resolution function by which experimental data are "broadened" and by which theoretical calculations must be "broadened" prior to comparison with experiments. The broadening width ω_E is given by the square root of the variance in Eq. (5.1.23). Note that the first two terms within the brackets correspond to the conventional expression for the width of the energy resolution function while the remaining terms are higher order corrections; i.e., to first order in powers of ω^2 we can write

$$\omega_E \simeq 2E_o \left\{ \left(\frac{\omega_l}{l} \right)^2 + \left(\frac{\omega_t}{t} \right)^2 \right\}^{1/2} \quad . \tag{5.1.24}$$

We note that this expression has the same form as Eq. (5.1.16) for the uncertainty in the mean energy. However, Δl and Δt in Eq. (5.1.16) are the uncertainties in the mean values of the length and time, while ω_l and ω_t in Eq. (5.1.24) are the standard deviations (widths) of the length and time distributions. It is clear that Δl and ω_l are completely different quantities (as are Δt and ω_t) as seen from the equations from which they are calculated.

Values for ω_E are given in Table 2. These values were generated from Eq. (5.1.23) rather than from the more severe approximation of Eq. (5.1.24).

5.1.5 *Uncertainty on* ω_E

To obtain an expression for the uncertainty on the width given by the square root of Eq. (5.1.23), we first note that a small increment of ω_E^2 can be written in the form

$$\delta(\omega_E^2) = q_1\delta(\omega_l^2) + q_2\delta(\omega_t^2) + q_3\delta l + q_4\delta t + [4l^{-3}\delta(\nu_l^3) + l^{-4}\delta(\mu_l^4) + 25t^{-4}\delta(\mu_t^4)]E_o^2 \quad . \tag{5.1.25}$$

We shall assume that the quantities within the square brackets in the preceding equation produce negligible effects; these terms will be dropped. Coefficients q_1, q_2, q_3, and q_4 in Eq. (5.1.25) can be evaluated directly by taking partial derivatives of Eq. (5.1.23):

$$q_1 = 4E_0^2l^{-2}(1 + 12\omega_t^2t^{-2} - \omega_l^2l^{-2}/2) \quad , \tag{5.1.26}$$

$$q_2 = 4E_0^2t^{-2}(1 + 12\omega_l^2l^{-2} - 9\omega_t^2t^{-2}/2) \quad , \tag{5.1.27}$$

$$q_3 = -2E_0^2l^{-1}(4\omega_l^2l^{-2} + 48\omega_l^2l^{-2}\omega_t^2t^{-2} + 6\nu_l^3l^{-3} + 2(\mu_l^4 - \omega_l^4)l^{-4}) + 4\omega_E^2l^{-1} \quad , \tag{5.1.28}$$

$$q_4 = -2E_0^2t^{-1}(4\omega_t^2t^{-2} + 48\omega_t^2t^{-2}\omega_l^2l^{-2} + 2(25\mu_t^4 - 9\omega_t^4)t^{-4}) - 4\omega_E^2t^{-1} \quad . \tag{5.1.29}$$

The square of the uncertainty in the variance is then given by squaring Eq. (5.1.25) and taking expectation values:

$$(\Delta(\omega_E^2))^2 = \langle(\delta(\omega_E^2))^2\rangle = q_1^2(\Delta(\omega_l^2))^2 + q_2^2((\Delta(\omega_t^2))^2 + q_3^2(\Delta l)^2 + q_4^2(\Delta t_0)^2 + 2q_1q_3\langle\delta\omega_l^2\delta l\rangle \quad . \tag{5.1.30}$$

Only the final term in Eq. (5.1.30) requires explanation. Since l and ω_l^2 are determined from the same set of parameters, the two are not independent. In Sect. 3 of this report we determined the partial derivatives of both ω_l^2 and l with respect to the ten independent parameters (f_W, d, W, s, Z, ω_W, r, λ, σ, L). Those partial derivatives may be used to evaluate

$$<\delta\omega_l^2 \delta l> = \sum_{i=1}^{10} \frac{\partial \omega_l^2}{\partial p_i} \left(\Delta p_i\right)^2 \frac{\partial l}{\partial p_i} \quad , \tag{5.1.31}$$

where $\{p\}$ represents those ten parameters. Note that the analogous term

$$2q_2q_4<\delta\omega_l^2 \delta t> \quad , \tag{5.1.32}$$

is zero here since ω_l^2 depends only on parameters a and b and not on t_0 or g. Values of $\Delta\omega_E$ are given in Table 2.

5.2 COMPARISON OF THE RESOLUTION FUNCTION WITH EXPERIMENT

To facilitate comparison of our calculated results with an experimental determination of the resolution function, we use the relation

$$E \simeq (72.3 l/t)^2 \quad , \tag{5.2.1}$$

with l in mm, t in ns, and E in ev, to rewrite Eq. (5.1.23) as

$$\begin{aligned} \omega_E^2 &= E_0^2 \left\{ (2\omega_l l^{-1})^2 + (2\omega_t t^{-1})^2 + \ldots \right\} \\ &\simeq E_0^2 \left\{ (2\omega_l l^{-1})^2 + (2\omega_t l^{-1}/72.3)^2 E \right\} \quad , \end{aligned} \tag{5.2.2}$$

or

$$(\omega_E/E)^2 \simeq b_1 + b_2 E \quad , \tag{5.2.3}$$

where $b_1 = (2\omega_l/l)^2$ and $b_2 = (2\omega_t/72.3\ l)^2$.

Since ω_l and l are energy dependent, $(\omega_E/E)^2$ is a non-linear function of energy. However, the energy dependence of l is weak enough that b_2 is essentially independent of energy. Table 4 presents results for the parameters b_1 and b_2 and their uncertainties and ω_E^2 as a function of energy.

Table 4. Values of b_1 and b_2 as a function of energy. Experimental values for the energy range 50 to 500 keV are $b_1 = (3.25 \pm 0.72) \times 10^{-8}$ and $b_2 = (1.75 \pm 0.18) \times 10^{-13}$, which are assumed to be independent of energy.

E (eV)	ω_E^2 (eV^2)	b_1	Δb_1	b_2 (1/eV)	Δb_2 (1/eV)	b_1+b_2E	$\Delta(b_1+b_2E)$	$(\omega_E/E)^2$
10.	1.050E−06	1.050E−08	1.657E−09	1.928E−13	2.550E−14	1.050E−08	1.657E−09	1.050E−08
1000.	1.434E−02	1.415E−08	2.384E−09	1.928E−13	2.550E−14	1.434E−08	2.384E−09	1.434E−08
2000.	6.425E−02	1.568E−08	2.686E−09	1.928E−13	2.550E−14	1.606E−08	2.686E−09	1.606E−08
5000.	4.797E−01	1.822E−08	3.185E−09	1.928E−13	2.550E−14	1.919E−08	3.187E−09	1.919E−08
10000.	2.254E+00	2.061E−08	3.638E−09	1.928E−13	2.550E−14	2.254E−08	3.647E−09	2.254E−08
20000.	1.092E+01	2.346E−08	4.151E−09	1.928E−13	2.550E−14	2.731E−08	4.182E−09	2.731E−08
50000.	9.440E+01	2.812E−08	4.932E−09	1.928E−13	2.550E−14	3.776E−08	5.094E−09	3.776E−08
100000.	5.175E+02	3.247E−08	5.812E−09	1.928E−13	2.550E−14	5.175E−08	6.347E−09	5.175E−08
200000.	3.005E+03	3.656E−08	7.560E−09	1.928E−13	2.550E−14	7.512E−08	9.119E−09	7.512E−08
300000.	8.509E+03	3.670E−08	9.251E−09	1.928E−13	2.550E−14	9.454E−08	1.200E−08	9.455E−08
400000.	1.779E+04	3.407E−08	1.075E−08	1.928E−13	2.550E−14	1.112E−07	1.482E−08	1.112E−07
700000.	7.642E+04	2.099E−08	1.132E−08	1.928E−13	2.550E−14	1.560E−07	2.114E−08	1.560E−07
1000000.	2.046E+05	1.176E−08	7.325E−09	1.928E−13	2.550E−14	2.046E−07	2.653E−08	2.046E−07
2000000.	1.564E+06	5.254E−09	1.021E−09	1.928E−13	2.550E−14	3.909E−07	5.101E−08	3.909E−07
5000000.	2.423E+07	5.039E−09	8.845E−10	1.928E−13	2.550E−14	9.691E−07	1.275E−07	9.691E−07
10000000.	1.933E+08	5.044E−09	8.848E−10	1.928E−13	2.550E−14	1.933E−06	2.550E−07	1.933E−06
20000000.	1.545E+09	5.045E−09	8.849E−10	1.928E−13	2.550E−14	3.861E−06	5.100E−07	3.861E−06

Johnson, Kernohan, and Winters (JO83) have analyzed isolated narrow resonances with a single-level R-function code, using a Gaussian resolution function, to obtain values of b_1 and b_2 (or equivalently, ω_l and ω_t). The argon transmission measurement on which their analysis is based was performed immediately following our nickel measurement and utilized the same experimental setup. Based on the analysis of 13 resonances from 50 to 500 keV, they obtained values of $b_1 = (3.25 \pm 0.72) \times 10^{-8}$ and $b_2 = (1.75 \pm 0.18) \times 10^{-13}$. Averaging our values of b_1 and b_2 from Table 4 from 50 to 400 keV, we obtain $b_1 = (3.36 \pm 0.77) \times 10^{-8}$ and $b_2 = (1.93 \pm 0.26) \times 10^{-13}$, both values being consistent with their results.

5.3 COMPUTER PROGRAM FLIP1

The computer program FLIP1 was designed to evaluate the various expectation values, variances, higher moments, and uncertainties described in Sects. 3, 4, and 5 of this report. The code is organized in a manner similar to this report: quantities for the individual components of flight-path length are generated first, in subroutines TAH20X (for the tantalum water target, Sect. 3.1 of this report) and DETECT (for the detector end, Sect. 3.3), and the total mean flight-path length l (with other moments and uncertainties) is produced from those individual results in subroutine COMBIN (Sect. 3.4). Quantities for the individual components of time are generated and combined in subroutine TIME (Sect. 4). The energy and its uncertainty and the energy resolution width and its uncertainty are generated from the length and time components in subroutine ENERGY (Sect. 5).

Additional subroutines are included to (1) produce plots of the distribution functions $\rho_{l_1}(x_1)$ (subroutine PLOT, Sect. 3.1) and $\rho_{l_3}(x_3)$ (subroutine PLTDET, Sect. 3.3), and (2) output both the input parameter values and values of the generated quantities. Tables 1 through 4 of this report were generated in subroutine DSPLAY.

No attempt has been made to cast this code into user-friendly format with convenient methods of changing parameter values, since the code is not expected to be used for a series of production runs. However, by isolating each component of length into a separate subroutine, we expect to have facilitated the substitution of more accurate distribution functions, for example.

Appendix C contains a listing of FLIP1; one of the output files produced by the code is given in Appendix D.

6. SUMMARY AND CONCLUSIONS

With the goal of developing expressions for the mean neutron energy and its uncertainty and the energy resolution function and its uncertainty, we have developed approximate analytic forms for the necessary distribution functions from which the desired quantities can be determined. The distribution functions for the neutrons which come from the Ta target and surrounding water moderator and the distribution function for neutrons which interact in the NE110 detector were found to be dependent on the neutron energy. From these results we obtained expressions for the mean energy-dependent flight-path length and its uncertainty and found as much as a 20-mm difference in the mean effective flight-path length, due to the energy dependence. This difference is much larger than the uncertainty in the flight-path length at any energy. From the distribution functions we also calculated the contribution to the width of the energy resolution function from the components of the flight-path length and the uncertainty on the width as functions of energy.

We then developed distribution functions for the t-o-f, i.e., expressions for the neutron burst width and the data-acquisition channel width. From these we evaluated the mean t-o-f and its associated uncertainty. We also evaluated the contribution to the width of the energy resolution function from the time distribution functions and the associated uncertainty.

Having developed the above information for the length and time distributions, we then used those results to develop an expression for the energy distribution function $\rho(\epsilon)$. From this expression, we found the mean neutron energy and its uncertainty. In addition to the conventional energy term [Eq. (5.1.10)], our expression for the mean energy contains small correction terms associated with the widths of the length and time distributions. Neglecting the small corrections to the conventional expression for the neutron energy, the expression for the energy uncertainty is the conventional expression [Eq. (5.1.16)], with the usual dependence on the uncertainties Δl and Δt.

We identified the second moment of the energy distribution function about the mean as the width of the energy resolution function, but did not evaluate the expression [Eq. (5.1.2)] for the energy distribution function itself. (Evaluation of that expression would provide the shape of the resolution function.) Comparing our result for the width of the resolution function with that determined from measurement, we find agreement well within the uncertainty.

A number of aspects of this report could be studied in more detail. It is clear to us that we have used too simple a treatment of the neutrons emerging from the Ta target. Multiple scattering and attenuation within the Ta produce an asymmetric tail to $\rho_T(x_1)$, and in addition the process is energy dependent. The Ta target neutron emission should properly be ascertained by Monte Carlo calculations, similar to the treatment in CO83 for neutrons from the water moderator. Ideally, Monte Carlo calculations should be done for the complete (Ta + H_2O) target at one time. Proper treatment of the Ta would increase the value of $\omega_{l_1}^2$, the contribution to the width of the energy resolution function from the source end, and thus increase the width ω_E of the energy resolution function. However, it would probably not have a significant effect on the mean path length l_1. A correct treatment of the Ta would simply modify $\rho_T(x_1)$ to $\rho_T(x_1,E)$ and change its shape, but the formalism we have developed to propagate ρ_T would be unaffected.

When a proper treatment of the Ta becomes available, it would be worthwhile attempting to evaluate the integral for the energy distribution (i.e., resolution) function [Eq. (5.1.2)]. The resulting shape could then be parameterized and used as the resolution function in the computer code SAMMY (LA80) for analysis of resonance parameters. Again, the framework for the t-o-f energy and energy resolution function, and their uncertainties, which we have developed would still be valid, although requiring some modification to SAMMY.

One small point should be noted regarding the treatment of the NE110 detector. The face of the detector which matches onto the phototube is curved to match the phototube face. Thus the thickness L of the detector is not a constant 19 mm, but has about a 15% variation in thickness across its face which should be accounted for in the description of the distribution function for the detector [Eq. (3.3.1)]. Also, a Monte Carlo treatment of neutrons in the NE110 would be more correct than our "distance to first collision" approximation; however, these effects are not expected to change the results significantly.

In discussion of resolution functions, references are often made to a correction for broadening due to "electronics." We have not included such a term because our method of identifying ω_{t_1} (Sect. 4.1) with the observed width of the gamma flash automatically includes effects of the incident electron burst width, broadening due to electronics, time dependence of the electron energy during a pulse due to depletion of stored energy in the accelerator cavity, and any contribution to the resolution due to the bremsstrahlung process.

ACKNOWLEDGEMENTS

We wish to thank Francis Perey for useful discussions regarding the uncertainty analysis component of this work, Cleland Johnson for providing the results of the resolution function analysis of their argon data, and Sue Damewood for a careful typing of this report. This work is an extension of work described in report ORNL/TM-8203, and was partially sponsored by the Division of Reactor Research and Technology of the Department of Energy.

REFERENCES

CO83 C. Coceva, R. Simonini, and D. K. Olsen, "Calculation of the ORELA Neutron Moderator Spectrum and Resolution Function," *Nucl. Inst. Meth.* **211**, 459 (1983).

EN79 ENDF/B Summary Documentation, BNL-NCS-17541 (ENDF-201), 3rd ed. (ENDF/B-V), ed. R. Kinsey, available from the National Nuclear Data Center, Brookhaven National Laboratory, Upton, N. Y.)July 1979).

HA69 Engineering Drawing No. EA-023-D, "Flight Tube as-built, Data Sheet No. 2," September 1969, J. A. Harvey files. This drawing contains measurements from the center of the target room (which is also assumed to be the target center) to various benchmarks in the flight stations.

HA75 J. A. Harvey and N. W. Hill, "Comparison of the Neutron Intensity, Energy Resolution, and Backgrounds of an Unmoderated Tantalum Target, a Light-Water-Moderated Tantalum Target, and a Beryllium Target at the ORELA," p. 169 in *ORNL Physics Division 1974 Annual Report*, ORNL-5025 (May 1975).

JO83 C. H. Johnson, J. C. Kernohan, and R. R. Winters, "Resolution Function at 200 Meters for January 1981," informal note circulated at ORELA (January 1981).

LA80 N. M. Larson and F. G. Perey, *User's Guide for SAMMY: A Computer Model for Multilevel R-Matrix Fits to Neutron Data Using Bayes' Equations,* ORNL/TM-7485, ENDF-297, Oak Ridge National Laboratory, Oak Ridge, Tenn. (November 1980).

LA83 D. C. Larson, N. M. Larson, J. A. Harvey, N. W. Hill, and C. H. Johnson, *Application of New Techniques to ORELA Neutron Transmission Measurements and Their Uncertainty Analysis: The Case of Natural Nickel From 2 keV to 20 MeV,* ORNL/TM-8203, ENDF-333, Oak Ridge National Laboratory, Oak Ridge, Tenn. (October 1983).

LA84 D. C. Larson, N. M. Larson, J. A. Harvey, and F. G. Perey, "Measurement of the 200, 80, and 18 m Flight Path Lengths and their Uncertainties," ORNL/TM-9097, in preparation.

LE70 T. A. Lewis, "Notes on Target Activation Study" done in 1970. Private communication, 1984.

APPENDIX A. MOMENTS OF DISTRIBUTION FUNCTIONS

In Sects. 3 and 4 of this report, we evaluated the first, second, third, and fourth moments about the mean of the length and time distribution functions, respectively. In this appendix we (1) relate the moments about the origin to the the moments about the mean; and (2) derive the moments of a combined distribution function. It is these moments about the origin of the combined distribution which enter into our determination of the resolution broadening function.

We begin by developing some notations. Let $\rho_\alpha(y)$ be an arbitrary distribution function for some variable y. This distribution function has a mean which we shall call Y_α and which is given by

$$Y_\alpha = <y>_\alpha = \int y \rho_\alpha(y) dy \quad . \tag{A.1}$$

The variance ω_α^2 for this distribution function is the "second moment about the mean," or

$$\omega_\alpha^2 = <(y - Y_\alpha)^2>_\alpha = <y^2>_\alpha - Y_\alpha^2 \quad , \tag{A.2}$$

where $<y^2>_\alpha$ is the "second moment about the origin," or

$$<y^2>_\alpha = \int y^2 \rho_\alpha(y) dy \quad . \tag{A.3}$$

In like manner the "third and fourth moments about the mean" are defined:

$$\nu_\alpha^3 = <(y - Y_\alpha)^3>_\alpha = \int (y - Y_\alpha)^3 \rho_\alpha(y) dy \tag{A.4}$$

and

$$\mu_\alpha^4 = <(y - Y_\alpha)^4>_\alpha = \int (y - Y_\alpha)^4 \rho_\alpha(y) dy \quad . \tag{A.5}$$

Expanding the integrand of Eq. (A.4) gives

$$\nu_\alpha^3 = <y^3>_\alpha - 3<y^2>_\alpha Y_\alpha + 2Y_\alpha^3 \tag{A.6}$$

or

$$<y^3>_\alpha = \nu_\alpha^3 + 3\omega_\alpha^2 Y_\alpha + Y_\alpha^3 \quad . \tag{A.7}$$

Similarly, Eq. (A.5) becomes

$$\mu_\alpha^4 = <y^4>_\alpha - 4<y^3>_\alpha Y_\alpha + 6<y^2>_\alpha Y_\alpha^2 - 3Y_\alpha^4 \tag{A.8}$$

or

$$<y^4>_\alpha = \mu_\alpha^4 + 4\nu_\alpha^3 Y_\alpha + 6\omega_\alpha^2 Y_\alpha^2 + Y_\alpha^4 \quad . \tag{A.9}$$

We now wish to convolute two arbitrary distributions to obtain moments of the combined distribution. For example, in Sect. 3.4 we set $x = x_1 + x_2 + x_3$; in Sect. 4.3 we set $t_n = t_2 - t_1$. Let us assume that we have $s = y \pm z$, where $\rho_\beta(z)$ is the distribution for variable z. The distribution function for s is then

$$\rho(s) = \int \rho_\alpha(y)dy \int \rho_\beta(z)dz\, \delta(s - (y \pm z)) \quad . \tag{A.10}$$

The mean of this distribution is

$$S = <s> = \int s\rho(s)ds = <y>_\alpha \pm <z>_\beta = Y \pm Z \quad . \tag{A.11}$$

The second moment about the mean is

$$\begin{aligned} \omega_s^2 &= <(s - S)^2> = \int \rho_\alpha(y)dy \int \rho_\beta(z)dz\ (((y \pm z) - (Y \pm Z))^2) \\ &= <(y - Y)^2>_\alpha \pm 2<y - Y>_\alpha <z - Z>_\beta + <(z - Z)^2>_\beta \\ &= \omega_\alpha^2 + \omega_\beta^2 \quad . \end{aligned} \tag{A.12}$$

Similarly the third moment is

$$\nu_s^3 = \nu_\alpha^3 \pm \nu_\beta^3 \quad , \tag{A.13}$$

and the fourth is

$$\mu_s^4 = \mu_\alpha^4 + 6\omega_\alpha^2\omega_\beta^2 + \mu_\beta^2 \quad . \tag{A.14}$$

APPENDIX B. EXPECTATION VALUES OF NEGATIVE POWERS OF τ

In Sect. 4.3 of this report we described the distribution function for the time of flight and evaluated the mean and variance of that distribution. In this appendix we derive approximate expressions for the expectation values of negative powers of τ. These approximations are needed to evaluate our expression for E as given in Sect. 5, which involves inverse powers of τ.

The fraction $1/\tau$ may be written in the form

$$\frac{1}{\tau} = \frac{1}{t} \quad \frac{1}{1 + y} \quad , \tag{B.1}$$

where y is given by

$$y = \frac{\tau - t}{t} \quad . \tag{B.2}$$

Thus the expectation value of τ^{-m} may be written as

$$\begin{aligned} <\tau^{-m}>_t &= \int \tau^{-m} \rho(\tau) d\tau \\ &= t^{-m} \int \rho_{t_1}(\tau_1) d\tau_1 \int \rho_{t_2}(\tau_2) d\tau_2 \left[1 + \frac{\tau_2 - \tau_1 - t_0 - t}{t} \right]^{-m} \quad , \end{aligned} \tag{B.3}$$

or, substituting $t = t_2 - t_1 - t_0$ into the numerator of the fraction, with $t_1 = 0$,

$$<\tau^{-m}>_t = t^{-m} \int \rho_{t_1}(\tau_1) d\tau_1 \int \rho_{t_2}(\tau_2) d\tau_2 \left[1 + \frac{(\tau_2 - t_2) - (\tau_1)}{t} \right]^{-m} \quad . \tag{B.4}$$

Since $\rho_{t_1}(\tau_1)$ is large only for small τ_1, and $\rho_{t_2}(\tau_2)$ is non-zero only for τ_2 near t_2, it is sufficient to replace $1/(1 + y)$ by a value which is correct only for small y. Note that by "y" we now mean

$$y = \frac{\tau_2 - t_2 - \tau_1}{t} \quad , \tag{B.5}$$

so that the fraction $1/(1 + y)$ becomes

$$\frac{1}{1 + y} \simeq 1 - y + y^2 - y^3 + y^4 \quad , \tag{B.6}$$

where terms higher than fourth order in y have been dropped. Squaring Eq. (B-6) gives

$$(1 + y)^{-2} \simeq 1 - 2y + 3y^2 - 4y^3 + 5y^4 \quad , \tag{B.7}$$

and squaring Eq. (B.7) gives

$$(1 + y)^{-4} \simeq 1 - 4y + 10y^2 - 20y^3 + 35y^4 \quad . \tag{B.8}$$

The expectation value of τ^{-k}, where k is 2 or 4, can then be found directly once the expectation values of the powers of y are known. From the definition of y, Eq. (B.2), we see that

$$<y^n>_t = <(\tau - t)^n>_t t^{-n} \quad , \tag{B.9}$$

so that

$$<\tau^{-2}> \simeq t^{-2}(1 - 0 + 3\omega_t^2 t^{-2} - 4\nu_t^3 t^{-3} + 5\mu_t^4 t^{-4}) \quad , \tag{B.10}$$

where the ν_t^3 term is retained for the sake of completeness; in this specific case ν_t^3 is zero. Values of ω_t^2 and μ_t^4 are given in Sect. 4. Similarly, we have

$$<\tau^{-4}> \simeq t^{-4}(1 - 0 + 10\omega_t^2 t^{-2} - 20\nu_t^3 t^{-3} + 35\mu_t^4 t^{-4}) \quad . \tag{B.11}$$

Finally, we note that

$$<\tau^{-2}>^2 \simeq t^{-4}(1 + 6\omega_t^2 t^{-2} - 8\nu_t^3 t^{-3} + 10\mu_t^4 t^{-4} + 9\omega_t^4 t^{-4}) \tag{B.12}$$

to fourth order in t^{-1}.

APPENDIX C. FORTRAN LISTING OF FLIP1

```
C
C       PURPOSE -- GENERATE MOMENTS OF ENERGY DISTRIBUTION
C                  BY COMBINING THE VARIOUS COMPONENTS OF
C                  LENGTH AND TIME
C
C       JANUARY, 1984
C
C *** INPUT      INTERNAL TO PROGRAM, NOT FROM EXTERNAL FILES
C *** OUTPUT     TAH2O.ODF  (FOR PLOTS OF ENERGY VS ENERGY-DEPENDENT
C ***                        QUANTITIES FOR WATER-TANTULUM TARGET)
C ***            XXXXXX.ODF (FOR PLOT OF DISTRIBUTION IN TARGET, AT E=XXXXXX)
C ***            XXXXXX.DET (FOR PLOT OF DISTRIBUTION IN DETECTOR)
C ***            FOR25.DAT (COMPLETE OUTPUT)
C ***            FOR26.DAT (DEBUG OUTPUT)
C ***            FOR27.DAT (SUMMARY OUTPUT, AS INCLUDED IN TM REPORT)
C ***
C ***
C *****************************************************************
C ***
C *** NOTATION USED IN VARIABLE NAMES
C ***
C ***   EL                              FLIGHT PATH LENGTH
C ***   ELL1,ELL2,ELL2                  THREE COMPONENTS OF FPL
C ***
C ***           1 (ONE)                 TARGET (TANTALUM + WATER)
C ***                                   WATER,WATR,WA REFER TO
C ***                                     WATER COMPONENT OF TARGET
C ***                                   TA REFERS TO TANTULUM PART
C ***                                     WITH PARAMETERS UUUUUU,
C ***                                     WWWWWW,SSSSSS,RRRRRR
C ***
C ***           2 (TWO)                 FLIGHT TUBE
C ***
C ***           3 (THREE)               DETECTOR END, WITH PARAMETERS
C ***                                     ALMBDA,THICKN,CROSSS
C ***
C ***
C ***   TIME OR TIM OR TI               "TOTAL" TIME
C ***
C ***           T1                      PULSE COMPONENT (BRST)
C ***           T2                      CHANNEL COMPONENT (CHNL)
C ***           TZERO                   T-SUB-ZERO
C ***
C ***
C ***   ENERGY, EN                      ENERGY
C ***
C ***
C ***   PREFIXES WITH SPECIAL MEANING
C ***
C ***   D.....                          UNCERTAINTY
C ***   D2....                          SQUARED UNCERTAINTY
C ***   W.....                          WIDTH
C ***   W2....                          SQUARED WIDTH (VARIANCE)
C ***   V3....                          THIRD MOMENT ABOUT MEAN
C ***   U4....                          FOURTH MOMENT ABOUT MEAN
```

```
C ***
C ***   D2W2..                                 SQUARED UNCERTAINTY ON
C ***                                            VARIANCE
C ***   DW2...                                 UNCERTAINTY ON VARIANCE
C ***   D2W...                                 SQUARED UNCERTAINTY ON
C ***                                            WIDTH
C ***   DW....                                 UNCERTAINTY ON WIDTH
C ***
C ***   PER...                                 PERCENT UNCERTAINTY
C ***   DEL...                                 DELTA ... (ABSOLUTE
C ***                                            UNCERTAINTY)
C ***
C ***   CV....                                 COVARIANCE TWEEN .. & ..
C ***
C ***
C ***   SUFFIXES
C ***   .....Z,....ZZ,...ZZZ,..ZZZZ            USED AS FILLER SO THERE
C ***                                            ARE ALWAYS SIX CHARACTERS
C ***
C ****************************************************************
C ***
C *** GENERAL NOTES
C ***
C ***   ALL DISTANCES ARE IN UNITS OF MILLIMETERS (MM)
C ***   ALL TIMES ARE IN NANOSECONDS (NS)
C ***   ALL ENERGIES ARE IN ELECTRON-VOLTS (EV)
C ***
C ****************************************************************
C
C
C
      COMMON /TOTAL/ ENZZZZ(17), FUDGEZ(17), DENZZZ(17),
     *     D2ENZZ(17), WENZZZ(17), W2ENZZ(17), DWENZZ(17),
     *     DW2ENZ(17), D2W2EN(17), WWEL2Z(17), WWTIM2(17),
     *     WWEL3Z(17), WWTIM3(17), WWELTI(17), WWEL4Z(17),
     *     WWTIM4(17), PW2W2L(17), PW2W2T(17), PW2LZZ(17),
     *     PW2TIM(17)
C
      COMMON /ELXXXX/ ELZZZZ(17), DLZZZZ(17), D2LZZZ(17),
     *     WLZZZZ(17), DWLZZZ(17), W2LZZZ(17), DW2LZZ(17),
     *     D2W2LZ(17), V3LZZZ(17), U4LZZZ(17), CVLW2Z(17)
C
      COMMON /ELL1XX/ DWAZZZ(17), WWAZZZ(17), FWAZZZ(17),
     *     FTNZZZ(17), ELL1ZZ(17), DL1ZZZ(17), D2L1ZZ(17),
     *     WL1ZZZ(17), DWL1ZZ(17), W2L1ZZ(17), DW2L1Z(17),
     *     D2W2L1(17), V3L1ZZ(17), U4L1ZZ(17), DFWAZZ(17),
     *     CVL1W2(17)
C
      COMMON /TAWATV/ PERDWA, PERWWA, WATER1, WATER2, WATER3,
     *     WWATR1, WWATR2, WWATR3, UUUUUU, WWWWWW, SSSSSS,
     *     DELUUU, DELWWW, DELSSS, RRRRRR, DELRRR, EMMMMM,
     *     PEREMM, ABSUNC
C
```

```
      COMMON /ELL3XX/ CROSSS(17), ELL3ZZ(17), DL3ZZZ(17),
     *     D2L3ZZ(17), WL3ZZZ(17), DWL3ZZ(17), W2L3ZZ(17),
     *     DW2L3Z(17), D2W2L3(17), V3L3ZZ(17), U4L3ZZ(17),
     *     CVL3W2(17)
      COMMON /DETECV/ ALMBDA, THICKN, PERLMB, PERTHI, PERCRO
C
      COMMON /TIMER/ TZEROZ, DTZERO, AFWHMZ, DAFWHM, BCHNLZ,
     *     DBCHNL, TSCALE
      COMMON /T1XXXX/ T1ZZZZ, DT1ZZZ, D2T1ZZ, WT1ZZZ, DWT1ZZ,
     *     W2T1ZZ, DW2T1Z, D2W2T1, V3T1ZZ, U4T1ZZ, CVT1W2
      COMMON /T2XXXX/ T2ZZZZ, DT2ZZZ, D2T2ZZ, WT2ZZZ, DWT2ZZ,
     *     W2T2ZZ, DW2T2Z, D2W2T2, V3T2ZZ, U4T2ZZ, CVT2W2
      COMMON /TIMEXX/ TIMEZZ(17), DTIMEZ(17), D2TIME(17),
     *     WTIMEZ, DWTIME, W2TIME, DW2TIM, D2W2TZ, V3TIME,
     *     U4TIME, CVTW2Z
C
      COMMON /ALLZZZ/ EEEEEE(17), ELL2ZZ, DL2ZZZ, SHORTZ,
     *     IEGRID, IPLOT
C
      LOGICAL SHORTZ
      DATA SHORTZ /.TRUE./
C
      DATA EEEEEE /10.0,1000.,2000.,5000.,10000.,20000.,50000.,
     *     100000.,200000.,300000.,400000.,700000.,1000000.,
     *     2000000.,5000000.,10000000.,20000000./
C
      DATA IEGRID /17/
      DATA IPLOT /3/
C
      CALL TAH2O
      CALL QQQTAH
      CALL DETECT
      CALL QQQDET
      CALL COMBIN
      CALL QQQCOM
      CALL OUTCMP
      CALL PLOT13
      CALL TIME
      CALL ENERGY
      CALL QQQTIM
      CALL QQQENE
      CALL DSPLAY
C
      STOP
      END
C
C
      SUBROUTINE TAH2O
C *** PURPOSE -- ORGANIZE TREATMENT OF TANTALUM-WATER TARGET
      CALL OUTTAH
      CALL TAH2OX
      CALL PLT
      RETURN
      END
```

```
      SUBROUTINE OUTTAH
C
C *** PURPOSE -- OUTPUT THE INPUT FOR TA-H2O CALCULATION
C
      COMMON /TAWATV/ PERDWA, PERWWA, WATER1, WATER2, WATER3,
     *     WWATR1, WWATR2, WWATR3, UUUUUU, WWWWWW, SSSSSS,
     *     DELUUU, DELWWW, DELSSS, RRRRRR, DELRRR, EMMMMM,
     *     PEREMM, ABSUNC
C
      COMMON /ALLZZZ/ EEEEEE(17), ELL2ZZ, DL2ZZZ, SHORTZ,
     *     IEGRID, IPLOT
      LOGICAL SHORTZ
C
      W2PLUS = 0.5*WWWWWW + SSSSSS
      UW2ZZZ = UUUUUU + W2PLUS
      RDELWW = DELWWW/WWWWWW*100.0
      RDELRR = DELRRR/RRRRRR*100.0
      RDELSS = DELSSS/SSSSSS*100.0
C
      WRITE (25,99999)
      WRITE (25,99998) UUUUUU, DELUUU
      WRITE (25,99997) WWWWWW
      WRITE (25,99996) DELWWW, RDELWW
      WRITE (25,99995) SSSSSS
      WRITE (25,99994) DELSSS, RDELSS
      WRITE (25,99993) UW2ZZZ
      WRITE (25,99992) RRRRRR
      WRITE (25,99991) DELRRR, RDELRR
      WRITE (25,99990) WATER1, WATER2, WATER3
      WRITE (25,99989) WWATR1, WWATR2, WWATR3
      WRITE (25,99988) PERDWA
      WRITE (25,99987) PERWWA
      WRITE (25,99986) ABSUNC
      WRITE (25,99985) EMMMMM
      WRITE (25,99984) PEREMM
      IF (SHORTZ) GO TO 10
C
      WRITE (5,99998) UUUUUU, DELUUU
      WRITE (5,99997) WWWWWW
      WRITE (5,99996) DELWWW, RDELWW
      WRITE (5,99995) SSSSSS
      WRITE (5,99994) DELSSS, RDELSS
      WRITE (5,99993) UW2ZZZ
      WRITE (5,99992) RRRRRR
      WRITE (5,99991) DELRRR, RDELRR
      WRITE (5,99990) WATER1, WATER2, WATER3
      WRITE (5,99989) WWATR1, WWATR2, WWATR3
      WRITE (5,99988) PERDWA
      WRITE (5,99987) PERWWA
      WRITE (5,99986) ABSUNC
      WRITE (5,99985) EMMMMM
      WRITE (5,99984) PEREMM
C
```

```
   10 CONTINUE
C
      WRITE (25,99983)
      IF (.NOT.SHORTZ) WRITE (5,99983)
C
      RETURN
99999 FORMAT (/25H ****** TARGET END ******)
99998 FORMAT (46H    UUU = DISTANCE TO SURFACE OF TA TARGET        ,
     *       15H               =, F7.3, 4H +/-, F7.3)
99997 FORMAT (46H    WWW = WIDTH OF TA TARGET                      ,
     *       15H               =, F7.3)
99996 FORMAT (46H DELWWW = ERROR ON WWW                            ,
     *       15H               =, F7.3, 2H =, F5.1, 8H PERCENT)
99995 FORMAT (46H    SSS = ESTIMATE OF MULTIPLE SCATTERING IN T,
     *       15HA TARGET       =, F7.3)
99994 FORMAT (46H DELSSS = ERROR ON SSS                            ,
     *       15H               =, F7.3, 2H =, F5.1, 8H PERCENT)
99993 FORMAT (46H    UW2 = UUU + WWW/2 + SSS = DISTANCE TO MEAN,
     *       15H OF TA TARGET =, F7.3)
99992 FORMAT (46H    RRR = RADIUS OF CIRCULAR DISTRIBUTION IN T,
     *       15HA TARGET       =, F7.3)
99991 FORMAT (46H DELRRR = ERROR ON RRRRRR                         ,
     *       15H               =, F7.3, 2H =, F5.1, 8H PERCENT)
99990 FORMAT (/44H DWA(E) =    MEAN OF DISTRIBUTION IN WATER =,
     *       F5.1, F6.2, 8H*LN(E) +, F6.3, 9H*LN(E)**2)
99989 FORMAT (44H WWA(E) = STD DEV OF DISTRIBUTION IN WATER =,
     *       F5.1, F6.2, 8H*LN(E) +, F6.3, 9H*LN(E)**2)
99988 FORMAT (44H PERDWA = UNCERTAINTY ON MEAN DWA (E)       =,
     *       F5.1, 8H PERCENT)
99987 FORMAT (44H PERWWA = UNCERTAINTY ON STD DEV WWA (E)    =,
     *       F5.1, 8H PERCENT)
99986 FORMAT (/45H ABSUNC = ABSOLUTE UNCERTAINTY ON FRACTION FR,
     *       20HOM TA AND FROM H2O =, F6.2)
99985 FORMAT (46H    EMM = ENERGY AT WHICH THE TWO FRACTIONS AR,
     *       19HE EQUAL           =, F9.0)
99984 FORMAT (46H PEREMM = RELATIVE UNCERTAINTY IN EMM = DEL(EM,
     *       19HM)/EMM            =, F6.1, 8H PERCENT///)
99983 FORMAT (46H                                    ERROR     DI,
     *       44HSTANCE   WIDTH                        WIDTH/
     *       49H                                     ON      TO ME,
     *       49HAN      OF     MEAN OF     UNCERT.    OF       UNCE,
     *       3HRT./43H  ENERGY      FRACTN      FRACTN      FRACTN    ,
     *       49H OF WATER   WATER   TA+WATER     ON      TA+WATER ,
     *       6H    ON/40H   (EV)        OF TA   OF WATER  OF WATE,
     *       49HR    DISTN      DISTN       DISTN      MEAN       DIST,
     *       11HN     WIDTH, //31H      EN          FTA         FWA   ,
     *       49H    DFWA       ELWATR      WWATR       ELL1       DL1   ,
     *       20H      WL1        DWL1)
      END
```

```
      SUBROUTINE TAH2OX
C
C *** PURPOSE -- GENERATE MOMENTS OF WATER-TANTALUM DISTRIBUTION
C
      COMMON /ELL1XX/ DWAZZZ(17), WWAZZZ(17), FWAZZZ(17),
     *     FTNZZZ(17), ELL1ZZ(17), DL1ZZZ(17), D2L1ZZ(17),
     *     WL1ZZZ(17), DWL1ZZ(17), W2L1ZZ(17), DW2L1Z(17),
     *     D2W2L1(17), V3L1ZZ(17), U4L1ZZ(17), DFWAZZ(17),
     *     CVL1W2(17)
C
      COMMON /TAWATV/ PERDWA, PERWWA, WATER1, WATER2, WATER3,
     *     WWATR1, WWATR2, WWATR3, UUUUUU, WWWWWW, SSSSSS,
     *     DELUUU, DELWWW, DELSSS, RRRRRR, DELRRR, EMMMMM,
     *     PEREMM, ABSUNC
C
      COMMON /ALLZZZ/ EEEEEE(17), ELL2ZZ, DL2ZZZ, SHORTZ,
     *     IEGRID, IPLOT
      LOGICAL SHORTZ
      DIMENSION IPP(17)
      DATA IPP /1,2,3,4,5,6,7,8,9,10,11,12,13,14,15,16,17/
C
      DATA WATER1 /22.8/, WATER2 /-1.60/, WATER3 /0.283/,
     *     WWATR1 /10.0/, WWATR2 /-0.63/, WWATR3 /0.112/,
     *     UUUUUU /0.0/, WWWWWW /36.6/, SSSSSS /6.0/, RRRRRR
     *     /9.20/, DELUUU /2.0/, DELWWW /5.492/, DELSSS /1.8/,
     *     DELRRR /1.840/, EMMMMM /300000./, PEREMM /30.0/,
     *     PERDWA /10.0/, PERWWA /10.0/
C
      W2PLUS = 0.5*WWWWWW + SSSSSS
      UW2ZZZ = UUUUUU + W2PLUS
      PERDWA = PERDWA*0.01
      PERWWA = PERWWA*0.01
      PEREMM = PEREMM*0.01
C
C
      IPL = 1
      DO 10 IE=1,IEGRID
C
C *** GENERATE FRACTION FROM TA AND FRACTION FROM H2O
            QQQQQQ = EEEEEE(IE)*ALOG(3.0)/EMMMMM
            EQQQQQ = EXP(QQQQQQ)
            FWAZZZ(IE) = 2.0/(1.0+EQQQQQ)
            FTNZZZ(IE) = 1.0 - FWAZZZ(IE)
            DFWAZZ(IE) = 0.5*FWAZZZ(IE)**2*EQQQQQ*QQQQQQ*PEREMM +
     *           ABSUNC
C
```

```
C *** DETERMINE PARAMETERS OF WATER DISTRIBUTION
          ELOG = ALOG(EEEEEE(IE))
          DWAZZZ(IE) = WATER1 + WATER2*ELOG + WATER3*ELOG**2
          WWAZZZ(IE) = WWATR1 + WWATR2*ELOG + WWATR3*ELOG**2
          ELWATR = DWAZZZ(IE)
          DLWATR = ELWATR*PERDWA
          W2WATR = WWAZZZ(IE)**2
          DW2WAT = 2.0*W2WATR*PERWWA
          V3WATR = 0.0
          U4WATR = 3.0*WWAZZZ(IE)**4
          FFWATR = FWAZZZ(IE)
          DFWATR = DFWAZZ(IE)
C
C *** DETERMINE PARAMETERS OF TANTALUM DISTRIBUTION
          ELTNTL = UUUUUU + WWWWWW/2.0 + SSSSSS
          D2LTNT = DELUUU**2 + DELWWW**2/4.0 + DELSSS**2
          DLTNTL = SQRT(D2LTNT)
          W2TNTL = RRRRRR**2/4.0
          DW2TNT = RRRRRR*DELRRR/2.0
          V3TNTL = 0.0
          U4TNTL = RRRRRR**4/8.0
          FFTNTL = FTNZZZ(IE)
C
C *** COMBINATION OF WATER AND TANTALUM
          FFWFFT = FFWATR*FFTNTL
          FTMNFW = FFTNTL - FFWATR
          ELWATN = ELWATR - ELTNTL
C
C *** GENERATE CONTRIBUTION TO ELL1, W2L1, V3L1, AND U4L1 FROM
C ***   WATER DISTRIBUTION
          ELL1ZZ(IE) = FFWATR*ELWATR
          W2L1ZZ(IE) = FFWATR*W2WATR
          V3L1ZZ(IE) = FFWATR*V3WATR
          U4L1ZZ(IE) = FFWATR*V4WATR
C
C *** GENERATE CONTRIBUTION FROM TANTALUM DISTRIBUTION
          ELL1ZZ(IE) = ELL1ZZ(IE) + FFTNTL*ELTNTL
          W2L1ZZ(IE) = W2L1ZZ(IE) + FFTNTL*W2TNTL
          V3L1ZZ(IE) = V3L1ZZ(IE) + FFTNTL*V3TNTL
          U4L1ZZ(IE) = U4L1ZZ(IE) + FFTNTL*U4TNTL
C
C *** GENERATE CONTRIBUTION FROM COMBINATION
          W2L1ZZ(IE) = W2L1ZZ(IE) + FFWFFT*ELWATN**2
          V3L1ZZ(IE) = V3L1ZZ(IE) + FFWFFT*ELWATN*
     *          ( 3.0*(W2WATR-W2TNTL) + FTMNFW*ELWATN**2 )
          U4L1ZZ(IE) = U4L1ZZ(IE) + FFWFFT*ELWATN**2*
     *          (FFTNTL*W2WATR+FTWATR*W2TNTL) +
     *          FFWFFT*(FFWATR**3-FFTNTL**3)*ELWATN**4
C
```

```
C *** NOW THE ASSOCIATED UNCERTAINTIES
            PLFWAT = ELWATN
            PLLWAT = FFWATR
            PLLTNT = FFTNTL
            PW2FWA = W2WATR - W2TNTL + FTMNFW*ELWATN**2
            PW2W2W = FFWATR
            PW2LWT = FFWFFT*2.0*ELWATN
            PW2W2T = FFTNTL
            D2L1ZZ(IE) = (PLFWAT*DFWATR)**2 + (PLLWAT*DLWATR)**2
     *           + (PLLTNT*DLTNTL)**2
            D2W2L1(IE) = (PW2FWA*DFWATR)**2 + (PW2W2W*DW2WAT)**2
     *           + (PW2W2T*DW2TNT)**2 +
     *           PW2LWT**2*(DLWATR**2+D2LTNT)
            CVL1W2(IE) = PLFWAT*PW2FWA*DFWATR**2 +
     *           PLLWAT*PW2LWT*DLWATR**2 - PLLTNT*PW2LWT*D2LTNT
C
C *** OBTAIN WIDTH (AND UNCERTAINTIES) FROM VARIANCE
            WL1ZZZ(IE) = SQRT(W2L1ZZ(IE))
            DL1ZZZ(IE) = SQRT(D2L1ZZ(IE))
            DW2L1Z(IE) = SQRT(D2W2L1(IE))
            DWL1ZZ(IE) = 0.5*DW2L1Z(IE)/WL1ZZZ(IE)
C
C *** WRITE RESULTS
            WRITE (25,99999) EEEEEE(IE), FTNZZZ(IE), FWAZZZ(IE),
     *           DFWAZZ(IE), DWAZZZ(IE), WWAZZZ(IE), ELL1ZZ(IE),
     *           DL1ZZZ(IE), WL1ZZZ(IE), DWL1ZZ(IE)
C
C *** PLOT SOME OF THE DISTRIBUTIONS
            IF (IPP(IPL).NE.IE) GO TO 10
            CALL PLOT(EEEEEE(IE), FTNZZZ(IE), FWAZZZ(IE),
     *           DWAZZZ(IE), WWAZZZ(IE), ELL1ZZ(IE), WL1ZZZ(IE),
     *           IPL, UUUUUU, WWWWWW, UW2ZZZ, RRRRRR)
            IPL = IPL + 1
   10 CONTINUE
C
      WRITE (25,99998)
      DO 20 IE=1,IEGRID
            CRL1W2 = 0.0
            IF (DL1ZZZ(IE)*DW2L1Z(IE).NE.0.0) CRL1W2 =
     *           CVL1W2(IE)/(DL1ZZZ(IE)*DW2L1Z(IE))
            WRITE (25,99997) EEEEEE(IE), D2L1ZZ(IE),
     *           D2W2L1(IE), CVL1W2(IE), CRL1W2
   20 CONTINUE
C
      RETURN
99999 FORMAT (F10.0, 3F10.4, 6F10.3)
99998 FORMAT (/45H        EN       D2L1     D2W2L1     CVL1W2    C,
     *     5HRL1W2)
99997 FORMAT (F10.0, 6F10.3)
      END
```

```
      SUBROUTINE DETECT
C
C *** PURPOSE -- GENERATE CONTRIBUTION TO LENGTH FROM DETECTOR
C ***             END OF FLIGHT PATH
C
      COMMON /ELL3XX/ CROSSS(17), ELL3ZZ(17), DL3ZZZ(17),
     *     D2L3ZZ(17), WL3ZZZ(17), DWL3ZZ(17), W2L3ZZ(17),
     *     DW2L3Z(17), D2W2L3(17), V3L3ZZ(17), U4L3ZZ(17),
     *     CVL3W2(17)
      COMMON /DETECV/ ALMBDA, THICKN, PERLMB, PERTHI, PERCRO
C
      COMMON /ALLZZZ/ EEEEEE(17), ELL2ZZ, DL2ZZZ, SHORTZ,
     *     IEGRID, IPLOT
C
      LOGICAL SHORTZ
C
      DATA ALMBDA /0.0047/, THICKN /19.0/, PERLMB /0.02/,
     *     PERTHI /0.05/, PERCRO /0.05/
C
      DATA CROSSS /27.200,27.17,27.02,26.60,25.91,24.69,21.7/,
     *     18.51,14.80,11.999,11.24,8.72,7.28,4.89,3.02,2.22,
     *     2.03/
C
CCCCCCCCCCCCCCCCCCCCCCCCCCCCCCCCCCCCCCCCCCCCCCCCCCC
CCCC INPUT CCCCCCCCCCCCCCCCCCCCCCCCCCCCCCCCCCCCCCCC
CCCC
CCCC  CROSSS = CROSS SECTION FOR NE110 AT ENERGY E
CCCC           NE110 = CH1.104
CCCC  SSIGMA = CROSS SECTION ALSO
CCCC  DSIGMA = UNCERTAINTY ON CROSS SECTION FOR NE110
CCCC  PERCRO = PERCENT UNCERTAINTY ON CROSS SECTION
CCCC
CCCC  THICKN = THICKNESS OF NE110 IN CM
CCCC  DTHICK = UNCERTAINTY ON THICKN
CCCC  PERTHI = PERCENT UNCERTAINTY ON THICKN
CCCC
CCCC  ALMBDA = DENSITY OF NE110 * .6023 / 12+1.104
CCCC           (DENSITY OF NE110 IS 1.032G/CM3)
CCCC  DLMBDA = UNCERTAINTY ON ALMBDA
CCCC  PERLMB = PERCENT UNCERTAINTY ON ALMBDA
CCCC
CCCC OUTPUT CCCCCCCCCCCCCCCCCCCCCCCCCCCCCCCCCCCCCCC
CCCC
CCCC  ELL3ZZ = MEAN DISTANCE TO FIRST SCATTER FROM FRONT
CCCC             OF DETECTOR
CCCC  DL3ZZZ = UNCERTAINTY ON ELL3ZZ
CCCC  WL3ZZZ = STANDARD DEVIATION OF DISTRIBUTION
CCCC             CENTERED ABOUT ELL3ZZ
CCCC  DWL3ZZ = UNCERTAINTY (STD DEV) ON WL3ZZZ
CCCC
CCCC  OUTPUT IS IN MILLIMETERS
CCCCCCCCCCCCCCCCCCCCCCCCCCCCCCCCCCCCCCCCCCCCCCCCCCC
```

```
      WRITE (25,99999)
C
      DLMBDA = PERLMB*ALMBDA
      DTHICK = PERTHI*THICKN
      PPPPPP = 100.0*PERCRO
      WRITE (25,99998) ALMBDA, DLMBDA
      WRITE (25,99997) THICKN, DTHICK
      WRITE (25,99994) PPPPPP
      WRITE (25,99996)
C
      DO 10 IE=1,IEGRID
          SSIGMA = CROSSS(IE)
          RSTZZZ = ALMBDA*SSIGMA*THICKN
          RST2ZZ = RSTZZZ**2
          EXPRST = EXP(RSTZZZ)
          DENOMN = 1.0 - EXPRST
          ELL3ZZ(IE) = (1.0/RSTZZZ + 1.0/DENOMN)*THICKN
C
          XXXXXX = 1.0/RST2ZZ - EXPRST/DENOMN**2
          W2L3ZZ(IE) = XXXXXX*THICKN**2
          WL3ZZZ(IE) = SQRT(XXXXXX)*THICKN
C
          PLRSTX = -XXXXXX*RSTZZZ*THICKN
          PLTHXX = ELL3ZZ(IE) + PLRSTX
          D2L3ZZ(IE) = PLRSTX**2*(PERLMB**2+PERCRO**2) +
     *        (PLTHXX*PERTHI)**2
          DL3ZZZ(IE) = SQRT(D2L3ZZ(IE))
C
          XXXXXX = 2.0/(RST2ZZ*RSTZZZ) +
     *        EXPRST*(1.0+EXPRST)/DENOMN**3
          PW2RST = -XXXXXX*RSTZZZ*THICKN**2
          PW2THI = 2.0*W2L3ZZ(IE)+PW2RST
          D2W2L3(IE) = PW2RST**2*(PERLMB**2+PERCRO**2) +
     *        (PW2THI*PERTHI)**2
          DW2L3Z(IE) = SQRT(D2W2L3(IE))
          DWL3ZZ(IE) = DW2L3Z(IE)/(2.0*WL3ZZZ(IE))
C
          CVL3W2(IE) = PLRSTX*PW2RST*(PERLMB**2+PERCRO**2) +
     *        PLTHXX*PW2THI*PERTHI**2
C
          V3L3ZZ(IE) = XXXXXX*THICKN**3
          XXXXXX = 9.0/RST2ZZ**2 - 6.0*EXPRST/(RSTZZZ*DENOMN)**2
     *        -EXPRST*(1.0+EXPRST+EXPRST**2)/DENOMN**4
          U4L3ZZ(IE) = XXXXXX*THICKN**4
          CRL3W2 = CVL3W2(IE)/(DL3ZZZ(IE)*DW2L3Z(IE))
```

```
C
          WRITE (25,99995) EEEEEE(IE), SSIGMA, ELL3ZZ(IE),
     *         DL3ZZZ(IE), WL3ZZZ(IE), DWL3ZZ(IE),
     *         V3L3ZZ(IE), U4L3ZZ(IE), D2L3ZZ(IE),
     *         D2W2L3(IE), CVL3W2(IE), CRL3W2
C
          IEE=IE
          CALL PLTDET(EEEEEE(IE), ELL3ZZ(IE), WL3ZZZ(IE),
     *         CROSSS(IE), ALMBDA, THICKN, IEE)
C
   10 CONTINUE
      RETURN
C
99999 FORMAT (//27H ****** DETECTOR END ******)
99998 FORMAT (/10H    RHO = , F8.6, 5H +/- , F8.6)
99997 FORMAT (10H THICKN = , F8.4, 5H +/- , F8.4)
99994 FORMAT (/10H PERCRO = , F8.4,
     *    37H PERCENT UNCERTAINTY ON CROSS SECTION/)
99996 FORMAT (/45H    ENERGY   CRSSCTN     ELL3        DL3        ,
     *    49H WL3        DWL3      V3L3        U4L3        D2L3 ,
     *    35H      D2W2L3      CVL3W2      CRL3W2)
99995 FORMAT (F10.0, 6F10.3, 3X, 6G12.5)
      END
```

```
      SUBROUTINE COMBIN
C
C *** PURPOSE -- COMBINE THE VARIOUS COMPONENTS OF FLIGHT-PATH-
C ***            LENGTH AND WRITE THEM ON UNIT 25
C
      COMMON /ELXXXX/ ELZZZZ(17), DLZZZZ(17), D2LZZZ(17),
     *     WLZZZZ(17), DWLZZZ(17), W2LZZZ(17), DW2LZZ(17),
     *     D2W2LZ(17), V3LZZZ(17), U4LZZZ(17), CVLW2Z(17)
      COMMON /ELL1XX/ DWAZZZ(17), WWAZZZ(17), FWAZZZ(17),
     *     FTNZZZ(17), ELL1ZZ(17), DL1ZZZ(17), D2L1ZZ(17),
     *     WL1ZZZ(17), DWL1ZZ(17), W2L1ZZ(17), DW2L1Z(17),
     *     D2W2L1(17), V3L1ZZ(17), U4L1ZZ(17), DFWAZZ(17),
     *     CVL1W2(17)
      COMMON /TAWATV/ PERDWA, PERWWA, WATER1, WATER2, WATER3,
     *     WWATR1, WWATR2, WWATR3, UUUUUU, WWWWWW, SSSSSS,
     *     DELUUU, DELWWW, DELSSS, RRRRRR, DELRRR, EMMMMM,
     *     PEREMM, ABSUNC
      COMMON /ELL3XX/ CROSSS(17), ELL3ZZ(17), DL3ZZZ(17),
     *     D2L3ZZ(17), WL3ZZZ(17), DWL3ZZ(17), W2L3ZZ(17),
     *     DW2L3Z(17), D2W2L3(17), V3L3ZZ(17), U4L3ZZ(17),
     *     CVL3W2(17)
      COMMON /ALLZZZ/ EEEEEE(17), ELL2ZZ, DL2ZZZ, SHORTZ,
     *     IEGRID, IPLOT
      LOGICAL SHORTZ
      DATA ELL2ZZ /201440.0/, DL2ZZZ /5.0/
C
      WRITE (25,99999)
C
      DO 10 IE=1,IEGRID
           ELZZZZ(IE) = ELL1ZZ(IE) + ELL2ZZ + ELL3ZZ(IE)
           D2LZZZ(IE) = D2L1ZZ(IE) + DL2ZZZ**2 + D2L3ZZ(IE)
           DLZZZZ(IE) = SQRT(D2LZZZ(IE))
           W2LZZZ(IE) = W2L1ZZ(IE) + W2L3ZZ(IE)
           WLZZZZ(IE) = SQRT(W2LZZZ(IE))
           D2W2LZ(IE) = D2W2L1(IE) + D2W2L3(IE)
           DW2LZZ(IE) = SQRT(D2W2LZ(IE))
           DWLZZZ(IE) = 0.5*DW2LZZ(IE)/WLZZZZ(IE)
           CVLW2Z(IE) = CVL1W2(IE) + CVL3W2(IE)
           V3LZZZ(IE) = V3L3ZZ(IE) + V3L1ZZ(IE)
           U4LZZZ(IE) = U4L3ZZ(IE) + U4L1ZZ(IE) +
     *          6.0*W2L3ZZ(IE)*W2L1ZZ(IE)
C
           WRITE (25,99998) EEEEEE(IE), ELZZZZ(IE), DLZZZZ(IE),
     *          WLZZZZ(IE), DWLZZZ(IE)
           IF (.NOT.SHORTZ) WRITE (5,99998) EEEEEE(IE), ELZZZZ(IE),
     *          DLZZZZ(IE), WLZZZZ(IE), DWLZZZ(IE)
   10 CONTINUE
      RETURN
C
99999 FORMAT (///40H ****** COMBINE THE THREE LENGTHS ******//
     *     51H    ENERGY         EL         DL         WL         DWL)
99998 FORMAT (F10.0, F12.3, 5F10.3)
      END
```

```
      SUBROUTINE OUTCMP
C *** PURPOSE -- WRITE ON UNIT 25 COMPONENTS OF WIDTHS ETC FOR FPL
C
      COMMON /ELXXXX/ ELZZZZ(17), DLZZZZ(17), D2LZZZ(17),
     *     WLZZZZ(17), DWLZZZ(17), W2LZZZ(17), DW2LZZ(17),
     *     D2W2LZ(17), V3LZZZ(17), U4LZZZ(17), CVLW2Z(17)
      COMMON /ELL1XX/ DWAZZZ(17), WWAZZZ(17), FWAZZZ(17),
     *     FTNZZZ(17), ELL1ZZ(17), DL1ZZZ(17), D2L1ZZ(17),
     *     WL1ZZZ(17), DWL1ZZ(17), W2L1ZZ(17), DW2L1Z(17),
     *     D2W2L1(17), V3L1ZZ(17), U4L1ZZ(17), DFWAZZ(17),
     *     CVL1W2(17)
      COMMON /ELL3XX/ CROSSS(17), ELL3ZZ(17), DL3ZZZ(17),
     *     D2L3ZZ(17), WL3ZZZ(17), DWL3ZZ(17), W2L3ZZ(17),
     *     DW2L3Z(17), D2W2L3(17), V3L3ZZ(17), U4L3ZZ(17),
     *     CVL3W2(17)
      COMMON /ALLZZZ/ EEEEEE(17), ELL2ZZ, DL2ZZZ, SHORTZ,
     *     IEGRID, IPLOT
      LOGICAL SHORTZ
C
      WRITE (25,99999)
      WRITE (25,99998)
      DO 10 IE=1,IEGRID
          WRITE (25,99997) EEEEEE(IE), ELZZZZ(IE), ELL2ZZ,
     *           ELL1ZZ(IE), ELL3ZZ(IE)
   10 CONTINUE
C
      WRITE (25,99996)
      WRITE (25,99995)
      DO 20 IE=1,IEGRID
          WRITE (25,99994) EEEEEE(IE), ELZZZZ(IE), DLZZZZ(IE),
     *           DL1ZZZ(IE), DL2ZZZ, DL3ZZZ(IE)
   20 CONTINUE
C
      WRITE (25,99993)
      WRITE (25,99992)
      DO 30 IE=1,IEGRID
          D2L2ZZ = DL2ZZZ**2
          WRITE (25,99994) EEEEEE(IE), ELZZZZ(IE), D2LZZZ(IE),
     *           D2L1ZZ(IE), D2L2ZZ, D2L3ZZ(IE)
   30 CONTINUE
C
      WRITE (25,99991)
      WRITE (25,99990)
      DO 40 IE=1,IEGRID
          WRITE (25,99989) EEEEEE(IE), ELZZZZ(IE), WLZZZZ(IE),
     *           WL1ZZZ(IE), WL3ZZZ(IE)
   40 CONTINUE
C
      WRITE (25,99988)
      WRITE (25,99987)
      DO 50 IE=1,IEGRID
          WRITE (25,99986) EEEEEE(IE), ELZZZZ(IE), W2LZZZ(IE),
     *           W2L1ZZ(IE), W2L3ZZ(IE)
   50 CONTINUE
```

```
      WRITE (25,99985)
      WRITE (25,99984)
      DO 60 IE=1,IEGRID
          WRITE (25,99983) EEEEEE(IE), ELZZZZ(IE), WLZZZZ(IE),
     *         DWLZZZ(IE)
   60 CONTINUE
C
      WRITE (25,99982)
      WRITE (25,99981)
      DO 70 IE=1,IEGRID
          WRITE (25,99980) EEEEEE(IE), DW2LZZ(IE), DW2L1Z(IE),
     *         DW2L3Z(IE)
   70 CONTINUE
C
      WRITE (25,99979)
      WRITE (25,99978)
      DO 80 IE=1,IEGRID
          WRITE (25,99980) EEEEEE(IE), CVLW2Z(IE), CVL1W2(IE),
     *         CVL3W2(IE)
   80 CONTINUE
      RETURN
99999 FORMAT (//44H *** COMPONENTS OF FLIGHT PATH LENGTH EL ***)
99998 FORMAT (/44H     ENERGY        EL           ELL2     ELL1   ,
     *     10H   ELL3    )
99997 FORMAT (1X, F10.0, F12.3, F13.3, 2F8.3)
99996 FORMAT (//44H *** COMPONENTS OF UNCERTAINTY ON FLIGHT PAT,
     *     12HH LENGTH ***)
99995 FORMAT (/45H     ENERGY        EL           DL          DL1   ,
     *     19H     DL2        DL3 )
99994 FORMAT (1X, F10.0, F12.3, 8F10.3)
99993 FORMAT (//44H *** COMPONENTS (SQUARED) OF UNCERTAINTY ON ,
     *     22HFLIGHT PATH LENGTH ***)
99992 FORMAT (/45H     ENERGY         EL          D2L       D2L1   ,
     *     19H    D2L2        D2L3)
99991 FORMAT (//44H *** COMPONENTS OF WIDTH "WL" OF FLIGHT PATH,
     *     24H LENGTH DISTRIBUTION ***)
99990 FORMAT (/45H     ENERGY         EL         WL          WL1    ,
     *     7H    WL3)
99989 FORMAT (1X, F10.0, F12.3, 3F10.3)
99988 FORMAT (//23H *** DITTO, SQUARED ***)
99987 FORMAT (/45H     ENERGY       EL          W2L        W2L1    ,
     *     8H   W2L3 )
99986 FORMAT (1X, F10.0, F12.3, 3F10.3)
99985 FORMAT (//44H *** UNCERTAINTY ON WIDTH OF FPL DISTRIBUTIO,
     *     5HN ***)
99984 FORMAT (/43H     ENERGY       EL          WL         DWL )
99983 FORMAT (1X, F10.0, F12.3, 8F10.3)
99982 FORMAT (//44H *** UNCERTAINTY ON VARIANCE OF FPL DISTRIBU,
     *     8HTION ***)
99981 FORMAT (/46H     ENERGY       DW2L       DW2L1       DW2L3)
99980 FORMAT (1X, F10.0, 8F12.3)
99979 FORMAT (//44H *** COVARIANCE ON FLIGHT PATH LENGTH DISTRI,
     *     6HBUTION)
99978 FORMAT (/47H     ENERGY       CVLW2       CVL1W2       CVL3W2)
      END
```

```
      SUBROUTINE TIME
C
C *** PURPOSE -- GENERATE MOMENTS OF TIME DISTRIBUTIONS
C
      COMMON /TIMER/ TZEROZ, DTZERO, AFWHMZ, DAFWHM, BCHNLZ,
     *     DBCHNL, TSCALE
      COMMON /T1XXXX/ T1ZZZZ, DT1ZZZ, D2T1ZZ, WT1ZZZ, DWT1ZZ,
     *     W2T1ZZ, DW2T1Z, D2W2T1, V3T1ZZ, U4T1ZZ, CVT1W2
      COMMON /T2XXXX/ T2ZZZZ, DT2ZZZ, D2T2ZZ, WT2ZZZ, DWT2ZZ,
     *     W2T2ZZ, DW2T2Z, D2W2T2, V3T2ZZ, U4T2ZZ, CVT2W2
      COMMON /TIMEXX/ TIMEZZ(17), DTIMEZ(17), D2TIME(17),
     *     WTIMEZ, DWTIME, W2TIME, DW2TIM, D2W2TZ, V3TIME,
     *     U4TIME, CVTW2Z
C
      COMMON /ALLZZZ/ EEEEEE(17), ELL2ZZ, DL2ZZZ, SHORTZ,
     *     IEGRID, IPLOT
C
      LOGICAL SHORTZ
C
      DATA AFWHMZ /7.5/, DAFWHM /0.5/, BCHNLZ /1.0/, DBCHNL
     *     /0.0010/, DTZERO /0.288675/, TSCALE /0.00002/
C     DTZERO IS 1/SQRT(12.0)
C
C
C *** T-SUB-1
      D2T1ZZ = 0.0
      WT1ZZZ = AFWHMZ/(2.0*SQRT(2.0*ALOG(2.0)))
      DWT1ZZ = DAFWHM/(2.0*SQRT(2.0*ALOG(2.0)))
      W2T1ZZ = WT1ZZZ*WT1ZZZ
      DW2T1Z = 2.0*WT1ZZZ*DWT1ZZ
      D2W2T1 = DW2T1Z**2
      V3T1ZZ = 0.0
      U4T1ZZ = 3.0*WT1ZZZ
C
C *** PRINTOUT FOR T-SUB-1 AND T-SUB-2
      WRITE (25,99999)
      WRITE (25,99998) WT1ZZZ, DWT1ZZ, AFWHMZ, DAFWHM,
     *     BCHNLZ, DBCHNL, DTZERO, DTZERO, TSCALE, TSCALE
C
C *** T-SUB-2
      D2T2ZZ = 0.0
      WT2ZZZ = BCHNLZ/SQRT(12.0)
      W2T2ZZ = BCHNLZ*BCHNLZ/12.0
      DWT2ZZ = DBCHNL/SQRT(12.0)
      DW2T2Z = (BCHNLZ/6.0)*DBCHNL
      D2W2T2 = DW2T2Z**2
      V3T2ZZ = 0.0
      U4T2ZZ = (BCHNLZ/2.0)**4/5.0
C
```

```
C *** COMBINE THE TWO
      W2TIME = W2T2ZZ + W2T1ZZ
      WTIMEZ = SQRT(W2TIME)
      V3TIME = 0.0
      U4TIME = U4T2ZZ + U4T1ZZ + 6.0*W2T2ZZ*W2T1ZZ
      D2W2TZ = D2W2T2 + D2W2T1
      DW2TIM = SQRT(D2W2TZ)
      DWTIME = DW2TIM/(2.0*WTIMEZ)
      CVTW2Z = CVT1W2 + CVT2W2
C
      WRITE (25,99997)
      WRITE (25,99996) WT1ZZZ, DWT1ZZ, W2T1ZZ, DW2T1Z, D2W2T1,
     *     V3T1ZZ, U4T1ZZ
      WRITE (25,99995) WT2ZZZ, DWT2ZZ, W2T2ZZ, DW2T2Z, D2W2T2,
     *     V3T2ZZ, U4T2ZZ
      WRITE (25,99994) WTIMEZ, DWTIME, W2TIME, DW2TIM, D2W2TZ,
     *     V3TIME, U4TIME
      RETURN
C
99999 FORMAT (///30H ****** TIME RESOLUTION ******)
99998 FORMAT (/37H   ASTD = WIDTH (STD.DEV.) OF BURST =, F8.5,
     *     5H +/- , F8.5/35H  AFWHM = WIDTH (FWHM) OF BURST    ,
     *     2H =, F8.5, 5H +/- , F8.5/23H   CHNL = WIDTH OF DETE,
     *     14HCTOR-CHANNEL =, F8.5, 5H +/- , F8.5/10H DTZERO = ,
     *     27HUNCERTAINTY IN TZERO      =, F8.5, 2H =, 1PE10.3/
     *     37H TSCALE = RELATIVE TIME-UNCERTAINTY =, 0PF8.5,
     *     2H =, 1PE10.3)
99997 FORMAT (/45H          ??         WT?         DWT?         W2T? ,
     *     47H       DW2T?       D2W2T?         V3T?         U4T?)
99996 FORMAT (12H        ONE   , 7G12.4)
99995 FORMAT (12H        TWO   , 7G12.4)
99994 FORMAT (12H      TOTAL   , 7G12.4)
      END
```

```
      SUBROUTINE ENERGY
C
C *** PURPOSE -- GENERATE ENERGY UNCERTAINTY AND MOMENTS OF THE
C ***            ENERGY-RESOLUTION FUNCTION
C
      COMMON /TOTAL/ ENZZZZ(17), FUDGEZ(17), DENZZZ(17),
     *     D2ENZZ(17), WENZZZ(17), W2ENZZ(17), DWENZZ(17),
     *     DW2ENZ(17), D2W2EN(17), WWEL2Z(17), WWTIM2(17),
     *     WWEL3Z(17), WWTIM3(17), WWELTI(17), WWEL4Z(17),
     *     WWTIM4(17), PW2W2L(17), PW2W2T(17), PW2LZZ(17),
     *     PW2TIM(17)
C
      COMMON /ELXXXX/ ELZZZZ(17), DLZZZZ(17), D2LZZZ(17),
     *     WLZZZZ(17), DWLZZZ(17), W2LZZZ(17), DW2LZZ(17),
     *     D2W2LZ(17), V3LZZZ(17), U4LZZZ(17), CVLW2Z(17)
C
      COMMON /TIMER/ TZEROZ, DTZERO, AFWHMZ, DAFWHM, BCHNLZ,
     *     DBCHNL, TSCALE
      COMMON /TIMEXX/ TIMEZZ(17), DTIMEZ(17), D2TIME(17),
     *     WTIMEZ, DWTIME, W2TIME, DW2TIM, D2W2TZ, V3TIME,
     *     U4TIME, CVTW2Z
C
      COMMON /ALLZZZ/ EEEEEE(17), ELL2ZZ, DL2ZZZ, SHORTZ,
     *     IEGRID, IPLOT
C
C
      WRITE (25,99999)
      WRITE (25,99998)
      DO 30 IE=1,IEGRID
           TMTZER = 72.297*ELZZZZ(IE)/SQRT(EEEEEE(IE))
           TIMEZZ(IE) = TMTZER
           D2TIME(IE) = DTZERO**2 + (TMTZER*TSCALE)**2
           DTIMEZ(IE) = SQRT(D2TIME(IE))
           FUDGE1 = W2LZZZ(IE)/ELZZZZ(IE)**2
           FUDGE2 = 3.0*W2TIME/TMTZER**2
           FUDGE3 = 5.0*U4TIME/TMTZER**4
           FUDGE4 = 3.0* (W2LZZZ(IE)/ELZZZZ(IE)**2) *
     *          (W2TIME/TMTZER**2)
           FUDGEZ(IE) = FUDGE1 + FUDGE2 + FUDGE3 + FUDGE4
           ENZZZZ(IE) = EEEEEE(IE)*(1.0+FUDGEZ(IE))
           TMTZZZ = 72.297*ELZZZZ(IE)/SQRT(ENZZZZ(IE))
C
           D2ENZZ(IE) = EEEEEE(IE)**2*4.0 *
     *          ( D2LZZZ(IE)/ELZZZZ(IE)**2 + D2TIME(IE)/TMTZER**2 )
           DENZZZ(IE) = SQRT(D2ENZZ(IE))
C
           AAEL2Z = 2.0*WLZZZZ(IE)/ELZZZZ(IE)
           WWEL2Z(IE) = AAEL2Z**2
           AATIM2 = 2.0*WTIMEZ/TMTZER
           WWTIM2(IE) = AATIM2**2
           WWEL3Z(IE) = 4.0*V3LZZZ(IE)/ELZZZZ(IE)**3
           AAEL3Z = SQRT(WWEL3Z(IE))
           WWTIM3(IE) = 0.0
```

```
         AATIM3 = 0.0
         WWELTI(IE) = 3.0*WWEL2Z(IE)*WWTIM2(IE)
         AAELTI = SQRT(WWELTI(IE))
         WWEL4Z(IE) = (U4LZZZ(IE)-W2LZZZ(IE)**2)/ELZZZZ(IE)**4
         AAEL4Z = SQRT(WWEL4Z(IE))
         WWTIM4(IE) = (25.0*U4TIME-9.0*W2TIME**2)/TMTZER**4
         AATIM4 = SQRT(WWTIM4(IE))
         W2ENZZ(IE) = EEEEEE(IE)**2*(WWEL2Z(IE)+WWTIM2(IE)
     *        +WWEL3Z(IE)+WWELTI(IE)+WWTIM3(IE)+WWEL4Z(IE)
     *        +WWTIM4(IE))
         WENZZZ(IE) = SQRT(W2ENZZ(IE))
C
         XAW2LZ = (1.0+3.0*WWTIM2(IE)-WWEL2Z(IE)/8.0)
     *        *4.0/ELZZZZ(IE)**2
         PW2W2L(IE) = XAW2LZ*EEEEEE(IE)**2
         XAW2TI = (1.0+3.0*WWEL2Z(IE)-9.0*WWTIM2(IE)/8.0)
     *        *4.0/TMTZER**2
         PW2W2T(IE) = XAW2TI*EEEEEE(IE)**2
         XAELZZ = -2.0*( WWEL2Z(IE)*(1.0+3.0*WWTIM2(IE))
     *        + WWEL3Z(IE)*1.5 + WWEL4Z(IE)*2.0 ) / ELZZZZ(IE)
         PW2LZZ(IE) = XAELZZ*EEEEEE(IE)**2 +
     *        4.0*W2ENZZ(IE)/ELZZZZ(IE)
         XATIME = -2.0*( WWTIM2(IE)*(1.0+3.0*WWEL2Z(IE))
     *        + 2.0*WWTIM4(IE) ) / TMTZER
         PW2TIM(IE) = XATIME*EEEEEE(IE)**2 -
     *        4.0*W2ENZZ(IE)/TMTZER
C
         D2W2EN(IE) = PW2W2L(IE)**2*D2W2LZ(IE) +
     *        PW2W2T(IE)**2*DW2TIM**2 +
     *        PW2LZZ(IE)**2*D2LZZZ(IE) +
     *        PW2TIM(IE)**2*D2TIME(IE) +
     *        2.0*PW2W2L(IE)*PW2LZZ(IE)*CVLW2Z(IE)
     *        + 2.0*PW2W2T(IE)*PW2TIM(IE)*CVTW2Z
         DW2ENZ(IE) = SQRT(D2W2EN(IE))
         DWENZZ(IE) = DW2ENZ(IE)/(2.0*WENZZZ(IE))
C
         WRITE (25,99997) TMTZER, TMTZZZ, FUDGE1, FUDGE2, FUDGE3,
     *        FUDGE4, AAEL2Z, AATIM2, AAEL3Z, AATIM3, AAELTI,
     *        AAEL4Z, AATIM4
   30 CONTINUE
C
      WRITE (25,99994)
      DO 40 IE=1,IEGRID
         WRITE (25,99993) EEEEEE(IE), W2ENZZ(IE), WWEL2Z(IE),
     *        WWTIM2(IE), WWEL3Z(IE), WWELTI(IE), WWTIM3(IE),
     *        WWEL4Z(IE), WWTIM4(IE)
   40 CONTINUE
```

```
C
      WRITE (25,99996)
      DO 50 IE=1,IEGRID
           XX = DENZZZ(IE)/ENZZZZ(IE)
           YY = WENZZZ(IE)/ENZZZZ(IE)
           ZZ = DWENZZ(IE)/WENZZZ(IE)
           WRITE (25,99995) EEEEEE(IE), ENZZZZ(IE), FUDGEZ(IE),
     *          DENZZZ(IE), XX, WENZZZ(IE), YY, DWENZZ(IE), ZZ
   50 CONTINUE
      RETURN
C
99999 FORMAT (///28H ****** FINAL RESULTS ******)
99998 FORMAT (///43H     T-TO     T-TOX    FUDGE1    FUDGE2    FUD,
     *     49HGE3   FUDGE4   AAEL2   AATIM2    AAEL3   AATIM3   ,
     *     25H AAELTI   AAEL4    AATIM4)
99997 FORMAT (1X, 2F9.0, 1P11G9.2)
99994 FORMAT (//'    ENERGY        W2EN          WWEL2       WWTIM2         WW
     *EL3       WWELTI       WWTIM3       WWEL4       WWTIM4')
99993 FORMAT (F10.0, 1P8G12.4)
99996 FORMAT (//44H      ENERGY   ADJ. ENE.      FUDGE         DEN,
     *     49H       DEN/EN         WEN         WEN/EN         DWEN ,
     *     12H    DWEN/WEN)
99995 FORMAT (1X, F10.0, F11.0, 1P7G12.3)
      END
```

```
      SUBROUTINE DSPLAY
C
C *** PURPOSE -- WRITE TABLES FOR TM REPORT
C
      COMMON /TOTAL/ ENZZZZ(17), FUDGEZ(17), DENZZZ(17),
     *      D2ENZZ(17), WENZZZ(17), W2ENZZ(17), DWENZZ(17),
     *      DW2ENZ(17), D2W2EN(17), WWEL2Z(17), WWTIM2(17),
     *      WWEL3Z(17), WWTIM3(17), WWELTI(17), WWEL4Z(17),
     *      WWTIM4(17), PW2W2L(17), PW2W2T(17), PW2LZZ(17),
     *      PW2TIM(17)
C
      COMMON /ELXXXX/ ELZZZZ(17), DLZZZZ(17), D2LZZZ(17),
     *      WLZZZZ(17), DWLZZZ(17), W2LZZZ(17), DW2LZZ(17),
     *      D2W2LZ(17), V3LZZZ(17), U4LZZZ(17), CVLW2Z(17)
C
      COMMON /ELL1XX/ DWAZZZ(17), WWAZZZ(17), FWAZZZ(17),
     *      FTNZZZ(17), ELL1ZZ(17), DL1ZZZ(17), D2L1ZZ(17),
     *      WL1ZZZ(17), DWL1ZZ(17), W2L1ZZ(17), DW2L1Z(17),
     *      D2W2L1(17), V3L1ZZ(17), U4L1ZZ(17), DFWAZZ(17),
     *      CVL1W2(17)
C
      COMMON /ELL3XX/ CROSSS(17), ELL3ZZ(17), DL3ZZZ(17),
     *      D2L3ZZ(17), WL3ZZZ(17), DWL3ZZ(17), W2L3ZZ(17),
     *      DW2L3Z(17), D2W2L3(17), V3L3ZZ(17), U4L3ZZ(17),
     *      CVL3W2(17)
C
      COMMON /TIMEXX/ TIMEZZ(17), DTIMEZ(17), D2TIME(17),
     *      WTIMEZ, DWTIME, W2TIME, DW2TIM, D2W2TZ, V3TIME,
     *      U4TIME, CVTW2Z
C
      COMMON /ALLZZZ/ EEEEEE(17), ELL2ZZ, DL2ZZZ, SHORTZ,
     *      IEGRID, IPLOT
C
C
      WRITE (27,99999)
      WRITE (27,99998)
      DO 10 IE=1,IEGRID
           EL1PL3 = ELL1ZZ(IE) + ELL3ZZ(IE)
           DL1PL3 = SQRT(D2L1ZZ(IE)+D2L3ZZ(IE))
           DEOE = DENZZZ(IE)/EEEEEE(IE)
           WRITE (27,99997) EEEEEE(IE), DENZZZ(IE), DEOE, ELZZZZ(IE),
     *           DLZZZZ(IE), ELL1ZZ(IE), DL1ZZZ(IE), ELL3ZZ(IE),
     *           DL3ZZZ(IE), EL1PL3, DL1PL3
   10 CONTINUE
C
      WRITE (27,99996)
      WRITE (27,99995)
      DO 20 IE=1,IEGRID
           WOE = WENZZZ(IE)/EEEEEE(IE)
           WRITE (27,99994) EEEEEE(IE), WENZZZ(IE), WOE, DWENZZ(IE),
     *           WLZZZZ(IE), DWLZZZ(IE), WL1ZZZ(IE), DWL1ZZ(IE),
     *           WL3ZZZ(IE), DWL3ZZ(IE)
   20 CONTINUE
```

```
C
      WRITE (27,99993)
      WRITE (27,99992)
      DO 30 IE=1,IEGRID
           WRITE (27,99991) EEEEEE(IE), W2LZZZ(IE), V3LZZZ(IE),
     *          U4LZZZ(IE)
   30 CONTINUE
C
      WRITE (27,99990)
      WRITE (27,99989)
      DO 40 IE=1,IEGRID
           B1 = 4.0*W2LZZZ(IE)/ELZZZZ(IE)**2
           D2B1 = B1**2 * (D2W2LZ(IE)/W2LZZZ(IE)**2
     *          -4.0*CVLW2Z(IE)/(W2LZZZ(IE)*ELZZZZ(IE))+
     *          4.0*D2LZZZ(IE)/ELZZZZ(IE)**2)
           DB1 = SQRT(D2B1)
           B2 = 4.0*W2TIME/(72.297*ELZZZZ(IE))**2
           D2B2 = B2**2 * (D2W2TZ/W2TIME**2 +
     *          4.0*D2LZZZ(IE)/ELZZZZ(IE)**2)
           DB2 = SQRT(D2B2)
           B1PB2E = B1 + B2*EEEEEE(IE)
           D2BBEZ = D2B1 + 16.0/TIMEZZ(IE)**4 *
     *          (D2W2TZ+4.0*D2TIME(IE)/TIMEZZ(IE)**2)
           DBBEZZ = SQRT(D2BBEZ)
           W2OEN2 = W2ENZZ(IE)/EEEEEE(IE)**2
           WRITE (27,99988) EEEEEE(IE), W2ENZZ(IE), B1, DB1, B2,
     *          DB2, B1PB2E, DBBEZZ, W2OEN2
   40 CONTINUE
      RETURN
C
99999 FORMAT (/// 8H TABLE 1)
99998 FORMAT (/51H        ENERGY     DELTA E   DE/ENERGY          L        ,
     *     48H DELTA L      L1      DELTA L1      L3      DELTA L3,
     *     25H     L1+L3   DELTA (L1+L3))
99997 FORMAT (F13.3, F11.3, 1PG12.3, 0PF12.3, 7F10.3)
99996 FORMAT (/// 8H TABLE 2)
99995 FORMAT (//45H        ENERGY          WEN  WEN/ENERGY       DWE,
     *     49HN       WL          DWL          WL1       DWL1         W,
     *     12HL3       DWL3)
99994 FORMAT (F13.3, F11.3, 1PG12.3, 0P/F10.3)
99993 FORMAT (/// 8H TABLE 3)
99992 FORMAT (/41H      ENERGY         W2L         V3L        U4L)
99991 FORMAT (1X, F10.0, 3F10.2)
99990 FORMAT (/// 8H TABLE 4)
99989 FORMAT (/41H      ENERGY          W2EN           B1         ,
     *     48H   DB1            B2            DB2           B1+B2*E,
     *     30H   D(B1+B2*E)   W2EN/ENERGY**2)
99988 FORMAT (1X, F10.0, 1P8E13.3)
      END
```

```
      SUBROUTINE PLT
C
C *** PURPOSE -- MAKE PLOT FILES FOR ENERGY-DEPENDENT
C ***            PARAMETERS OF TANTALUM-WATER DISTRIBUTION
C
      COMMON /ELL1XX/ DWAZZZ(17), WWAZZZ(17), FWAZZZ(17),
     *     FTNZZZ(17), ELL1ZZ(17), DL1ZZZ(17), D2L1ZZ(17),
     *     WL1ZZZ(17), DWL1ZZ(17), W2L1ZZ(17), DW2L1Z(17),
     *     D2W2L1(17), V3L1ZZ(17), U4L1ZZ(17), DFWAZZ(17),
     *     CVL1W2(17)
C
      COMMON /ALLZZZ/ EEEEEE(17), ELL2ZZ, DL2ZZZ, SHORTZ,
     *     IEGRID, IPLOT
      LOGICAL SHORTZ
C
      IU = 21
      INS = 9
      IFB = 3
      MODE = 3
      NDSTRT = 0
      NEW = 1
      CALL ODFIO(IU, 'TAH2O.ODF', IFB, NEW, INS, IEGRID, MODE,
     *     NDSTRT, -1, 0)
      CALL OUTODF(IU, IFB, INS, 1, MODE, NDSTRT, 1, IEGRID,
     *     EEEEEE, 1)
      CALL OUTODF(IU, IFB, INS, 2, MODE, NDSTRT, 1, IEGRID,
     *     FTNZZZ, 1)
      CALL OUTODF(IU, IFB, INS, 3, MODE, NDSTRT, 1, IEGRID,
     *     FWAZZZ, 1)
      CALL OUTODF(IU, IFB, INS, 4, MODE, NDSTRT, 1, IEGRID,
     *     DWAZZZ, 1)
      CALL OUTODF(IU, IFB, INS, 5, MODE, NDSTRT, 1, IEGRID,
     *     WWAZZZ, 1)
      CALL OUTODF(IU, IFB, INS, 6, MODE, NDSTRT, 1, IEGRID,
     *     ELL1ZZ, 1)
      CALL OUTODF(IU, IFB, INS, 7, MODE, NDSTRT, 1, IEGRID,
     *     DL1ZZZ, 1)
      CALL OUTODF(IU, IFB, INS, 8, MODE, NDSTRT, 1, IEGRID,
     *     WL1ZZZ, 1)
      CALL OUTODF(IU, IFB, INS, 9, MODE, NDSTRT, 1, IEGRID,
     *     DWL1ZZ, 1)
      CLOSE (UNIT=21)
      RETURN
      END
```

```
      SUBROUTINE PLOT13
C
C *** PURPOSE -- MAKE PLOT FILES FOR ENERGY-DEPENDENT
C ***            L1+L3 AND UNCERTAINTY THEREON
C
      COMMON /ELL1XX/ DWAZZZ(17), WWAZZZ(17), FWAZZZ(17),
     *     FTNZZZ(17), ELL1ZZ(17), DL1ZZZ(17), D2L1ZZ(17),
     *     WL1ZZZ(17), DWL1ZZ(17), W2L1ZZ(17), DW2L1Z(17),
     *     D2W2L1(17), V3L1ZZ(17), U4L1ZZ(17), DFWAZZ(17),
     *     CVL1W2(17)
C
      COMMON /ELL3XX/ CROSSS(17), ELL3ZZ(17), DL3ZZZ(17),
     *     D2L3ZZ(17), WL3ZZZ(17), DWL3ZZ(17), W2L3ZZ(17),
     *     DW2L3Z(17), D2W2L3(17), V3L3ZZ(17), U4L3ZZ(17),
     *     CVL3W2(17)
C
      COMMON /ALLZZZ/ EEEEEE(17), ELL2ZZ, DL2ZZZ, SHORTZ,
     *     IEGRID, IPLOT
      LOGICAL SHORTZ
C
      DIMENSION DDUMMY(17)
C
C
      IU = 21
      INS = 3
      IFB = 3
      MODE = 3
      NDSTRT = 0
      NEW = 1
      CALL ODFIO(IU, 'L1PL3.ODF', IFB, NEW, INS, IEGRID, MODE,
     *     NDSTRT, -1, 0)
C
      DO 10 IE=1,IEGRID
           DDUMMY(IE) = ELL1ZZ(IE) + ELL3ZZ(IE)
   10 CONTINUE
C
      CALL OUTODF(IU, IFB, INS, 1, MODE, NDSTRT, 1, IEGRID,
     *     EEEEEE, 1)
      CALL OUTODF(IU, IFB, INS, 2, MODE, NDSTRT, 1, IEGRID,
     *     DDUMMY, 1)
C
      DO 20 IE=1,IEGRID
           DDUMMY(IE) = SQRT(D2L1ZZ(IE)+D2L3ZZ(IE))
   20 CONTINUE
C
      CALL OUTODF(IU, IFB, INS, 3, MODE, NDSTRT, 1, IEGRID,
     *     DDUMMY, 1)
      CLOSE (UNIT=21)
      RETURN
      END
```

```
      SUBROUTINE PLOT(E, FTNZZZ, FWAZZZ, D, WTA, ELL1ZZ,
     *     WL1ZZZ, IPL, U, W, UW2, R)
C
C *** PURPOSE -- GENERATE ODF FILE FOR TA-WATER DISTRIBUTION
C
      DIMENSION Q(501), RHO(501)
      DOUBLE PRECISION FILE(17)
      DATA FILE /10H0      .ODF, 10H1      .ODF, 10H2      .ODF,
     *     10H5      .ODF, 10H10     .ODF, 10H20     .ODF,
     *     10H50     .ODF, 10H100    .ODF, 10H200    .ODF,
     *     10H300    .ODF, 10H400    .ODF, 10H700    .ODF,
     *     10H1000   .ODF, 10H2000   .ODF, 10H5000   .ODF,
     *     10H10000 .ODF, 10H20000 .ODF/
      DATA IQQ /501/
C
      QMIN = AMIN1(-(U+W),-ELL1ZZ-3.*WL1ZZZ)
      QMAX = AMAX1(0.,-ELL1ZZ+3.*WL1ZZZ)
C       TYPE 99, QMIN, QMAX
      DELQ = (QMAX-QMIN)/500.
      DO 10 IQ=1,IQQ
           Q(IQ) = -(QMIN+DELQ*(IQ-1))
   10 CONTINUE
C
      AH2O = FWAZZZ/(SQRT(2.*3.141592654)*WTA)
      ATA = FTNZZZ*2./(3.141592654*R*R)
      DEN = 2.*WTA**2
      DO 20 IQ=1,IQQ
           RHO(IQ) = EXP(-(Q(IQ)-D)**2/DEN)*AH2O
           IF (Q(IQ).GE.UW2-R .AND. Q(IQ).LE.UW2+R) RHO(IQ) =
     *           RHO(IQ) + ATA*SQRT((R-UW2+Q(IQ))*(R+UW2-Q(IQ)))
   20 CONTINUE
C
      DO 30 IQ=1,IQQ
           Q(IQ) = -Q(IQ)
   30 CONTINUE
C
C
      IU = 22
      INS = 2
      IFB = 3
      MODE = 3
      NDSTRT = 0
      NEW = 1
      CALL ODFIO(IU, FILE(IPL), IFB, NEW, INS, IQQ, MODE,
     *     NDSTRT, -1, 0)
      CALL OUTODF(IU, IFB, INS, 1, MODE, NDSTRT, 1, IQQ, Q, 1)
      CALL OUTODF(IU, IFB, INS, 2, MODE, NDSTRT, 1, IQQ, RHO, 1)
      CLOSE(UNIT=IU)
      RETURN
      END
```

```
      SUBROUTINE PLTDET(E, EL, W, S, R, T, IPL)
C
C *** PURPOSE -- GENERATE ODF FILES FOR DETECTOR-END DISTRIBUTION (L3)
C
      DIMENSION Q(501), RHO(501)
      DOUBLE PRECISION FILE(17)
      DATA FILE /10H0      .DET, 10H1      .DET, 10H2      .DET,
     *     10H5      .DET, 10H10     .DET, 10H20     .DET,
     *     10H50     .DET, 10H100    .DET, 10H200    .DET,
     *     10H300    .DET, 10H400    .DET, 10H700    .DET,
     *     10H1000   .DET, 10H2000   .DET, 10H5000   .DET,
     *     10H10000 .DET, 10H20000 .DET/
      DATA IQQ /501/
C
      QMIN = EL-3.0*W
      QMAX = EL+3.0*W
C       TYPE 99, QMIN, QMAX
      DELQ = (QMAX-QMIN)/500.
      DO 10 IQ=1,IQQ
           Q(IQ) = (QMIN+DELQ*(IQ-1))
   10 CONTINUE
C
      RS = R*S
      RST = RS*T
      A = RS/(1.0-EXP(-RST))
      DO 20 IQ=1,IQQ
           IF (Q(IQ).GE.0. .AND. Q(IQ).LE.T)
     *          RHO(IQ) = A*EXP(-RS*Q(IQ))
   20 CONTINUE
C
      IU = 22
      INS = 2
      IFB = 3
      MODE = 3
      NDSTRT = 0
      NEW = 1
      CALL ODFIO(IU, FILE(IPL), IFB, NEW, INS, IQQ, MODE,
     *     NDSTRT, -1, 0)
      CALL OUTODF(IU, IFB, INS, 1, MODE, NDSTRT, 1, IQQ, Q, 1)
      CALL OUTODF(IU, IFB, INS, 2, MODE, NDSTRT, 1, IQQ, RHO, 1)
      CLOSE(UNIT=IU)
      RETURN
      END
```

```
      SUBROUTINE QQQTAH
C WRITE DEBUG-PRINT FOR TANTALUM-WATER ARRAYS
      COMMON /ELL1XX/ DWAZZZ(17), WWAZZZ(17), FWAZZZ(17),
     *     FTNZZZ(17), ELL1ZZ(17), DL1ZZZ(17), D2L1ZZ(17),
     *     WL1ZZZ(17), DWL1ZZ(17), W2L1ZZ(17), DW2L1Z(17),
     *     D2W2L1(17), V3L1ZZ(17), U4L1ZZ(17), DFWAZZ(17),
     *     CVL1W2(17)
      COMMON /TAWATV/ PERDWA, PERWWA, WATER1, WATER2, WATER3,
     *     WWATR1, WWATR2, WWATR3, UUUUUU, WWWWWW, SSSSSS,
     *     DELUUU, DELWWW, DELSSS, RRRRRR, DELRRR, EMMMMM,
     *     PEREMM, ABSUNC
      DIMENSION AAAAAA(19)
      EQUIVALENCE (AAAAAA(1),PERDWA)
      CALL QQQZZZ(6HDWA    , 6HWWA    , 6HFWA    , 6HFTN    , DWAZZZ,
     *     WWAZZZ, FWAZZZ, FTNZZZ)
      CALL QQQZZZ(6HELL1   , 6HDL1    , 6HD2L1   , 6HWL1    , ELL1ZZ,
     *     DL1ZZZ, D2L1ZZ, WL1ZZZ)
      CALL QQQZZZ(6HDWL1   , 6HW2L1   , 6HDW2L1  , 6HD2W2L1, DWL1ZZ,
     *     W2L1ZZ, DW2L1Z, D2W2L1)
C
      CALL QQQZZZ(6HV3L1   , 6HU4L1   , 6HDFWA   , 6HCVL1W2, V3L1ZZ,
     *     U4L1ZZ, DFWAZZ, CVL1W2)
      CALL QQQXXX(AAAAAA, 19)
      RETURN
      END
C
C
C
      SUBROUTINE QQQDET
C *** PURPOSE -- DEBUG-PRINT FOR DETECTOR ARRAYS (L3)
      COMMON /ELL3XX/ CROSSS(17), ELL3ZZ(17), DL3ZZZ(17),
     *     D2L3ZZ(17), WL3ZZZ(17), DWL3ZZ(17), W2L3ZZ(17),
     *     DW2L3Z(17), D2W2L3(17), V3L3ZZ(17), U4L3ZZ(17),
     *     CVL3W2(17)
      COMMON /DETECV/ ALMBDA, THICKN, PERLMB, PERTHI, PERCRO
      DIMENSION AAAAAA(5)
      EQUIVALENCE (AAAAAA(1),ALMBDA)
      CALL QQQZZZ(6HCROSSS, 6HELL3   , 6HDL3    , 6HD2L3   , CROSSS,
     *     ELL3ZZ, DL3ZZZ, D2L3ZZ)
      CALL QQQZZZ(6HWL3    , 6HDWL3   , 6HW2L3   , 6HDW2L3  , WL3ZZZ,
     *     DWL3ZZ, W2L3ZZ, DW2L3Z)
      CALL QQQZZZ(6HD2W2L3, 6HV3L3   , 6HU4L3   , 6HCVL3W2, D2W2L3,
     *     V3L3ZZ, U4L3ZZ, CVL3W2)
      CALL QQQXXX(AAAAAA, 5)
      RETURN
      END
```

```
      SUBROUTINE QQQCOM
C *** PURPOSE -- DEBUG-PRINT LENGTH ARRAYS
      COMMON /ELXXXX/ ELZZZZ(17), DLZZZZ(17), D2LZZZ(17),
     *     WLZZZZ(17), DWLZZZ(17), W2LZZZ(17), DW2LZZ(17),
     *     D2W2LZ(17), V3LZZZ(17), U4LZZZ(17), CVLW2Z(17)
      COMMON /ALLZZZ/ EEEEEE(17), ELL2ZZ, DL2ZZZ, SHORTZ,
     *     IEGRID, IPLOT
      DIMENSION AAAAAA(2)
      EQUIVALENCE (AAAAAA(1),ELL2ZZ)
      CALL QQQZZZ(6HEL    , 6HDL    , 6HD2L   , 6HWL    , ELZZZZ,
     *     DLZZZZ, D2LZZZ, WLZZZZ)
      CALL QQQZZZ(6HW2L   , 6HDWL   , 6HDW2L  , 6HD2W2L , W2LZZZ,
     *     DWLZZZ, DW2LZZ, D2W2LZ)
      CALL QQQXXX(AAAAAA, 2)
      RETURN
      END
C
C
C
      SUBROUTINE QQQTIM
C *** PURPOSE -- DEBUG-PRINT TIME ARRAYS
      COMMON /TIMER/ TZEROZ, DTZERO, AFWHMZ, DAFWHM, BCHNLZ,
     *     DBCHNL, TSCALE
      COMMON /T1XXXX/ T1ZZZZ, DT1ZZZ, D2T1ZZ, WT1ZZZ, DWT1ZZ,
     *     W2T1ZZ, DW2T1Z, D2W2T1, V3T1ZZ, U4T1ZZ, CVT1W2
      COMMON /T2XXXX/ T2ZZZZ, DT2ZZZ, D2T2ZZ, WT2ZZZ, DWT2ZZ,
     *     W2T2ZZ, DW2T2Z, D2W2T2, V3T2ZZ, U4T2ZZ, CVT2W2
      COMMON /TIMEXX/ TIMEZZ(17), DTIMEZ(17), D2TIME(17),
     *     WTIMEZ, DWTIME, W2TIME, DW2TIM, D2W2TZ, V3TIME,
     *     U4TIME, CVTW2Z
      DIMENSION AAAAAA(6), BBBBBB(11), CCCCCC(11), DDDDDD(8)
      EQUIVALENCE (AAAAAA(1),TZEROZ), (BBBBBB(1),T1ZZZZ),
     *     (CCCCCC(1),T2ZZZZ), (DDDDDD(1),WTIMEZ)
      CALL QQQXXX(AAAAAA, 6)
      CALL QQQXXX(BBBBBB, 11)
      CALL QQQXXX(CCCCCC, 11)
      CALL QQQZZZ(6HTIME  , 6HDTIME , 6HD2TIME, 6H      , TIMEZZ,
     *     DTIMEZ, D2TIME, X)
      CALL QQQXXX(DDDDDD, 8)
      RETURN
      END
```

```
      SUBROUTINE QQQENE
C *** PURPOSE -- DEBUG-PRINT ENERGY ARRAYS
      COMMON /TOTAL/ ENZZZZ(17), FUDGEZ(17), DENZZZ(17),
     *     D2ENZZ(17), WENZZZ(17), W2ENZZ(17), DWENZZ(17),
     *     DW2ENZ(17), D2W2EN(17), WWEL2Z(17), WWTIM2(17),
     *     WWEL3Z(17), WWTIM3(17), WWELTI(17), WWEL4Z(17),
     *     WWTIM4(17), PW2W2L(17), PW2W2T(17), PW2LZZ(17),
     *     PW2TIM(17)
      COMMON /ALLZZZ/ EEEEEE(17), ELL2ZZ, DL2ZZZ, SHORTZ,
     *     IEGRID, IPLOT
      CALL QQQZZZ(6HEN    , 6HFUDGE , 6HDEN   , 6HD2EN  , ENZZZZ,
     *     FUDGEZ, DENZZZ, D2ENZZ)
      CALL QQQZZZ(6HWEN   , 6HW2EN  , 6HDWEN  , 6HDW2EN , WENZZZ,
     *     W2ENZZ, DWENZZ, DW2ENZ)
      CALL QQQZZZ(6HD2W2EN, 6HWWEL2 , 6HWWTIM2, 6HWWEL3 , D2W2EN,
     *     WWEL2Z, WWTIM2, WWEL3Z)
      CALL QQQZZZ(6HWWTIM3, 6HWWELTI, 6HWWEL4 , 6HWWTIM4, WWTIM3,
     *     WWELTI, WWEL4Z, WWTIM4)
      CALL QQQZZZ(6HPW2W2L, 6HPW2W2T, 6HPW2L  , 6HPW2TIM, PW2W2L,
     *     PW2W2T, PW2LZZ, PW2TIM)
      RETURN
      END
C
C
C
      SUBROUTINE QQQZZZ(A, B, C, D, E, F, G, H)
C *** PURPOSE -- DEBUG-PRINT ARRAYS
      DOUBLE PRECISION A, B, C, D, BLANK
      COMMON /ALLZZZ/ EEEEEE(17), ELL2ZZ, DL2ZZZ, SHORTZ,
     *     IEGRID, IPLOT
      DIMENSION E(IEGRID), F(IEGRID), G(IEGRID), H(IEGRID)
      DATA BLANK /10H          /
      WRITE (26,99999) A, B, C, D
      DO 10 I=1,IEGRID
           IF (D.NE.BLANK) WRITE (26,99998) E(I), F(I), G(I),
     *          H(I), E(I), F(I), G(I), H(I)
           IF (D.EQ.BLANK) WRITE (26,99997) E(I), F(I), G(I),
     *          E(I), F(I), G(I)
   10 CONTINUE
      RETURN
99999 FORMAT (/1X, 4(10X, A10))
99998 FORMAT (1X, 4F20.10, 2X, 1P4G10.2)
99997 FORMAT (1X, 3F20.10, 22X, 1P3G10.2)
      END
C
C
C
      SUBROUTINE QQQXXX(A, N)
C *** PURPOSE -- DEBUG-PRINT VARIABLES
      DIMENSION A(N)
      WRITE (26,99999) A
      RETURN
99999 FORMAT (//5F20.10/, (5F20.10))
      END
```

APPENDIX D. OUTPUT FROM FLIP1

```
****** TARGET END ******
   UUU = DISTANCE TO SURFACE OF TA TARGET                   =  0.000 +/- 2.000
   WWW = WIDTH OF TA TARGET                                 = 36.600
DELWWW = ERROR ON WWW                                       =  5.492 = 15.0 %
   SSS = ESTIMATE OF MULTIPLE SCATTERING IN TA TARGET       =  6.000
DELSSS = ERROR ON SSS                                       =  1.800 = 30.0 %
   UW2 = UUU + WWW/2 + SSS = DISTANCE TO MEAN OF TA TARGET  = 24.300
   RRR = RADIUS OF CIRCULAR DISTRIBUTION IN TA TARGET       =  9.200
DELRRR = ERROR ON RRRRRR                                    =  1.840 = 20.0 %

DWA(E) =    MEAN OF DISTRIBUTION IN WATER = 22.8 -1.60*LN(E) + 0.283*LN(E)**2
WWA(E) = STD DEV OF DISTRIBUTION IN WATER = 10.0 -0.63*LN(E) + 0.112*LN(E)**2
PERDWA = UNCERTAINTY ON MEAN DWA (E)      = 10.0 %
PERWWA = UNCERTAINTY ON STD DEV WWA (E)   = 10.0 %

ABSUNC = ABSOLUTE UNCERTAINTY ON FRACTION FROM TA AND FROM H2O =  0.00
   EMM = ENERGY AT WHICH THE TWO FRACTIONS ARE EQUAL           =  300000.
PEREMM = RELATIVE UNCERTAINTY IN EMM = DEL(EMM)/EMM            =  30.0 %
```

ENERGY (EV)	FRACTN OF TA	FRACTN OF WATR	ERROR ON FRACTN OF WATER	DISTANCE TO MEAN OF WATER DISTN	WIDTH OF WATER DISTN	MEAN OF TA+WATER DISTN	UNCER. ON MEAN	WIDTH OF TA+WATER DISTN	UNCER. ON WIDTH
EN	FTA	FWA	DFWA	ELWATR	WWATR	ELL1	DL1	WL1	DWL1
10.	0.0000	1.0000	0.0000	20.616	9.143	20.616	2.062	9.143	0.914
1000.	0.0018	0.9982	0.0005	25.252	10.992	25.250	2.521	10.984	1.098
2000.	0.0037	0.9963	0.0011	26.989	11.682	26.979	2.689	11.665	1.166
5000.	0.0092	0.9908	0.0027	29.702	12.759	29.653	2.943	12.718	1.268
10000.	0.0183	0.9817	0.0055	32.070	13.698	31.928	3.149	13.627	1.353
20000.	0.0366	0.9634	0.0110	34.711	14.746	34.330	3.349	14.631	1.438
50000.	0.0913	0.9087	0.0272	38.618	16.295	37.311	3.548	16.132	1.550
100000.	0.1811	0.8189	0.0531	41.890	17.592	38.705	3.623	17.411	1.693
200000.	0.3507	0.6493	0.0964	45.434	18.997	38.023	3.830	18.532	2.069
300000.	0.5000	0.5000	0.1236	47.633	19.868	35.966	4.205	18.549	2.530
400000.	0.6245	0.3755	0.1340	49.250	20.509	33.668	4.513	17.808	3.062
700000.	0.8569	0.1431	0.1021	52.529	21.809	28.338	4.442	13.560	4.236
1000000.	0.9499	0.0501	0.0536	54.711	22.673	25.823	4.009	9.478	3.918
2000000.	0.9987	0.0013	0.0029	59.158	24.436	24.346	3.841	4.850	1.024
5000000.	1.0000	0.0000	0.0000	65.454	26.930	24.300	3.845	4.600	0.920
10000000.	1.0000	0.0000	0.0000	70.532	28.942	24.300	3.845	4.600	0.920
20000000.	1.0000	0.0000	0.0000	75.883	31.062	24.300	3.845	4.600	0.920

EN	D2L1	D2W2L1	CVL1W2	CRL1W2
10.	4.250	279.534	-0.001	-0.000
1000.	6.353	581.896	0.022	0.000
2000.	7.231	739.553	0.142	0.002
5000.	8.663	1041.039	0.848	0.009
10000.	9.919	1359.711	2.770	0.024
20000.	11.215	1770.864	8.246	0.059
50000.	12.590	2501.383	29.807	0.168
100000.	13.126	3474.905	65.523	0.307
200000.	14.668	5881.645	119.601	0.407
300000.	17.684	8808.100	179.289	0.454
400000.	20.365	11892.838	247.042	0.502
700000.	19.733	13193.839	241.060	0.472
1000000.	16.073	5516.790	79.642	0.267
2000000.	14.752	98.667	-0.828	-0.022
5000000.	14.781	71.639	-0.000	-0.000
10000000.	14.781	71.639	-0.000	-0.000
20000000.	14.781	71.639	-0.000	-0.000

****** DETECTOR END ******

RHO = .004700 +/- .000094
THICKN = 19.0000 +/- 0.9500

PERCRO = 5.0000 % UNCERTAINTY ON CROSS SECTION

ENERGY	CRSSCTN	ELL3	DL3	WL3	DWL3	V3L3	U4L3
10.	27.200	5.986	0.220	4.788	0.191	89.786	1445.2
1000.	27.170	5.989	0.220	4.790	0.191	89.768	1445.7
2000.	27.020	6.005	0.220	4.796	0.191	89.672	1448.4
5000.	26.600	6.051	0.222	4.815	0.193	89.381	1455.7
10000.	25.910	6.127	0.224	4.844	0.196	88.827	1467.4
20000.	24.690	6.263	0.230	4.896	0.201	87.617	1486.9
50000.	21.770	6.600	0.244	5.015	0.213	83.459	1527.9
100000.	18.510	6.995	0.266	5.136	0.227	76.617	1563.9
200000.	14.800	7.466	0.296	5.256	0.242	65.962	1593.2
300000.	11.999	7.835	0.323	5.332	0.252	55.985	1608.1
400000.	11.240	7.937	0.331	5.350	0.255	53.016	1611.2
700000.	8.720	8.279	0.360	5.403	0.262	42.432	1619.3
1000000.	7.280	8.478	0.377	5.428	0.266	35.935	1622.3
2000000.	4.890	8.811	0.408	5.459	0.270	24.574	1624.4
5000000.	3.020	9.074	0.433	5.475	0.273	15.248	1606.7
10000000.	2.220	9.186	0.444	5.479	0.273	10.806	1435.7
20000000.	2.030	9.213	0.447	5.480	0.274	9.969	1479.5

ENERGY	D2L3	D2W2L3	CVL3W2	CRL3W2
10.	0.48246E-01	3.3363	0.36011	0.89758
1000.	0.48293E-01	3.3423	0.36065	0.89770
2000.	0.48528E-01	3.3721	0.36340	0.89832
5000.	0.49209E-01	3.4571	0.37126	0.90013
10000.	0.50398E-01	3.6010	0.38482	0.90331
20000.	0.52732E-01	3.8685	0.41079	0.90952
50000.	0.59736E-01	4.5716	0.48411	0.92639
100000.	0.70494E-01	5.4406	0.58595	0.94615
200000.	0.87554E-01	6.4788	0.72783	0.96637
300000.	0.10454	7.2399	0.85138	0.97863
400000.	0.10982	7.4353	0.88686	0.98144
700000.	0.12957	8.0308	1.0091	0.98923
1000000.	0.14245	8.3237	1.0809	0.99264
2000000.	0.16644	8.7130	1.2004	0.99678
5000000.	0.18750	8.9197	1.2917	0.99880
10000000.	0.19711	8.9797	1.3296	0.99935
20000000.	0.19945	8.9912	1.3384	0.99946

****** COMBINE THE THREE LENGTHS ******

ENERGY	EL	DL	WL	DWL
10.	201466.604	5.413	10.321	0.815
1000.	201471.238	5.604	11.983	1.009
2000.	201472.984	5.681	12.613	1.081
5000.	201475.703	5.806	13.599	1.188
10000.	201478.055	5.913	14.462	1.277
20000.	201480.592	6.022	15.429	1.365
50000.	201483.910	6.136	16.893	1.482
100000.	201485.699	6.180	18.153	1.625
200000.	201485.490	6.305	19.263	1.992
300000.	201483.803	6.541	19.300	2.432
400000.	201481.605	6.744	18.594	2.933
700000.	201476.617	6.698	14.596	3.936
1000000.	201474.301	6.420	10.922	3.403
2000000.	201473.156	6.318	7.302	0.710
5000000.	201473.375	6.322	7.151	0.628
10000000.	201473.486	6.323	7.154	0.628
20000000.	201473.514	6.323	7.155	0.628

*** COMPONENTS OF FLIGHT PATH LENGTH EL ***

ENERGY	EL	ELL2	ELL1	ELL3
10.	201466.604	201440.000	20.616	5.986
1000.	201471.238	201440.000	25.250	5.989
2000.	201472.984	201440.000	26.979	6.005
5000.	201475.703	201440.000	29.653	6.051
10000.	201478.055	201440.000	31.928	6.127
20000.	201480.592	201440.000	34.330	6.263
50000.	201483.910	201440.000	37.311	6.600
100000.	201485.699	201440.000	38.705	6.995
200000.	201485.490	201440.000	38.023	7.466
300000.	201483.803	201440.000	35.966	7.835
400000.	201481.605	201440.000	33.668	7.937
700000.	201476.617	201440.000	28.338	8.279
1000000.	201474.301	201440.000	25.823	8.478
2000000.	201473.156	201440.000	24.346	8.811
5000000.	201473.375	201440.000	24.300	9.074
10000000.	201473.486	201440.000	24.300	9.186
20000000.	201473.514	201440.000	24.300	9.213

*** COMPONENTS OF UNCERTAINTY ON FLIGHT PATH LENGTH ***

ENERGY	EL	DL	DL1	DL2	DL3
10.	201466.604	5.413	2.062	5.000	0.220
1000.	201471.238	5.604	2.521	5.000	0.220
2000.	201472.984	5.681	2.689	5.000	0.220
5000.	201475.703	5.806	2.943	5.000	0.222
10000.	201478.055	5.913	3.149	5.000	0.224
20000.	201480.592	6.022	3.349	5.000	0.230
50000.	201483.910	6.136	3.548	5.000	0.244
100000.	201485.699	6.180	3.623	5.000	0.266
200000.	201485.490	6.305	3.830	5.000	0.296
300000.	201483.803	6.541	4.205	5.000	0.323
400000.	201481.605	6.744	4.513	5.000	0.331
700000.	201476.617	6.698	4.442	5.000	0.360
1000000.	201474.301	6.420	4.009	5.000	0.377
2000000.	201473.156	6.318	3.841	5.000	0.408
5000000.	201473.375	6.322	3.845	5.000	0.433
10000000.	201473.486	6.323	3.845	5.000	0.444
20000000.	201473.514	6.323	3.845	5.000	0.447

*** COMPONENTS (SQUARED) OF UNCERTAINTY ON FLIGHT PATH LENGTH ***

ENERGY	EL	D2L	D2L1	D2L2	D2L3
10.	201466.604	29.298	4.250	25.000	0.048
1000.	201471.238	31.401	6.353	25.000	0.048
2000.	201472.984	32.279	7.231	25.000	0.049
5000.	201475.703	33.712	8.663	25.000	0.049
10000.	201478.055	34.969	9.919	25.000	0.050
20000.	201480.592	36.268	11.215	25.000	0.053
50000.	201483.910	37.650	12.590	25.000	0.060
100000.	201485.699	38.197	13.126	25.000	0.070
200000.	201485.490	39.755	14.668	25.000	0.088
300000.	201483.803	42.788	17.684	25.000	0.105
400000.	201481.605	45.475	20.365	25.000	0.110
700000.	201476.617	44.863	19.733	25.000	0.130
1000000.	201474.301	41.215	16.073	25.000	0.142
2000000.	201473.156	39.918	14.752	25.000	0.166
5000000.	201473.375	39.968	14.781	25.000	0.187
10000000.	201473.486	39.978	14.781	25.000	0.197
20000000.	201473.514	39.980	14.781	25.000	0.199

*** COMPONENTS OF WIDTH "WL" OF FLIGHT PATH LENGTH DISTRIBUTION ***

ENERGY	EL	WL	WL1	WL3
10.	201466.604	10.321	9.143	4.788
1000.	201471.238	11.983	10.984	4.790
2000.	201472.984	12.613	11.665	4.796
5000.	201475.703	13.599	12.718	4.815
10000.	201478.055	14.462	13.627	4.844
20000.	201480.592	15.429	14.631	4.896
50000.	201483.910	16.893	16.132	5.015
100000.	201485.699	18.153	17.411	5.136
200000.	201485.490	19.263	18.532	5.256
300000.	201483.803	19.300	18.549	5.332
400000.	201481.605	18.594	17.808	5.350
700000.	201476.617	14.596	13.560	5.403
1000000.	201474.301	10.922	9.478	5.428
2000000.	201473.156	7.302	4.850	5.459
5000000.	201473.375	7.151	4.600	5.475
10000000.	201473.486	7.154	4.600	5.479
20000000.	201473.514	7.155	4.600	5.480

*** DITTO, SQUARED ***

ENERGY	EL	W2L	W2L1	W2L3
10.	201466.604	106.524	83.597	22.927
1000.	201471.238	143.592	120.653	22.940
2000.	201472.984	159.078	136.075	23.003
5000.	201475.703	184.938	161.759	23.180
10000.	201478.055	209.154	185.686	23.469
20000.	201480.592	238.047	214.072	23.975
50000.	201483.910	285.380	260.229	25.151
100000.	201485.699	329.538	303.158	26.380
200000.	201485.490	371.080	343.452	27.628
300000.	201483.803	372.496	344.064	28.432
400000.	201481.605	345.737	317.111	28.626
700000.	201476.617	213.055	183.863	29.193
1000000.	201474.301	119.292	89.834	29.458
2000000.	201473.156	53.317	23.519	29.799
5000000.	201473.375	51.134	21.160	29.974
10000000.	201473.486	51.183	21.160	30.023
20000000.	201473.514	51.193	21.160	30.033

*** UNCERTAINTY ON WIDTH OF FPL DISTRIBUTION ***

ENERGY	EL	WL	DWL
10.	201466.604	10.321	0.815
1000.	201471.238	11.983	1.009
2000.	201472.984	12.613	1.081
5000.	201475.703	13.599	1.188
10000.	201478.055	14.462	1.277
20000.	201480.592	15.429	1.365
50000.	201483.910	16.893	1.482
100000.	201485.699	18.153	1.625
200000.	201485.490	19.263	1.992
300000.	201483.803	19.300	2.432
400000.	201481.605	18.594	2.933
700000.	201476.617	14.596	3.936
1000000.	201474.301	10.922	3.403
2000000.	201473.156	7.302	0.710
5000000.	201473.375	7.151	0.628
10000000.	201473.486	7.154	0.628
20000000.	201473.514	7.155	0.628

*** UNCERTAINTY ON VARIANCE OF FPL DISTRIBUTION ***

ENERGY	DW2L	DW2L1	DW2L3
10.	16.819	16.719	1.827
1000.	24.192	24.123	1.828
2000.	27.257	27.195	1.836
5000.	32.319	32.265	1.859
10000.	36.923	36.874	1.898
20000.	42.128	42.082	1.967
50000.	50.060	50.014	2.138
100000.	58.994	58.948	2.333
200000.	76.734	76.692	2.545
300000.	93.890	93.851	2.691
400000.	109.088	109.054	2.727
700000.	114.899	114.864	2.834
1000000.	74.331	74.275	2.885
2000000.	10.362	9.933	2.952
5000000.	8.975	8.464	2.987
10000000.	8.979	8.464	2.997
20000000.	8.979	8.464	2.999

*** COVARIANCE ON FLIGHT PATH LENGTH DISTRIBUTION

ENERGY	CVLW2	CVL1W2	CVL3W2
10.	0.360	-0.001	0.360
1000.	0.383	0.022	0.361
2000.	0.505	0.142	0.363
5000.	1.219	0.848	0.371
10000.	3.155	2.770	0.385
20000.	8.656	8.246	0.411
50000.	30.291	29.807	0.484
100000.	66.109	65.523	0.586
200000.	120.329	119.601	0.728
300000.	180.140	179.289	0.851
400000.	247.929	247.042	0.887
700000.	242.069	241.060	1.009
1000000.	80.723	79.642	1.081
2000000.	0.372	-0.828	1.200
5000000.	1.292	-0.000	1.292
10000000.	1.330	-0.000	1.330
20000000.	1.338	-0.000	1.338

****** TIME RESOLUTION ******

ASTD = WIDTH (STD.DEV.) OF BURST = 3.18496 +/- 0.21233
AFWHM = WIDTH (FWHM) OF BURST = 7.50000 +/- 0.50000
CHNL = WIDTH OF DETECTOR-CHANNEL = 1.00000 +/- 0.00100
DTZERO = UNCERTAINTY IN TZERO = 0.28867 = 2.887E-01
TSCALE = RELATIVE TIME-UNCERTAINTY = 0.00002 = 2.000E-05

??	WT?	DWT?	W2T?	DW2T?	D2W2T?	V3T?	U4T?
ONE	3.185	0.2123	10.14	1.353	1.829	0.0000	9.555
TWO	0.2887	0.2887E-03	0.8333E-01	0.1667E-03	0.2778E-07	0.0000	0.0125
TOTAL	3.198	0.2115	10.23	1.353	1.829	0.0000	14.64

****** FINAL RESULTS ******

T-TO	T-TOX	FUDGE1	FUDGE2	FUDGE3	FUDGE4
4605994.	4605994.	2.62E-09	1.45E-12	1.63E-25	3.80E-21
460610.	460610.	3.54E-09	1.45E-10	1.63E-21	5.12E-19
325703.	325703.	3.92E-09	2.89E-10	6.50E-21	1.13E-18
205996.	205996.	4.56E-09	7.23E-10	4.06E-20	3.29E-18
145663.	145663.	5.15E-09	1.45E-09	1.63E-19	7.45E-18
103000.	103000.	5.86E-09	2.89E-09	6.50E-19	1.70E-17
65144.	65144.	7.03E-09	7.23E-09	4.06E-18	5.08E-17
46064.	46064.	8.12E-09	1.45E-08	1.63E-17	1.17E-16
32572.	32572.	9.14E-09	2.89E-08	6.50E-17	2.64E-16
26595.	26595.	9.18E-09	4.34E-08	1.46E-16	3.98E-16
23032.	23032.	8.52E-09	5.78E-08	2.60E-16	4.93E-16
17410.	17410.	5.25E-09	1.01E-07	7.97E-16	5.31E-16
14566.	14566.	2.94E-09	1.45E-07	1.63E-15	4.25E-16
10300.	10300.	1.31E-09	2.89E-07	6.50E-15	3.80E-16
6514.	6514.	1.26E-09	7.23E-07	4.07E-14	9.11E-16
4606.	4606.	1.26E-09	1.45E-06	1.63E-13	1.82E-15
3257.	3257.	1.26E-09	2.89E-06	6.50E-13	3.65E-15

AAEL2	AATIM2	AAEL3	AATIM3	AAELTI	AAEL4	AATIM4
1.02E-04	1.39E-06	2.10E-07	0.00	2.46E-10	9.85E-10	1.13E-12
1.19E-04	1.39E-05	2.10E-07	0.00	2.86E-09	1.25E-09	1.13E-10
1.25E-04	1.96E-05	2.13E-07	0.00	4.26E-09	1.75E-09	2.26E-10
1.35E-04	3.10E-05	2.31E-07	0.00	7.26E-09	2.49E-09	5.65E-10
1.44E-04	4.39E-05	2.71E-07	0.00	1.09E-08	3.12E-09	1.13E-09
1.53E-04	6.21E-05	3.61E-07	0.00	1.65E-08	3.81E-09	2.26E-09
1.68E-04	9.82E-05	6.08E-07	0.00	2.85E-08	4.77E-09	5.65E-09
1.80E-04	1.39E-04	9.43E-07	0.00	4.33E-08	5.43E-09	1.13E-08
1.91E-04	1.96E-04	1.45E-06	0.00	6.50E-08	5.80E-09	2.26E-08
1.92E-04	2.40E-04	1.80E-06	0.00	7.98E-08	5.57E-09	3.39E-08
1.85E-04	2.78E-04	1.97E-06	0.00	8.88E-08	5.04E-09	4.52E-08
1.45E-04	3.67E-04	1.81E-06	0.00	9.22E-08	3.46E-09	7.91E-08
1.08E-04	4.39E-04	1.29E-06	0.00	8.25E-08	2.37E-09	1.13E-07
7.25E-05	6.21E-04	2.79E-07	0.00	7.80E-08	1.33E-09	2.26E-07
7.10E-05	9.82E-04	8.64E-08	0.00	1.21E-07	1.50E-09	5.65E-07
7.10E-05	1.39E-03	7.27E-08	0.00	1.71E-07	1.46E-09	1.13E-06
7.10E-05	1.96E-03	6.98E-08	0.00	2.42E-07	1.47E-09	2.26E-06

ENERGY	W2EN	WWEL2	WWTIM2	WWEL3
10.	1.0500E-06	1.0498E-08	1.9283E-12	4.3914E-14
1000.	1.4343E-02	1.4150E-08	1.9282E-10	4.4161E-14
2000.	6.4247E-02	1.5676E-08	3.8563E-10	4.5485E-14
5000.	0.4797	1.8224E-08	9.6406E-10	5.3212E-14
10000.	2.254	2.0610E-08	1.9281E-09	7.3585E-14
20000.	10.92	2.3456E-08	3.8561E-09	1.3054E-13
50000.	94.40	2.8119E-08	9.6398E-09	3.6934E-13
100000.	517.5	3.2470E-08	1.9279E-08	8.8908E-13
200000.	3005.	3.6563E-08	3.8559E-08	2.1167E-12
300000.	8509.	3.6703E-08	5.7839E-08	3.2246E-12
400000.	1.7791E+04	3.4067E-08	7.7120E-08	3.8983E-12
700000.	7.6423E+04	2.0994E-08	1.3497E-07	3.2911E-12
1000000.	2.0457E+05	1.1755E-08	1.9281E-07	1.6526E-12
2000000.	1.5636E+06	5.2540E-09	3.8563E-07	7.7994E-14
5000000.	2.4228E+07	5.0389E-09	9.6408E-07	7.4595E-15
10000000.	1.9332E+08	5.0437E-09	1.9282E-06	5.2854E-15
20000000.	1.5445E+09	5.0447E-09	3.8563E-06	4.8759E-15

ENERGY	WWELTI	WWTIM3	WWEL4	WWTIM4
10.	6.0729E-20	0.0000	9.6976E-19	-1.2784E-24
1000.	8.1854E-18	0.0000	-1.5568E-18	-1.2783E-20
2000.	1.8136E-17	0.0000	-3.0790E-18	-5.1130E-20
5000.	5.2707E-17	0.0000	-6.2105E-18	-3.1955E-19
10000.	1.1921E-16	0.0000	-9.7397E-18	-1.2781E-18
20000.	2.7134E-16	0.0000	-1.4535E-17	-5.1122E-18
50000.	8.1319E-16	0.0000	-2.2777E-17	-3.1949E-17
100000.	1.8780E-15	0.0000	-2.9490E-17	-1.2779E-16
200000.	4.2294E-15	0.0000	-3.3684E-17	-5.1117E-16
300000.	6.3686E-15	0.0000	-3.1030E-17	-1.1502E-15
400000.	7.8818E-15	0.0000	-2.5412E-17	-2.0448E-15
700000.	8.5007E-15	0.0000	-1.1982E-17	-6.2630E-15
1000000.	6.7998E-15	0.0000	-5.6229E-18	-1.2782E-14
2000000.	6.0784E-15	0.0000	1.7594E-18	-5.1130E-14
5000000.	1.4574E-14	0.0000	2.2414E-18	-3.1956E-13
10000000.	2.9175E-14	0.0000	2.1383E-18	-1.2782E-12
20000000.	5.8362E-14	0.0000	2.1650E-18	-5.1129E-12

ENERGY	ADJ. ENE.	FUDGE	DEN	DEN/EN
10.	10.	2.626E-09	6.699E-04	6.699E-05
1000.	1000.	3.682E-09	6.853E-02	6.853E-05
2000.	2000.	4.208E-09	0.138	6.917E-05
5000.	5000.	5.279E-09	0.351	7.021E-05
10000.	10000.	6.598E-09	0.711	7.114E-05
20000.	20000.	8.756E-09	1.44	7.215E-05
50000.	50000.	1.426E-08	3.67	7.341E-05
100000.	100000.	2.258E-08	7.43	7.430E-05
200000.	200000.	3.806E-08	15.3	7.636E-05
300000.	300000.	5.255E-08	23.8	7.929E-05
400000.	400000.	6.636E-08	32.8	8.191E-05
700000.	700000.	1.065E-07	59.1	8.438E-05
1000000.	1000000.	1.475E-07	85.0	8.504E-05
2000000.	2000001.	2.905E-07	186.	9.314E-05
5000000.	5000004.	7.243E-07	579.	1.157E-04
10000000.	10000015.	1.447E-06	1.458E+03	1.458E-04
20000000.	20000058.	2.894E-06	3.845E+03	1.923E-04

ENERGY	WEN	WEN/EN	DWEN	DWEN/WEN
10	1.025E-03	1.025E-04	8.088E-05	7.893E-02
1000.	0.120	1.198E-04	9.953E-03	8.311E-02
2000.	0.253	1.267E-04	2.120E-02	8.363E-02
5000.	0.693	1.385E-04	5.752E-02	8.305E-02
10000.	1.50	1.501E-04	0.121	8.091E-02
20000.	3.31	1.653E-04	0.253	7.657E-02
50000.	9.72	1.943E-04	0.655	6.746E-02
100000.	22.7	2.275E-04	1.40	6.133E-02
200000.	54.8	2.741E-04	3.33	6.071E-02
300000.	92.2	3.075E-04	5.86	6.349E-02
400000.	133.	3.335E-04	8.89	6.664E-02
700000.	276.	3.949E-04	18.7	6.777E-02
1000000.	452.	4.523E-04	29.3	6.485E-02
2000000.	1.250E+03	6.252E-04	81.6	6.525E-02
5000000.	4.922E+03	9.844E-04	324.	6.578E-02
10000000.	1.390E+04	1.390E-03	917.	6.595E-02
20000000.	3.930E+04	1.965E-03	2.595E+03	6.604E-02

INTERNAL DISTRIBUTION

1. L. S. Abbott
2. H. P. Carter
3. J. W. T. Dabbs
4. G. de Saussure
5. J. K. Dickens
6. G. F. Flanagan
7. R. Gwin
8-12. J. A. Harvey
13. D. M. Hetrick
14. N. W. Hill
15. C. H. Johnson
16-20. D. C. Larson
21-25. N. M. Larson
26. R. L. Macklin
27. F. C. Maienschein
28. G. S. McNeilly
29. B. D. Murphy
30. D. K. Olsen
31. R. W. Peelle
32. F. G. Perey
33. R. R. Spencer
34. L. W. Weston
35. G. E. Whitesides/ CS Library
36. A. Zucker
37. P. W. Dickson, Jr. (consultant)
38. G. H. Golub (consultant)
39. H. J. C. Kouts (consultant)
40. D. Steiner (consultant)
41. Central Research Library
42. ORNL Y-12 Technical Library
43. Document Reference Section
44. Laboratory Records
45. Laboratory Records-RC
46. ORNL Patent Section

EXTERNAL DISTRIBUTION

47. Office of Assistant Manager for Energy Research and Development, Department of Energy, Oak Ridge Operations Office, Oak Ridge, TN 37831
48-49. Director, Reactor Research and Development, USDOE, Washington, DC 20545
50. Dr. W. P. Poenitz, Argonne National Laboratory, 9700 South Cass Ave., Argonne, IL 60439
51. Mr. Philip B. Hemmig, Chief, Physics Branch, Reactor Research and Technology, Office of Energy Technology, U.S. Department of Energy, Washington, DC 20545
52. Dr. R. C. Block, Department of Nuclear Engineering, Rensselaer Polytechnic Institute, Troy, NY 12181
53. Dr. Donald L. Smith, Building 314, Applied Physics Division, Argonne National Laboratory, 9700 South Cass Ave., Argonne, IL 60439
54. Dr. S. L. Whetstone, Division of Nuclear Physics, Office of Energy Research, U.S. Department of Energy, Room G-315, Washington, DC 20545
55. Dr. M. R. Bhat, Building 197D, National Nuclear Data Center, Brookhaven National Laboratory, Upton, NY 11973
56. Dr. G. F. Auchampaugh, Los Alamos Scientific Laboratory, MS 442, P-3, Los Alamos, NM 87545

EXTERNAL DISTRIBUTION (contd)

57. Dr. R. F. Carlton, Middle Tennessee State University, Physics Department, Box 407, Murfreesboro, TN 37132
58. Dr. E. C. Lynn, Nuclear Physics Division, Atomic Energy Research Establishment, Harwell, Didcot, Oxon, OX11, ORA, United Kingdom
59. Dr. M. G. Sowerby, Nuclear Physics Division, Bldg. 418, Atomic Energy Research Establishment, Harwell, Didcot, Oxon, OX11, ORA, United Kingdom
60. Dr. Roger White, Lawrence Livermore National Laboratory, P. O. Box 808, Livermore, CA 94550
61. Dr. R. R. Winters, Physics Department, Denison University, Granville, Ohio 43023
62. Dr. Herman Weigmann, Central Bureau for Nuclear Measurements, Steenweg naar Retie, B-2440, Geel, Belgium
63. Dr. G. L. Morgan, Los Alamos National Laboratory, P. O. Box 1663, Group P-15, MS D406, Los Alamos, NM 87545
64. Dr. C. Coceva, ENEA Comitato Nazionale, Centro Richerche Energie, Ezio Clemental, via G. Maxxini, 2, 40138, Bologna, Italy
65. Dr. O. A. Wasson, RADP-B119, National Bureau of Standards, Washington, DC 20234

66-92. Technical Information Center